INFORMATION TO USERS

This manuscript has been reproduced from the microfilm master. UMI films the text directly from the original or copy submitted. Thus, some thesis and dissertation copies are in typewriter face, while others may be from any type of computer printer.

The quality of this reproduction is dependent upon the quality of the copy submitted. Broken or indistinct print, colored or poor quality illustrations and photographs, print bleedthrough, substandard margins, and improper alignment can adversely affect reproduction.

In the unlikely event that the author did not send UMI a complete manuscript and there are missing pages, these will be noted. Also, if unauthorized copyright material had to be removed, a note will indicate the deletion.

Oversize materials (e.g., maps, drawings, charts) are reproduced by sectioning the original, beginning at the upper left-hand corner and continuing from left to right in equal sections with small overlaps. Each original is also photographed in one exposure and is included in reduced form at the back of the book.

Photographs included in the original manuscript have been reproduced xerographically in this copy. Higher quality 6" x 9" black and white photographic prints are available for any photographs or illustrations appearing in this copy for an additional charge. Contact UMI directly to order.

UMI

A Bell & Howell Information Company
300 North Zeeb Road, Ann Arbor MI 48106-1346 USA
313/761-4700 800/521-0600

CHROMATOGRAPHIC STUDY OF GEMINI SURFACTANTS

by

Lin Guo

A dissertation submitted to the Graduate Faculty in Chemistry in partial fulfillment of the requirements for the degree of Doctor of Philosophy, The City University of New York.

1999

This manuscript has been read and accepted for the Graduate Faculty in Chemistry in satisfaction of the dissertation requirement for the degree of Doctor of Philosophy.

9/17/98
Date

P. Gary Marshall
Chair of Examining Committee

12/22/98
Date

Gerald Koppel
Executive Officer

David C. Lorde

Milt Flam
Supervisory Committee

THE CITY UNIVERSITY OF NEW YORK

1998

Abstract

CHROMATOGRAPHIC STUDY OF GEMINI SURFACTANTS

by

Lin Guo

Adviser: Professor P. Gary Mennitt

The application of ion-interaction reversed-phase chromatography to ionic surfactants including three series of gemini surfactants and a series of alkanesulfonates has been demonstrated in this work. The satisfactory RP-HPLC analysis was obtained using 33 x 4.6 mm C18 columns, direct or indirect UV detection, and ion-interaction reagents.

The retention mechanism has been studied by using designed experiments and thermodynamic considerations. The results indicate that no matter what kind of ion-interaction reagents is used there are no tightly bonded ion-pairs, even though the analyte and the ion-interaction reagent co-elute. The oppositely charged ions are separated by the solvent molecules.

The linear correlations between log CMC and log k' or pC_{20} and log k' have been explored. These linear relationships exist when the surface and micellar properties of a series of surfactants follow the regularity with the increment of the carbon number in the straight alkyl chain. This work provides a supplementary method to the determination of CMC and pC_{20} values.

Acknowledgment

I would like to express my gratitude to Professor P. Gary Mennitt who served as my mentor for my Ph.D. research. His guidance and invaluable assistance during my entire research and throughout the writing of this dissertation led me to pursue my doctorate.

My gratitude extends to Professors Milton Rosen and David C Locke for serving on my Thesis Committee. I would like to thank Professor Milton Rosen for his expert advice in the area of the surfactant science and his support for experiment materials. I would also like to thank Professor David C Locke for his expert advice in the chromatographic science.

My special thanks to Professor Darryl Howery for his encouragement and support throughout my graduate study. Without his support, I would not have undertaken such a challenge. I would like to thank Professor Richard Pizer for his support and help specially during the early days of my graduate study. I would also like to acknowledge the entire staff of the Chemistry Department and my friends for their support.

Finally., I am most grateful to all of my family for their understanding and support throughout my graduate study: my parents Wude Guo and Xuecui Tao, my aunt Xueliang Tao, my husband Xinshun Ding, my daughter Yue Ding, and my brother Bo and his family.

Contents

List of Tables

List of Figures

Chapter 1

Correlation of Surfactant Properties with HPLC Measurements

1.1 Adsorption, Micellization and Their Measurement

A surfactant has a lipid-soluble portion connected to a water-soluble portion. This amphipathic structure provides surfactants with unique properties. One of the features of surfactants is the ability to adsorb at interfaces in a certain orientation. When a surfactant is mixed with a solvent, usually water, the structural group that has very little interaction with the solvent may cause distortion of the structure of the liquid solvent. This increases the free energy of the system. Therefore, the work required to bring a surfactant molecule to the surface is less than the work required to bring a solvent molecule to the surface. The surfactant will concentrate at the surface. In addition, the presence of the group that does interact with the solvent keeps the surfactant in the solvent. Thus, a bridge is formed between the two otherwise immiscible phases.

The concentration of a surfactant in the liquid phase required to produce a given amount of adsorption at the interface is a measure of the efficiency of adsorption. It

should relate to the minimum concentration of the surfactant in the bulk phase necessary to produce maximum (saturation) adsorption at the interface. This concentration can be determined by a complete γ vs. log C plot, where γ is the surface tension and C is the bulk phase concentration of a surfactant. When the surface (or interfacial) tension of the pure solvent has been decreased by about 20 dyne/cm, the surface excess concentration of the surfactant is close to its saturation value[1]. Therefore, the commonly used measurement of the adsorption efficiency is the negative logarithm of the concentration of a surfactant in the bulk phase required to produce a 20 dyne/cm reduction in the surface or interfacial tension of the solvent[2].

$$pC_{20} \equiv - \log C_{\Delta\gamma = -20} \qquad (1\text{-}1)$$

Where $C_{\Delta\gamma = -20}$ is the molar concentration of the surfactant in the liquid phase at adsorption equilibrium required to reduce the surface or interfacial tension of the solvent by 20 dyne/cm. In general, the adsorption efficiency at aqueous solution-air and aqueous solution-hydrocarbon interfaces increases linearly with an increase in the number of carbon atoms in the straight-chain hydrophobic group of a surfactant.

Micellization is another important property typically used to characterize surfactants. As described above, when the surfactants dissolve in water, the free energy of the system increases. Surfactant molecules adsorb at the surface with their hydrophobic groups pointing away from the aqueous

phase in order to minimize this free energy increase. With the interface saturated, additional free energy minimization occurs by aggregating the surfactant molecules into micelles with the hydrophobic groups toward the interior of the cluster and the hydrophilic groups toward the solvent. The concentration at which the micelles start to form is called the critical micelle concentration (CMC).

The CMC can be determined by measuring a variety of physical properties of the surfactant solutions. Some of these are electrical conductivity, surface tension, light scattering, and refractive index as shown in Figure 1-1[3]. The formation of the micelles causes breaks in the curves of those physical properties vs. concentration. The CMC can also be measured by other methods, such as adding some dyestuff to the surfactant solution. The spectral characteristics of dyestuff will change when the surfactant CMC is reached[4]. Recently, the determination of the CMC by capillary electrophoresis has been reported[5].

For homologous straight-chain ionic surfactants in aqueous solution, a linear relation between the CMC and the number of carbon atoms N in the hydrophobic chain is observed[6].

$$\log \mathrm{CMC} = A - BN \qquad (1\text{-}2)$$

where A is a constant for a particular ionic head group at a given temperature and B is a constant related to the hydrophobic chain. Homologous straight-chain ionic

surfactants, such as alkanesulfonates, alkyl sulfates, alkylammonium chlorides, and alkyltrimethylammonium bromides, in aqueous medium at 35 °C have a *B* value of about 0.3[7].

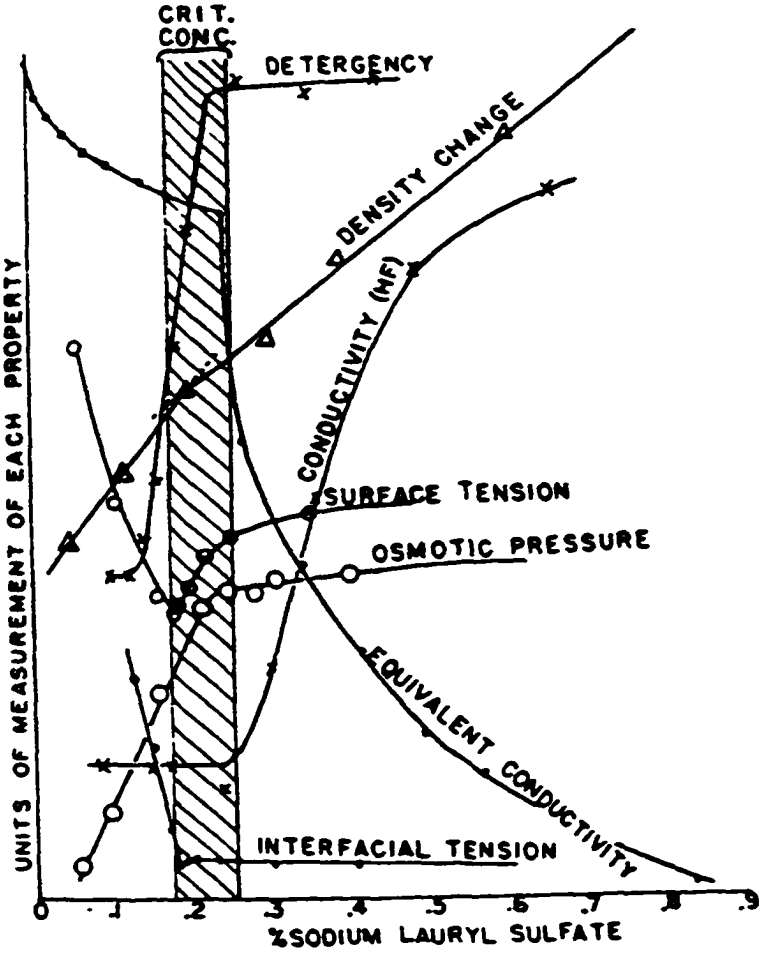

Figure 1-1 Changes in some physical properties of an aqueous solution of sodium dodecyl sulfate in the neighborhood of the critical micelle concentration[3].

1.2 Capacity Factor, k', in Chromatography

According to a committee of the International Union of Pure and Applied Chemistry, chromatography is "··· a method, used primarily for separation of the components of a sample, in which the components are distributed between two phases, one of which is stationary while the other moves. The stationary phase may be a solid, or a liquid supported on a solid, or a gel. The stationary phase may be packed in a column, spread as a layer, or distributed as a film ···. The mobile phase may be gaseous or liquid."[8]

In liquid chromatography (LC) the mobile phase is liquid. Early in the development of liquid chromatography, scientists realized that the improvement of efficiency in liquid chromatography could be achieved by using very small particles as the stationary phase and a high pressure difference along the column. This led to the development of high-performance liquid chromatography (HPLC). LC separations depend mainly on solubility differences of analytes in two phases. The compositions of the mobile phase and the stationary phase materials are both important. In normal-phase high-performance liquid chromatography, the stationary phase is polar and the mobile phase is relatively nonpolar. In reversed-phase high-performance liquid chromatography (RP-HPLC), the packing material has a nonpolar surface and the

mobile phase is relatively polar.

The difference in the equilibrium distribution of sample components between two phases results in the different migration rates of analytes. Ideally, it causes the components in a mixture to separate into bands along the column. Thus substances are separated. The migration rates are determined by the partition coefficient, K. The partition coefficient is the equilibrium constant for the process:

$$A_{mobile} \rightleftharpoons A_{stationary}$$

$$K = \frac{C_s}{C_m} \qquad (1\text{-}3)$$

Where C_s is the analyte concentration in the stationary phase and C_m is its concentration in the mobile phase.

The capacity factor, k', is an important parameter in chromatography. It is defined as the ratio of analyte mass in the stationary phase and the mobile phase[9] at equilibrium.

$$k' = \frac{(\text{mass of analyte})_s}{(\text{mass of analyte})_m} = \frac{m_s}{m_m} \qquad (1\text{-}4)$$

The relationship between the partition coefficient, K, and the capacity factor, k', is

$$K = k'\frac{V_m}{V_s} \qquad (1\text{-}5)$$

Where V_m and V_s are the volumes of the mobile and stationary phases respectively. The ratio V_m/V_s is called the phase ratio. Equation (1-5) relates the equilibrium distribution of

an analyte within the column, k', to the thermodynamic distribution coefficient, K. K is independent of a particular column, but the phase ratio and, therefore, k' are characteristic for the particular column.

Because it is impossible to measure the phase ratio, a more practical method is to relate k' directly to easily measurable quantities. Equation (1-4) represents the ratio of the probabilities that solute molecules stay in the stationary phase to the mobile phase. This is equal to the ratio of the time that solute molecules spend in the two phases[9],

$$k' = \frac{t_r - t_m}{t_m} = \frac{t_r'}{t_m} \qquad (1\text{-}6)$$

where t_r is called the retention time, which is the time required for an analyte to traverse the system. The t_m is the time it takes a solute to pass through the space occupied by the mobile phase. During this time all solutes migrate with the velocity of the mobile phase. The difference, $t_r - t_m$, is the adjusted retention time of an analyte, which is the time that an analyte spends in the stationary phase (where the analyte has zero velocity).

In the reversed-phase liquid chromatographic system, retention mainly depends on the polarity and the size of a molecule (or the size of the hydrophobic group). k' increases with decrease of the solute polarity, and with increase of the mobile phase polarity and the size of the hydrophobic group of an analyte.

1.3 Prediction of CMC and pC_{20} by log k'

The CMC and pC_{20} values reflect hydrophobic interactions of the surfactants with themselves. The self-association of hydrophobic molecules (or hydrocarbon chains of the amphipathic compounds) and adsorption onto the interface resemble the partition of a solute into the lipophilic phase in reversed-phase high performance liquid chromatography (RP-HPLC). Those processes can be considered as transfer of a hydrophobic chain from a hydrophilic environment to a lipophilic medium. Since the CMC and pC_{20} of a surfactant and its chromatographic mobility are fundamentally related phenomena, RP-HPLC measurements could constitute a means of estimating the CMC and pC_{20} value.

1.3.1 Work done by Castro group

In 1986, Victor Castro and coworkers proposed the use of RP-HPLC to predict the critical micelle concentration[10]. A treatment of RP-HPLC retention data for homologous series of α-olefin sulfonates and sodium alkanesulfonates led to a relationship with the CMC. The following is a summary of their work.

The Martin rule[11] summarizes the empirical observation that retention in reversed-phase systems increases with an increment of molecular size. For a homologous series, log k'

increases linearly with increasing number of carbon atoms.

$$\log k' = a + bN \qquad (1\text{-}7)$$

Where a is a constant for a functional group; b is a constant reflecting the hydrophobic interactions from the hydrocarbon chain; N is the number of carbon atoms in the straight chain of hydrocarbon.

Castro proposed that the standard free energy change of transfer, ΔG°_{LC}, of the analyte from a polar mobile phase to a nonpolar stationary phase is

$$\Delta G^{\circ}_{LC} = C_1 + C_2N \qquad (1\text{-}8)$$

C_1 and C_2 are constants.

In a homologous series of straight-chain surfactants, the following relationship holds.

$$\log \text{CMC} = A - BN \approx \text{const.} + \frac{\Delta G^{\circ}_{mic}}{2.3RT} \qquad (1\text{-}9)$$

Where A and B are constants relating log CMC to the number of carbon atoms. Castro concluded that ΔG°_{LC} in equation (1-8) and ΔG°_{mic} in (1-9) have the same meaning. Then by equalizing two ΔG°s and using equations (1-7), (1-8) and (1-9) they obtained A and a, B and b correlations.

$$A = \text{const.} - \log \frac{V_m}{V_s} - a \qquad (1\text{-}10)$$

$$B = b \qquad (1\text{-}11)$$

In order to predict log CMC, A had to be taken from one of the

known experimental CMC values in each series. The constant *B* was evaluated by a numerical treatment of their chromatographic results and extrapolation of data to a mobile phase of pure water. Part of their results are in Table 1-1.

But there are two questions associated with the above considerations:

(a) Micellization and adsorption at the stationary phase of RP-HPLC are two different processes, even though they are similar in some respects. The free energy change of transfer in HPLC is not identical to the free energy change of transfer in the micelle formation.

(b) Generally, $B \neq b$, since the increment per methylene unit may have a different effect in the two systems.

Table 1-1 Prediction of CMC values* (mmol/L) of sodium sulfonates[10]

Series	C_{12}		C_{14}		C_{16}		C_{18}	
	Pred	Expt	Pred	Expt	Pred	Expt	Pred	Expt
2-Alkenesulfonates	10	13	2.7	2.7**	0.73	0.61	0.20	0.18
3-Hydroxyalkanesulfonates	25.8	25.0	6.3	6.3**	1.54	1.6	0.38	0.38

* Experimental values were obtained from the literature.

** Standard values used for the calculation of A in equation (1-9).

1.3.2 Work done by Shaw group

In 1991, Roger Shaw and coworkers estimated CMCs of bile acids by RP-HPLC[12]. They used the free energy change of partition ΔG_p, equation (1-12), and the free energy change of micelle formation ΔG_m, equation (1-13), to derive correlation between the CMC and the relative capacity factor rk'.

$$\Delta G_p = - RT(\ln k' + r_o) \qquad (1\text{-}12)$$

$$\Delta G_m \approx RT(\ln [B]_c - s_o) \qquad (1\text{-}13)$$

Where k' is the capacity factor, r_o and s_o are constants, and $[B]_c$ is the CMC of the bile acid.

By assuming a linear free energy relationship of ΔG_p and ΔG_m, they obtained

$$\log \text{CMC} \propto - \log rk'$$

Where the relative capacity factor rk' is defined as

$$rk' = \frac{k'(x)}{k'(s)} \qquad (1\text{-}14)$$

x is for the analyte (bile acid) and s for the standard. Some of their results for CMCs of the bile acids are in Table 1-2 and Figure 1-2. There is a good agreement between measured and predicted values.

A test of the general validity of this method was to examine the CMC and rk' values of C_8-C_{14} sodium n-alkyl sulfates. Figure 1-3 is their plot of log CMC vs. log k' (instead of log rk' in their derived equation) for C_8-C_{14}

sodium *n*-alkyl sulfates in the aqueous solution. Here the CMC and *k'* data were taken from the literature. This graph clearly shows that, for some systems, there is a strong correlation of the CMC and *k'*.

The following are drawbacks in their work:

(a) Some assumptions were made for the constant s_o in equation (1-13). Those assumptions referred specifically to the bile acids used in their investigation.

(b) The relative capacity *rk'* is not a commonly used parameter in chromatography.

Table 1-2 log CMC (mM) and log *rk'* values for bile acids[12]

Bile acid*	log *rk'*	log CMC (measured)	log CMC (predicted)
C	-0.46	1.11	1.14
HDC	-0.44	1.10	1.12
UDC	-0.47	1.19	1.15
CDC	-0.10	0.85	0.81
DC	0.00**	0.70	0.72
TC	-0.51	1.08	1.11
TAC	-0.49	1.10	1.09
TCDC	-0.17	0.78	0.72
TACDC	-0.16	0.67	0.70
TDC	-0.88	0.60	0.61

* C: cholic acid; HDC: hyodeoxycholic acid; UDC: ursodeoxycholic acid; CDC: chenodeoxycholic acid; DC: deoxycholic acid; T: bile acids conjugated with taurine; A: allocholanic acid.

** Used as the standard in *rk'* calculation.

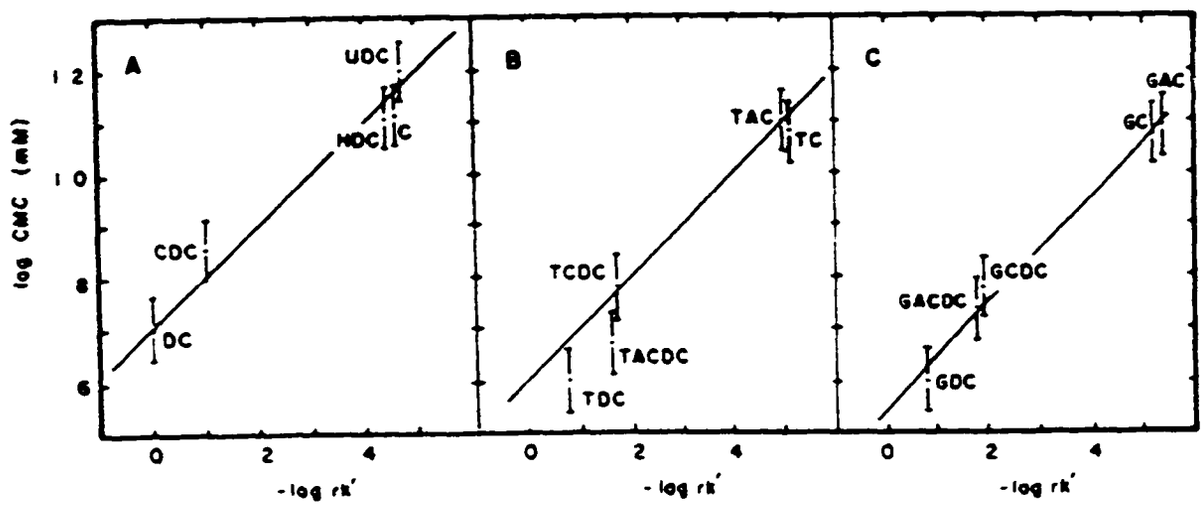

	intercept	slope
Left (free bile salt):	0.72	-0.93
Center (taurine conjugate):	0.52	-1.15
Right (glycine conjugate):	0.55	-1.02

Figure 1-2 Relationship between log CMC and log *rk'* for bile acids[12]

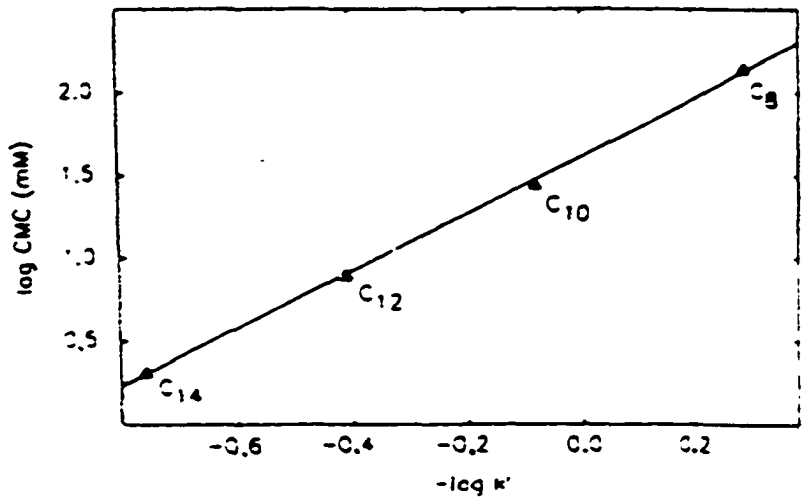

Intercept: 1.61 slope: -1.72

Figure 1-3 Relationship between log CMC and log *k'* for homologous *n*-alkyl sulfates[12]

1.4 Thermodynamic Consideration of CMC and k', pC_{20} and k' Correlations

The work done by the Castro group and the Shaw group shows that the relative prediction of the CMC is possible. But as has been discussed there are some problems and limitations in their theoretical considerations of the correlation between the CMC and k'. A search of the literature has not revealed the corresponding correlation of pC_{20} and k'.

A modified thermodynamic treatment of the CMC and k', pC_{20} and k' correlations is presented here. This theoretical approach is expected to overcome the drawbacks in the work of the Castro group and the Shaw group. The approach is also the theoretical foundation for this thesis.

1.4.1 The free energy change of transfer in HPLC, ΔG°_{LC}

With the usual assumption that phenomena occurring inside the column are well approximated by equilibrium, the free energy change of transfer, ΔG°_{LC}, for the analyte from a polar liquid environment to a nonpolar stationary phase in HPLC is

$$\Delta G^{\circ}_{LC} = - 2.3RT\log K \qquad (1\text{-}15)$$

Since $K = k'(V_m/V_s)$ (equation (1-5)), this can be rewritten as

$$\Delta G^{\circ}_{LC} = - 2.3RT\log\ (k'\frac{V_m}{V_s}) \qquad (1\text{-}16)$$

1.4.2 The free energy change of transfer in micelle formation, ΔG_{mic}

As previously indicated, for homologous straight chain surfactants, the empirical relation between the CMC and the total number of carbon atoms (N) in the hydrophobic group is

$$\log \text{CMC} = A - BN \qquad (1\text{-}2)$$

Where A and B are constants. The Castro group rather arbitrarily assumed a connection of this relationship with ΔG_{mic}; Rosen, however, showed theoretically the meaning of A and B[13]. The constant A reflects the free energy change involved in transferring the hydrophilic group from an aqueous environment to the micelle, whereas B reflects the free energy change involved in transferring a methylene unit of the hydrophobic group from an aqueous environment to the micelle.

$$A = \frac{- \Delta G_{mic}(-W) + k}{2.3RT} + \log \omega \qquad (1\text{-}17)$$

$$B = \frac{- \Delta G_{mic}(-CH_2-)}{2.3RT} \qquad (1\text{-}18)$$

$\Delta G_{mic}(-W)$ is the free energy change of transfer for the hydrophilic head group from an aqueous environment to the micelle. For ionic surfactants, $\Delta G_{mic}(-W)$ involves the

electrical energy of transferring the ionic hydrophilic group from an aqueous environment to the micelle. The constant k is defined by $k = \Delta G_{mic}(-CH_3) - \Delta G_{mic}(-CH_2-)$. ω is the molar concentration of water. $\Delta G_{mic}(-CH_2-)$ is the free energy change of transfer for a methylene unit of the hydrophobic group from an aqueous environment (a polar phase) to the interior of the micelle (a hydrocarbon phase). Values of $\Delta G_{mic}(-CH_2-)$ for all types of surfactants (nonionics, ionics and zwitterionics) with similar hydrocarbon chain are similar. One can assume that the contributions of $\Delta G_{mic}(-CH_3)$, $\Delta G_{mic}(-CH_2-)$ and $\Delta G_{mic}(-W)$ do not change with increase in the length of the hydrophobic group[13].

Equation (1-2) can be written as

$$\log CMC = A + \frac{\Delta G_{mic}(-CH_2-)}{2.3RT}N \qquad (1\text{-}19)$$

Thus,

$$N\Delta G_{mic}(-CH_2-) = 2.3RT\log CMC - 2.3RTA \qquad (1\text{-}20)$$

Because ΔG_{mic} can be separated into the following terms[13],

$$\Delta G_{mic} = \Delta G_{mic}(-CH_3) + (N-1)\Delta G_{mic}(-CH_2-) + \Delta G_{mic}(-W) \qquad (1\text{-}21)$$

Then,

$$\Delta G_{mic} = 2.3RT\log CMC + A' \qquad (1\text{-}22)$$

A' is a constant which includes $\Delta G_{mic}(-CH_3)$, $\Delta G_{mic}(-CH_2-)$, $\Delta G_{mic}(-W)$, and the constant A.

1.4.3 The relationship between ΔG°_{LC} and ΔG_{mic}

ΔG°_{LC} in equation (1-16) and ΔG_{mic} in equation (1-22) are different, but fundamentally related to each other. They both represent the transfer of solute molecules from a hydrophilic environment to a lipophilic medium and would thus be expected to be related by a linear free energy relationship. Thus, for a homologous series (with the same hydrophobic head group), we can write,

$$\Delta G_{mic} = m\Delta G^{o}_{LC} + \text{const.} \qquad (1\text{-}23)$$

In this equation, the const. represents the inherent difference in hydrophobicities and hydrophilicities of the environments of the HPLC system and the micelle formation. The m characterizes the different tendencies between adsorption onto the HPLC stationary phase (monomer adsorbing onto the interface) and self-association.

In equation (1-23), one can replace ΔG°_{LC} with equation (1-16), and ΔG_{mic} with equation (1-22),

$$\log CMC = - m\log k' - m\log \frac{V_m}{V_s} + \frac{\text{const.} - A'}{2.3RT} \qquad (1\text{-}24)$$

which can be written as

$$\log CMC = - m\log k' + c \qquad (1\text{-}25)$$

The CMC values of a homologous series of surfactants can be estimated from RP-HPLC data, once two CMCs for the series have been measured experimentally.

1.4.4 The free energy change in adsorption at the interface, ΔG°_{ad}, and the relationship between ΔG°_{LC} and ΔG°_{ad}

For homologous straight-chain surfactants, the adsorption efficiency factor, pC_{20}, is a linear function of the number of carbon atoms, N, in the hydrophobic group[14].

$$pC_{20} = [\frac{-\Delta G^{\circ}_{ad}(-CH_2-)}{2.3RT}]N + \text{const.}' \qquad (1\text{-}26)$$

$\Delta G^{\circ}_{ad}(-CH_2-)$ is the standard free energy change of transfer of one $-CH_2-$ group from the interior of the liquid phase to the interface under conditions where the surface (or interfacial) tension has been reduced by 20 dyne/cm. $\Delta G^{\circ}_{ad}(-CH_2-)$ is related to, but not the same as the $\Delta G_{mic}(-CH_2-)$ introduced in section 1.4.2. Comparing equation (1-26) with (1-19), they have similar forms except that the two ΔG terms and the constants have different values. Therefore doing the same derivation, one obtains a similar relation between pC_{20} and log k' for a homologous series.

$$pC_{20} = m'\log k' + c' \qquad (1\text{-}27)$$

1.5 Research Scope of RP-HPLC and CMC, pC_{20} of Surfactants

The following four series of surfactants were studied.

(1) Alkanesulfonates

$$C_nH_{2n+1}SO_3^-$$

(2) Aromatic quaternary ammonium geminis

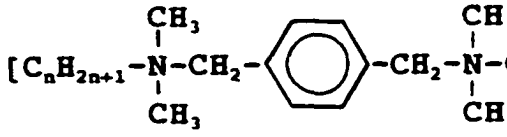

$(C_nN)_2Ar$

(3) Nonaromatic quaternary ammonium geminis (mono-ol)

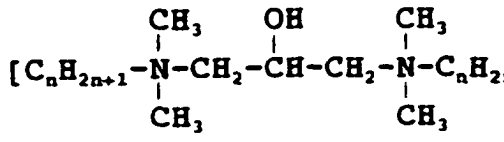

$(C_nN)_2OH$

(4) Nonaromatic quaternary ammonium geminis (di-ol)

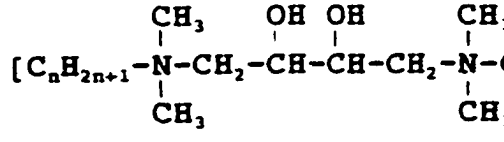

$(C_nN)_2(OH)_2$

The three series labelled above as $(C_nN)_2Ar$, $(C_nN)_2OH$ and $(C_nN)_2(OH)_2$ are gemini surfactants. Geminis are a new generation of surfactants. They have two hydrophilic groups and two hydrophobic groups per molecule. These structural characteristics result in unusually low CMC and C_{20} values in aqueous media. Compared with conventional surfactants with the same number of carbon atoms per hydrophobic group, the ionic gemini surfactants are about three orders more efficient at reducing the surface tension (C_{20}) and more than two orders more efficient in forming micelles (CMC)[15].

The experiments and data analysis were undertaken with two objectives. One was to confirm the predicted correlations of log CMC with log k', and pC_{20} with log k'. The results for these four series of surfactants are discussed in Chapters 4, 6 and 8. In general, linear relationships are observed, provided that a series of surfactants behaves normally. The work conducted here demonstrates that log k' from RP-HPLC could be used for prediction of log CMC and pC_{20}, even though there are limitations. But experimental results and thermodynamic considerations show no direct relationship can be written between m/m' (slopes in equations (1-25) and (1-7)) and CMC/C_{20}, m/m' and $\Delta G^{\circ}_{mic}/\Delta G^{\circ}_{ad}$ (see Chapter 8).

The other objective of the research is to study the chromatographic behavior of these homologous series of surfactants. This is discussed in Chapters 3, 5 and 7. Reversed-phase ion-interaction methodology has proven to be very useful for the separation of ionic surfactants which exhibit both hydrophobic and hydrophilic characteristics. Optimum separation conditions and retention mechanisms were studied. The calculated thermodynamic parameters (ΔG°, ΔH° and ΔS°) and equilibrium considerations were used to explain the mechanisms. The results give a better understanding of the retention process.

Chapter 2

Ion-Interaction Chromatography of Surfactants

2.1 Introduction

In reversed-phase chromatography, ionic species generally have little or no retention on the hydrophobic stationary phase and are eluted as an unresolved mixture. Addition to the mobile phase of a reagent ion with the opposite charge to the analyte ion can improve the retention of the ionic compound by effectively neutralizing the ionic charge. This added ion is referred to as an ion-interaction reagent or an ion-pairing reagent. This chromatographic process is called ion-interaction, or ion-pair, chromatography[16]. Ion-interaction chromatography is valuable for the separation of ionized and weakly ionized compounds.

The early work was done by Eksbory and Schill during the 1970s[17]. They were the first to apply ion-pair extraction techniques to modern liquid chromatography in both the normal- and reversed-phase mode[18]. In early studies of normal-phase chromatography the stationary phases were silica or cellulose column packings coated with a buffered aqueous solution which contained the ion-pairing reagent; and a relatively nonpolar

organic solvent was used as the mobile phase. The main limitation in the application of normal phase systems to ionic compounds is that the sample must be dissolved in the organic solvent prior to analysis. Early reversed-phase used an aqueous buffer containing a low concentration of an ion-pairing reagent as the mobile phase. A relatively nonpolar solvent, coated onto an inert support, served as the stationary phase. Reversed-phase ion-interaction chromatography quickly gained acceptance as a separation method. But both systems had problems with instability because of the leaching of the stationary liquid phase from its support[18]. Today, these problems have been overcome with the development of chemically bonded phases.

Many other workers expanded on this technique[19-23] and demonstrated its ability to separate a wide range of compounds. Ion-interaction chromatography can simultaneously separate samples containing neutral and ionized molecules. It uses conventional liquid chromatographic columns to provide greater versatility than fixed-site ion exchanger columns, and does not require any special or modified equipment.

Ion-interaction chromatography uses secondary chemical equilibria to control retention and selectivity in liquid chromatography. Several theoretical models, such as ion-pair, dynamic ion-exchange, electrostatic-interaction, and ion-interaction, have been proposed to describe the retention mechanism in reversed-phase liquid chromatography[24-26]:

The ion-pair model assumes that an ion pair is formed in the mobile phase prior to the sorption of the analyte onto the stationary phase. The solute capacity factor is governed by the equilibrium constants for ion-pair formation in the mobile phase, extraction of the ion-pair onto the stationary phase, and the dissociation of the ion-pair on the stationary phase. This model is successful at explaining retention in liquid-liquid chromatographic systems but it is somewhat limited when applied to chemically bonded phases.

The dynamic ion-exchange model assumes that the ion-pairing reagent is reversibly adsorbed onto the stationary phase through hydrophobic interaction. A dynamic ion exchanger is formed. Then the solute ion exchanges with the counterion of the ion-interaction reagent which is adsorbed onto the stationary phase. This process is combined with the equilibria for dissociation of the analyte ions in the mobile phase and the electrostatic interaction between the analyte ion and the ion-interaction reagent on the stationary phase. Here, the retention of ionic solutes is governed mainly by ionic interactions.

The electrostatic model is the most versatile but is mathematically complex and not very intuitive. This model assumes the formation of a surface potential between the bulk mobile phase and the stationary phase, which is caused by adsorption of ions onto the stationary phase. When the concentration of an ion-interaction reagent is varied, the

retention of the analyte will change because the surface potential changes.

The ion-interaction model can be described as an intermediate between the ion-pair model and the dynamic ion-exchange model, but does not require ion-pair formation and is not based on the ion-exchange. This model assumes a dynamic adsorption equilibrium of the ion-interaction ion on the stationary phase surface. The retention of the sample ion is due to the interaction, electrostatic and hydrophobic, with ion-interaction reagent and an additional hydrophobic interaction with the nonpolar stationary surface.

An additional advantage of ion-interaction chromatography is that it can provide a method of indirect detection for analytes lacking suitable chromophores or other properties commonly used for detection[27]. A constant concentration of a detectable ion is added to the mobile phase. It is distributed between the mobile phase and the stationary phase. This ion provides a fixed detector response. As analytes are eluted, the detector response will change as a result of their influence on the distribution of the detectable ion in the chromatographic system.

2.2 Related RP-HPLC Studies of Surfactants Using Ion-Interaction Chromatography

2.2.1 Analysis of alkanesulfonates

Alkanesulfonates, $C_nH_{2n+1}SO_3Na$, are one of the simplest types of anionic surfactants. They have high biodegradability if alkyl chains are straight and low toxicity. Most methods developed for the analysis of these compounds use reversed-phase ion-interaction chromatography on C_8 or C_{18} packings. Anion exchange columns are occasionally used for lower molecular weight products.

In the RP-HPLC analysis of alkanesulfonates, an ion-interaction reagent is added to the mobile phase. If indirect photometric detection is used then the ion-interaction reagent is chosen for its optical absorption characteristics. The ion-interaction occurs between the anionic surfactant and the cationic ion-interaction reagent. This interaction alters the retention behavior of alkanesulfonates and provides indirect detection when needed. A comprehensive review of HPLC analysis of anionic surfactants by Schmitt[28] has provided broad information on various HPLC separation methods. Since our attention is on RP-HPLC, part of our literature search results of RP-HPLC analysis of alkanesulfonates are shown in Table 2-1.

Table 2-1 RP-HPLC analysis of alkanesulfonates

Column	Mobile phase	Detector	Ref.
Merck LiChrosorb RP-8, 250 x 4.6 mm	Methanol/water, 1 x 10^{-2} *M* tetrabutylammonium sulfate	Refractive index	[29]
Waters μBondapak C_{18}, 300 x 3.9 mm	Methanol/water, 2 x 10^{-4} *M* cetylpyridinium chloride, pH 4.45, phosphate buffer	Indirect UV, 254 nm	[30]
Shandon reversed-phase, Hypersil SAS or Hypersil ODS, 150 x 4.6 mm	Acetone/water/NaH_2PO_4	Postcolumn reaction, extraction, and fluorescence detection	[31]
Altex Ultrasphere RP-18, 250 x 10 mm	Methanol/water, 1.1 x 10^{-3} *M* HNO_3	Moving-wire flame ionization detector	[10][32]
Merck LiChrosorb RP-8 or Shandon Hypersil ODS, 200 x 4.6 mm, 40°C	Gradient, methanol/water, 2.5 x 10^{-4} *M* in *N*-methylpyridinium chloride	Indirect UV, 260 nm	[33][34]

Table 2-1 (Continued)

Column	Mobile phase	Detector	Ref.
Hamilton polystyrene-divinylbenzene PRP-1, 250 x 4.1 mm	80:20 methanol/5 x 10^{-2} *M* aqueous ammonium acetate	ICAP detection of sulfur	[35]
Unspecified C18, 250 x 2 mm, 40°C	Gradient, THF/Water	Evaporative light scattering	[36]
Macherey-Nagel Nucleosil C18, 250 x 4 mm	90:10 or 80:20 methanol/water, containing 0.25 *M* $NaClO_4$	Refractive index	[37]
Hamilton polystyrene-divinylbenzene PRP-1, 50 x 4.1 mm	Acetonitrile/water, 10^{-4} *M* in iron(II) 1,10-phenanthroline salts, pH 6.0 adjusted with citrate or acetate buffer	Indirect visible, 510 nm	[38]
Unspecified alkyl coated packing, 150 x 4.6 mm	Methanol/water, containing 1 x 10^{-3} *M* NaH_2PO_4	Conductivity	[39]

2.2.2 Analysis of aromatic quaternary ammonium salts

Cationic surfactants are useful as fabric softeners, corrosion inhibitors, and antimicrobial agents. Benzylalkyldimethylammonium salts are one of the commonly used types of cationic surfactants.

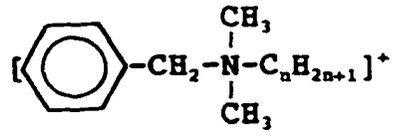

They are used as germicides, disinfectants, and sanitizers.

Aromatic quaternary ammonium salts can be analyzed by RP-HPLC using the ion-interaction method. Direct UV detection is suitable for these surfactants. A comprehensive review of HPLC analysis of cationic surfactants has been given by Schmitt[40]. Table 2-2 lists some details of RP-HPLC analysis of benzylalkyldimethylammonium salts.

Table 2-2 RP-HPLC analysis of benzylalkyldimethylammonium salts

Column	Mobile phase	Detector	Ref.
Hitachi Gel 3011 polystyrene-divinylbenzene, 500 x 4 mm	Methanol, 0.5 *M* $HClO_4$	UV, 220 nm	[41]
Waters μBondapak CN, 300 x 4.6 mm	60:40 acetonitrile/0.1 *M* aqueous sodium acetate, pH 5.0 adjusted with acetic acid	UV, 254 nm	[42]
Toyo Soda TSK Gel LS410 ODS/silica, 250 x 4 mm, 50 °C	85:15 methanol/0.4 *M* aqueous NaCl	UV, 210 nm	[43]
Toyo Soda TSK Gel LS410 ODS/silica, 200 x 6 mm, 50°C	85:15 methanol/1.0 *M* aqueous $NaClO_4$, pH 2.5 adjusted with H_3PO_4 (or 0.1 *M* aqueous $NaClO_4$, pH 3.5)	Refractive index	[44]

Table 2-2 (Continued)

Column	Mobile phase	Detector	Ref.
Various C18, phenyl and CN, 250 x 4.6 mm	Water/methanol, or acetonitrile, or THF, with 0.05-0.25 *M* ClO_4^-	UV, 215 nm	[45]
ß-cyclodextrin, 250 x 4.6 mm	70:30 water/acetonitrile or 50:50 water/methanol, 0.1 *M* various electrolytes, pH 3.3 adjusted with H_3PO_4	UV, 215 nm	[46]
Waters µBondapak CN, 150 x 4 mm	58:33:9 water (pH 2.2 adjusted with $HClO_4$)/ acetonitrile/2-propanol or 51:34:15 water (pH 2.2)/ acetonitrile/THF	UV, 214 nm	[47]

2.2.3 Analysis of nonaromatic quaternary ammonium salts

Ion-interaction RP-HPLC with indirect photometric detection can be used for the analysis of nonaromatic quaternary ammonium salts. An ion-interaction reagent with a UV chromophore is needed. Table 2-3 gives some examples of RP-HPLC analysis of fatty quaternary ammonium salts, which serve as the reference for our study of the nonaromatic quaternary ammonium geminis.

Table 2-3 RP-HPLC analysis of fatty quaternary ammonium salts

Column	Mobile phase	Detector	Ref.
Waters μBondapak Phenyl	3×10^{-4} *M* 1-phenethyl-2-picolinium ion in pH 4.6 acetate buffer	Indirect UV, 254 nm	[48]
Toyo Soda TSK Gel LS410 ODS/silica, 200 x 6 mm, 50°C	85:15 methanol/1.0 *M* aqueous $NaClO_4$, pH 2.5 adjusted with H_3PO_4 (or 0.1 *M* aqueous $NaClO_4$, pH 3.5)	Refractive index	[44]
Macherey-Nagel Nucleosil CN, 120 x 4.6 mm	55:45 methanol/water, 5×10^{-3} *M* *p*-toluenesulfonic acid	Indirect UV, 254 nm	[49]
Shandon Hypersil C8, 150 x 4.6 mm	60:60:5 methanol/acetonitrile/water, 5×10^{-2} *M* sodium carbonate and 1×10^{-1} *M* sodium bicarbonate	Postcolumn reaction	[50]

Table 2-3 (Continued)

Column	Mobile phase	Detector	Ref.
DuPont Zorbax C8, 250 x 4.6 mm or Alltech Nucleosil CN, 150 x 4.6 mm	25:75 methanol/water, 5×10^{-3} *M* *p*-toluenesulfonic acid	Indirect UV, 260 nm	[51]
Polymer Laboratories PLRP-S polystyrene-divinylbenzene, 250 x 4.6 mm	60:38:2 acetonitrile/water/ acetic acid, 5×10^{-3} *M* sodium *p*-xylenesulfonate	Indirect UV, 262 nm	[52]
Novapak CN, 100 x 8 mm	Methanol/water, 1×10^{-2} *M* to 5×10^{-2} *M* benzenesulfonic acid	Refractive index	[53]

2.3 Surfactants Studied in This Work

2.3.1 Alkanesulfonates

The ion-interaction reagent, dodecylpyridinium bromide, with indirect UV detection was used for the analysis of alkanesulfonates, $C_nH_{2n+1}SO_3^-$, (Chapter 3). The long hydrophobic chain of this reagent enhances its interaction with the hydrocarbon stationary phase and the pyridinium group provided a strong chromophore.

2.3.2 Gemini surfactants

As mentioned in Chapter 1, an important part of this work was the analysis of the following series of gemini surfactants. These have been synthesized by the Surfactant Research Institute at Brooklyn College. To our knowledge, the RP-HPLC analysis of these geminis has not appeared in the literature.

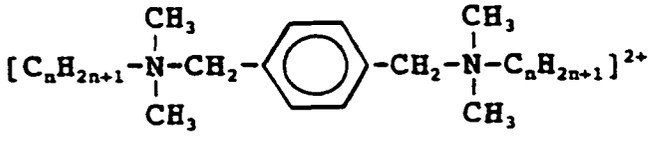

$(C_nN)_2Ar$

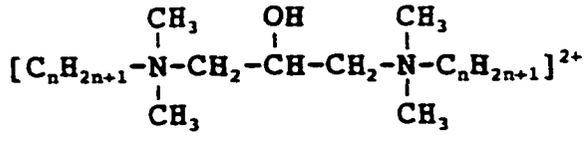

$(C_nN)_2OH$

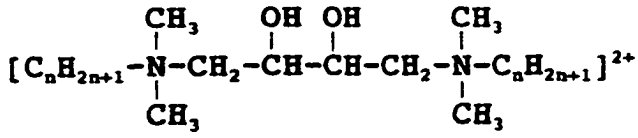

$(C_nN)_2(OH)_2$

Sodium perchlorate provided a suitable ion-interaction reagent in the analysis of the aromatic quaternary ammonium gemini surfactants, $(C_nN)_2Ar$, (Chapter 5). The perchlorate ion effectively interacts with the positively charged analyte ion and improves the separation.

Sodium *p*-toluenesulfonate and *p*-toluenesulfonic acid were used for the analysis of the nonaromatic quaternary ammonium gemini surfactants, $(C_nN)_2OH$ and $(C_nN)_2(OH)_2$, (Chapter 7). These ion-interaction reagents neutralize the charge of the analyte and enhance the interaction between the analyte and the hydrocarbon stationary phase. The aromatic group of these compounds provided a good probe for indirect UV detection.

Chapter 3

Chromatography of Alkanesulfonates

3.1 Introduction

As reviewed in Section 2.2.1, various reversed-phase packing materials, such as C8, C18, and polystyrenedivinylbenzene, have been applied to RP-HPLC analysis of alkanesulfonates. Mobile phases were often methanol-water or acetonitrile-water in combination with ion-interaction reagents. Since alkanesulfonates do not absorb in the UV region, various detection methods have been used including indirect UV, refractive index, postcolumn reaction, conductivity, and evaporative light scattering.

In order to become familiar with the technique of the ion-interaction RP-HPLC and to confirm the correlation of log k' with the CMC and pC_{20}, a series of alkanesulfonates were chromatographed. The experiments were carried out using 3x3 C18 columns (33 x 4.6 mm), methanol-water mobile phases, and a UV diode array detector. The ion-interaction reagent was dodecylpyridinium (DDP) bromide.

The 3x3 column is also called the high-speed column. Compared with commonly used longer columns (150 mm to 250 mm

in length, 4.6 mm ID, 5 μm particles) in the reviewed publications (Section 2.2.1), the 3x3 column decreases the separation time and requires less solvent. The price of the short column is about 1/5 to 1/3 of a 150 x 4.6 mm column packed with the similar material[54][55]. Therefore, our work provides an economic chromatographic method for the alkanesulfonate analysis based on the length of the straight alkyl chain.

Experiments designed to elucidate the ion-interaction retention mechanism were performed as well. The results suggest that even though oppositely charged ions co-elute, there is no tightly bonded ion-pair.

3.2 Experimental

3.2.1 Instrumentation

The Perkin-Elmer high-performance liquid chromatography system consisted of the following: a Model 250 Binary LC Pump, an ISS 200 Advanced LC Sample Processor, a LC-235 Photo Diode Array Detector, and a PE Nelson Model 1020LC Plus Personal Integrator. A Perkin-Elmer solvent selector was used in conjunction with the pump. The columns were Perkin-Elmer Pecosphere 3x3 C18 cartridge columns (33 x 4.6 mm, 3 μm particles).

A Perkin-Elmer Lambda 3B UV/Vis spectrophotometer with Perkin-Elmer computerized spectroscopy software (PECSS) was used for determining the absorption characteristics of the reagents.

A YSI Model 35 conductance meter was used for conductivity titrations.

3.2.2 Reagents

The series of *n*-alkanesulfonates, $C_nH_{2n+1}SO_3Na$, where n = 6, 8, 10, 12, 14, 17 and 18, and dodecylpyridinium (DDP) bromide were obtained from the Surfactant Research Institute at Brooklyn College. These compounds are the products of Research Plus Laboratories. Methanol and acetonitrile were Fisher Scientific and Sigma-Aldrich HPLC grade. Milli-Q water

was used. All sample solutions and mobile phase solvents were passed through 0.45 μm nylon filters (Sigma-Aldrich) prior to use. High purity grade helium gas from Prest-O-Sales was used for degassing.

3.2.3 Procedure

A homologous series of *n*-alkanesulfonates (C_6, C_8, C_{10}, C_{14}, C_{17}, and C_{18}) were chromatographed on 3x3 C18 columns at ambient temperature using various methanol-water mobile phase compositions. Dodecylpyridinium bromide (0.2 mM) was added to the mobile phase as an ion-interaction reagent and for indirect detection as well. Both isocratic and gradient conditions were used. Samples were dissolved in the mobile phases (0.5 mg/L in most experiments). Before each run the column was flushed with mobile phase for several minutes until equilibrium was reached as indicated by a stable pump pressure and a plateau detector baseline caused by UV absorption of the dodecylpyridinium ion. The UV detection was set at 255 nm. Various mobile phase compositions (from 55:45 CH_3OH:H_2O to 80:20 CH_3OH:H_2O) were tried in order to find the best chromatographic condition.

3.3 Results and Discussion

Typically, data were obtained for the individual surfactants. But mixtures of C_6, C_8, C_{10}, C_{14}, C_{17}, and C_{18} alkanesulfonates were analyzed to demonstrate the possibility of using a short column to separate them in a reasonable period of time. There is no dodecanesulfonate data, because its solubility is very low in the presence of dodecylpyridinium bromide. They both have a C_{12} alkyl group but carry opposite charges which leads to a strong interaction between them.

The chromatographic data are in Table 3-1. The data include the results of series of experiments in which the mobile phase composition and flow rate were varied. The number of data points (# of data) and the standard deviation (Stdev) of the log k' values are also shown in the table. The k' should be independent of the flow rate. The slight variation in log k' values from different flow rates may be caused by the change in the ambient temperature. The summary in the table is the average log k' over all data obtained at different flow rates but the same mobile phase composition. For clarity, these average log k' values are provided in Table 3-2.

Table 3-1 Chromatographic data of alkanesulfonates

Mobile phase: CH_3OH/H_2O + 0.2 m*M* dodecylpyridinium bromide
Temperature: ambient

$CH_3OH:H_2O$ (*V*:*V*)	Flow rate (mL/min)		C_6	C_8	C_{10}	C_{14}	C_{17}	C_{18}
55:45	1.0	# of data	1	-	-	-	-	-
		log *k'*	0.84	-	-	-	-	-
60:40	1.0	# of data	11	-	1	-	-	-
		log *k'*(avg.)	0.43	-	1.58	-	-	-
		Stdev	5.4E-2	-	-	-	-	-
	2.0	# of data	23	16	11	2	-	-
		log *k'*(avg.)	0.39	0.88	1.41	2.19	-	-
		Stdev	3.1E-2	3.3E-2	4.1E-2	8.7E-3	-	-
	Summary	log *k'*(avg.)	0.40	0.88	1.42	2.19	-	-
		Stdev	4.0E-2	3.3E-2	6.4E-2	8.7E-3	-	-

Table 3-1 (Continued)

$CH_3OH:H_2O$ (V:V)	Flow rate (mL/min)		C_6	C_8	C_{10}	C_{14}	C_{17}	C_{18}
65:35	1.5	# of data	1	1	-	-	-	-
		log k'	0.02	0.47	-	-	-	-
	2.0	# of data	3	3	4	1	-	-
		log k'(avg.)	0.01	0.37	0.87	1.85	-	-
		Stdev	3.0E-2	2.8E-2	8.6E-2	-	-	-
	Summary	log k'(avg.)	0.01	0.39	0.87	1.85	-	-
		Stdev	3.0E-2	5.6E-2	8.6E-2	-	-	-
70:30	1.0	# of data	4	-	4	4	-	-
		log k'(avg.)	-0.33	-	0.56	1.49	-	-
		Stdev	0.0E+0	-	1.9E-3	6.4E-3	-	-
	1.5	# of data	3	-	4	3	-	-
		log k'(avg.)	-0.38	-	0.47	1.41	-	-
		Stdev	4.0E-2	-	5.6E-2	7.8E-2	-	-
	2.0	# of data	14	5	13	11	4	-
		log k'(avg.)	-0.31	0.06	0.48	1.38	2.10	-
		Stdev	1.9E-2	2.3E-2	5.2E-2	6.6E-2	7.1E-2	-
	Summary	log k'(avg.)	-0.31	0.06	0.49	1.41	2.10	-
		Stdev	3.2E-2	2.3E-2	5.6E-2	7.4E-2	7.1E-2	-

Table 3-1 (Continued)

$CH_3OH:H_2O$ (V:V)	Flow rate (mL/min)		C_6	C_8	C_{10}	C_{14}	C_{17}	C_{18}
73:27	1.0	# of data	1	1	1	1	1	-
		log k'	-0.51	-0.09	0.32	1.15	1.79	-
	2.0	# of data	3	2	3	4	7	7
		log k'(avg.)	-0.44	-0.11	0.27	1.09	1.74	1.93
		Stdev	7.2E-2	0.00E+0	7.5E-3	5.9E-2	7.3E-2	7.6E-2
	Summary	log k'(avg.)	-0.46	-0.10	0.28	1.10	1.75	1.93
		Stdev	7.1E-2	8.8E-3	2.9E-2	6.0E-2	6.9E-2	7.6E-2
75:25	1.0	# of data	2	-	2	2	-	-
		log k'(avg.)	-0.78	-	0.09	0.94	-	-
		Stdev	0.0E+0	-	6.9E-3	2.9E-3	-	-
	2.0	# of data	-	-	-	-	1	-
		log k'	-	-	-	-	1.50	-
	Summary	log k'(avg.)	-0.78	-	0.09	0.94	1.5	-
		Stdev	0.0E+0	-	1.0E-2	0.0E+0	-	-

Table 3-1 (Continued)

$CH_3OH:H_2O$ (V:V)	Flow rate (mL/min)		C_6	C_8	C_{10}	C_{14}	C_{17}	C_{18}
80:20	1.0	# of data	1	-	1	1	-	-
		log k'	-1.24	-	-0.37	0.42	-	-
	2.0	# of data	-	-	-	-	1	-
		log k'	-	-	-	-	0.93	-
	Summary	log k'	-1.24	-	-0.37	0.42	0.93	-

Table 3-2 Summary of log k' of alkanesulfonates

Mobile phase: CH_3OH/H_2O + 0.2 *mM* dodecylpyridinium bromide
Temperature: ambient

$CH_3OH:H_2O$ (*V:V*)	C_6	C_8	C_{10}	C_{14}	C_{17}	C_{18}
60:40	0.40	0.88	1.42	2.19	-	-
65:35	0.01	0.39	0.87	1.85	-	-
70:30	-0.31	0.06	0.49	1.41	2.10	-
73:27	-0.46	-0.10	0.28	1.10	1.75	1.93
75:25	-0.78	-	0.09	0.94	1.50	-
80:20	-1.24	-	-0.37	0.42	0.93	-

3.3.1 log k', the number of carbon atoms, and the mobile phase composition

The data in Table 3-2 are shown graphically in Figure 3-1 which is a plot of log k' vs. the number of carbon atoms in the straight-chain. The linear relationship contained in the Martin Rule is observed.

$$\log k' = a + bN \qquad (1\text{-}7)$$

The log k' increases about 0.20 to 0.23 (slope b in equation (1-7)) per carbon atom. The intercept, however, decreases with an increase in the solvent strength (methanol percentage).

Figure 3-2 is the plot of log k' vs. CH_3OH volume fraction for alkanesulfonates. The plots are linear in the range of 60% to 80% methanol. This figure indicates log k' decreases about 0.8 to 0.9 with each 10% increase in CH_3OH volume fraction under the experimental conditions. In Figure 3-2 the slope of the C_{17} line is slightly off the trend from the other members. This might be attributable to the fact that data for this compound could only be obtained over a smaller methanol volume fraction range.

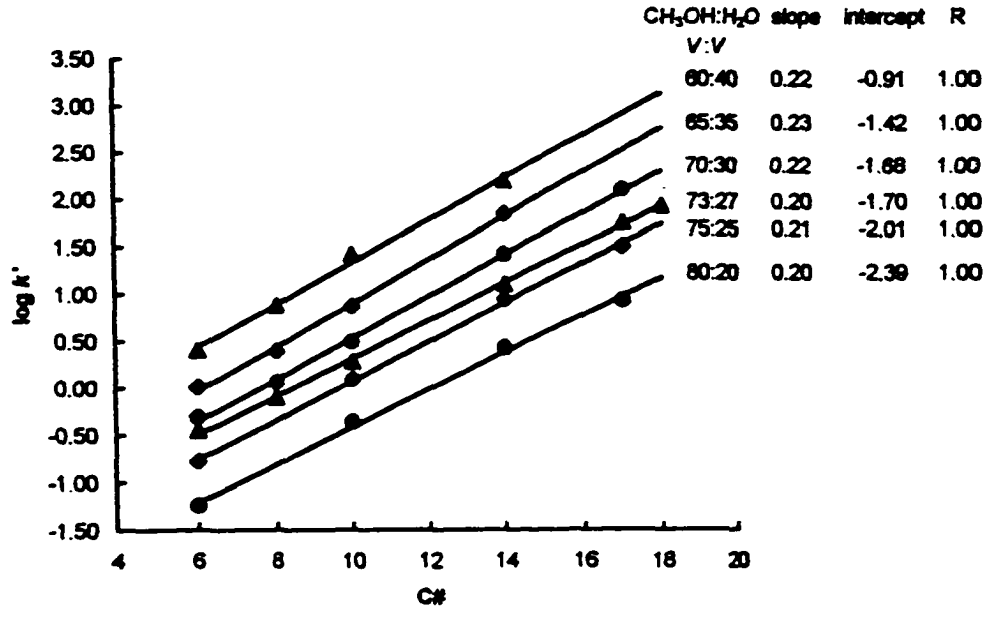

Figure 3-1 log k' vs. carbon number of $C_nH_{2n+1}SO_3Na$ (CH_3OH/H_2O + 0.2 mM dodecylpyridinium bromide, ambient temperature)

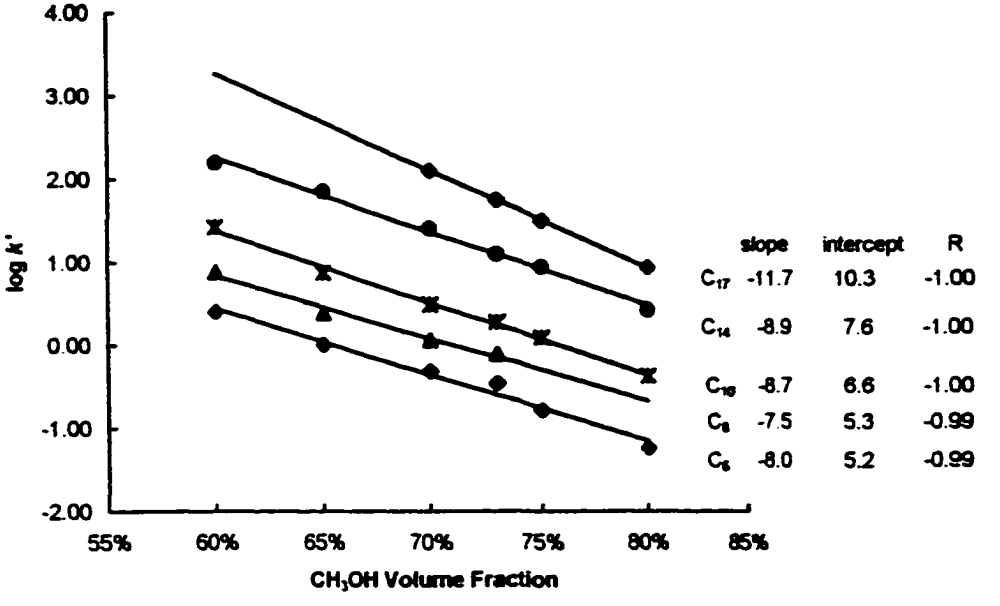

Figure 3-2 log *k'* vs. CH_3OH volume fraction in chromatography of $C_nH_{2n+1}SO_3Na$ (CH_3OH/H_2O, 0.2 m*M* dodecylpyridinium bromide, ambient temperature)

3.3.2 Separation of alkanesulfonates

Figures 3-3, 3-4, and 3-5 present some chromatograms of alkanesulfonates. Typically the impurities in a surfactant will be the adjacent upper and lower members in the series. For three adjacent members, baseline separation could be obtained with 33 x 4.6 mm C18 column and using the dodecylpyridinium ion as the ion-interaction and indirect detection reagent. The lower carbon number surfactants (C_6, C_8 and C_{10}) in the series can be well separated using a 60:40 or 65:35 CH_3OH:H_2O solvent. The middle ones can be separated with about 70:30 CH_3OH:H_2O mobile phase. A 75:25 CH_3OH:H_2O or higher CH_3OH% solvent is good for higher molecular weight alkanesulfonates (C_{16}, C_{17} and C_{18}).

There are two positive and negative peaks appearing at the beginning of each chromatogram. The first one occurs upon injection, and appears as a positive or negative peak. Its retention time is used as t_m in the equation (1-6) for k' calculations. The second peak has the same retention time as the dodecylpyridinium ion and is discussed in Section 3.4.1.

The variations in the peak areas between each replicated run are less than 5% at ambient temperature.

The gradient method was tested. The change of the solvent composition readjusts the adsorption equilibrium of the ion interaction reagent in the column. This causes a large baseline shift during the chromatographic run.

Therefore the isocratic method is more suitable for the indirect detection with a strong background adsorption.

The limit of quantitative measurement and the linear range were not studied. The lowest concentration used in the experiments is approximately 0.6 m*M* (0.15 mg/mL, 3 x 10^{-9} moles of the sample for injection of 5 μL). From chromatograms in Figures 3-3 to 3-5 one can estimate that the detection limit is lower than this value. The upper concentration limit for chromatography is restricted by the low solubility of alkanesulfonates in the presence of dodecylpyridinium ions.

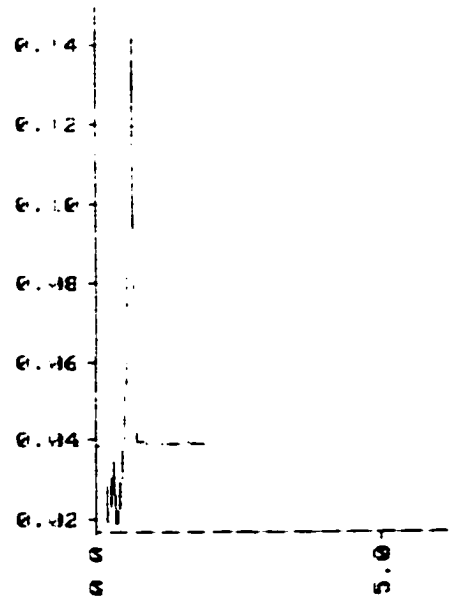

(a) C_6(0.5 mg/mL)

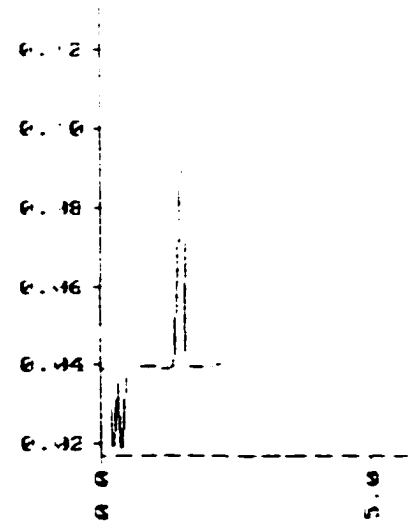

(b) C_8(0.5 mg/mL)

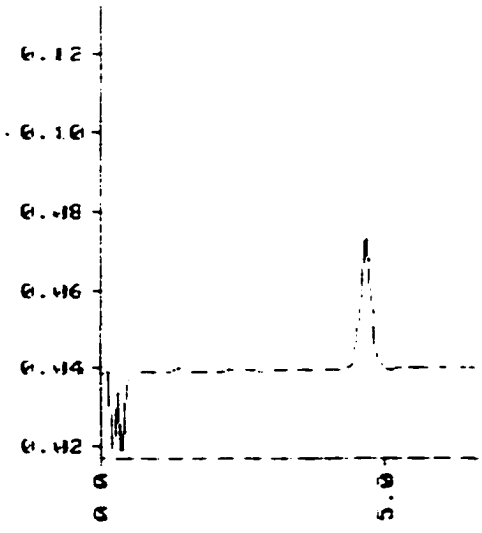

(c) C_{10}(0.5 mg/mL)

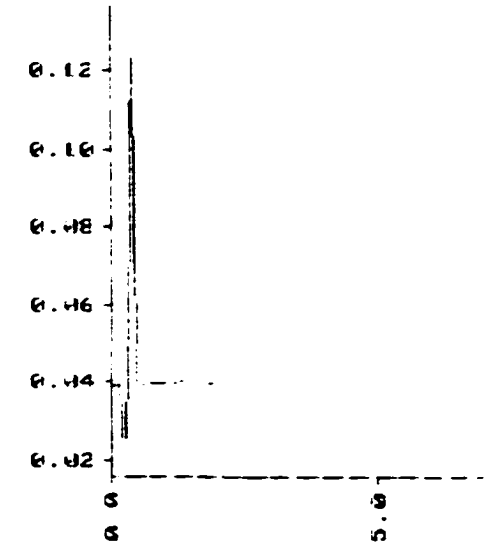

(d) DDP(0.5 mg/mL)

Figure 3-3 Chromatograms of alkanesulfonates with 60% CH_3OH in mobile phase

Mobile phase:	60% CH_3OH, 40% H_2O, 0.2 mM DDP
UV detection:	255 nm
Flow rate:	2.0 mL/min
Column:	3x3 C18 (33 x 4.6 mm)
Injection Volume:	3 μL
Temperature:	ambient

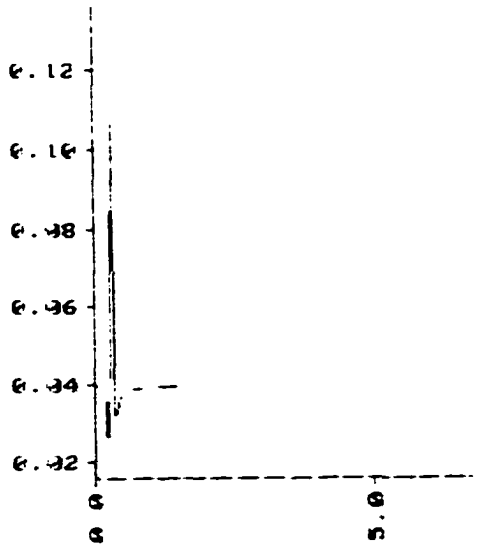

(a) C_6(0.5 mg/mL)

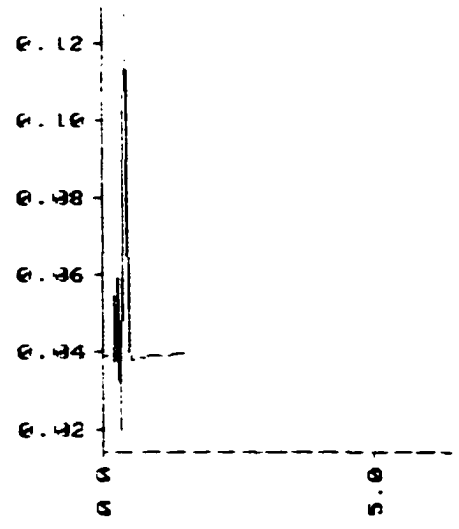

(b) C_8(0.5 mg/mL)

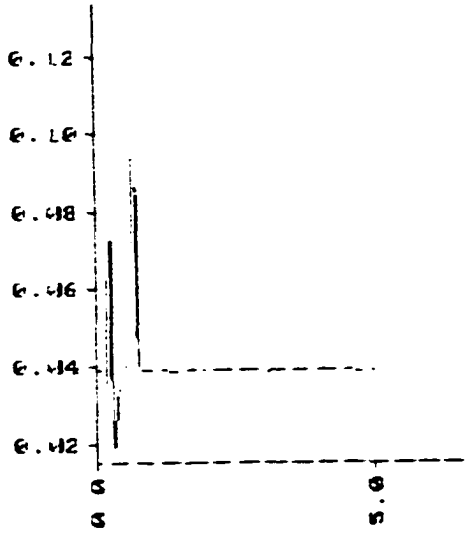

(c) C_{10}(0.5 mg/mL)

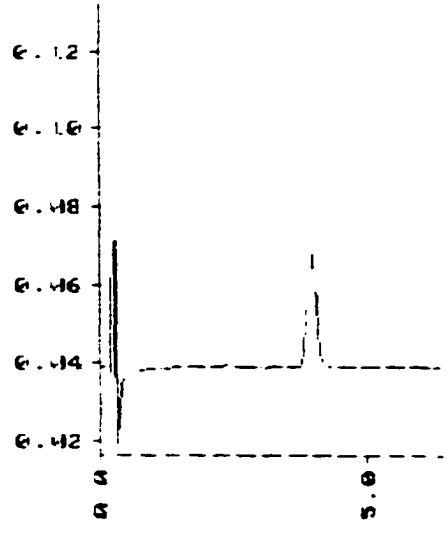

(d) C_{14}(0.5 mg/mL)

Figure 3-4 Chromatograms of alkanesulfonates with 70% CH_3OH in mobile phase

Mobile phase:	70% CH_3OH, 30% H_2O, 0.2 m*M* DDP
UV detection:	255 nm
Flow rate:	2.0 mL/min
Column:	3x3 C18 (33 x 4.6 mm)
Injection Volume:	3 μL
Temperature:	ambient

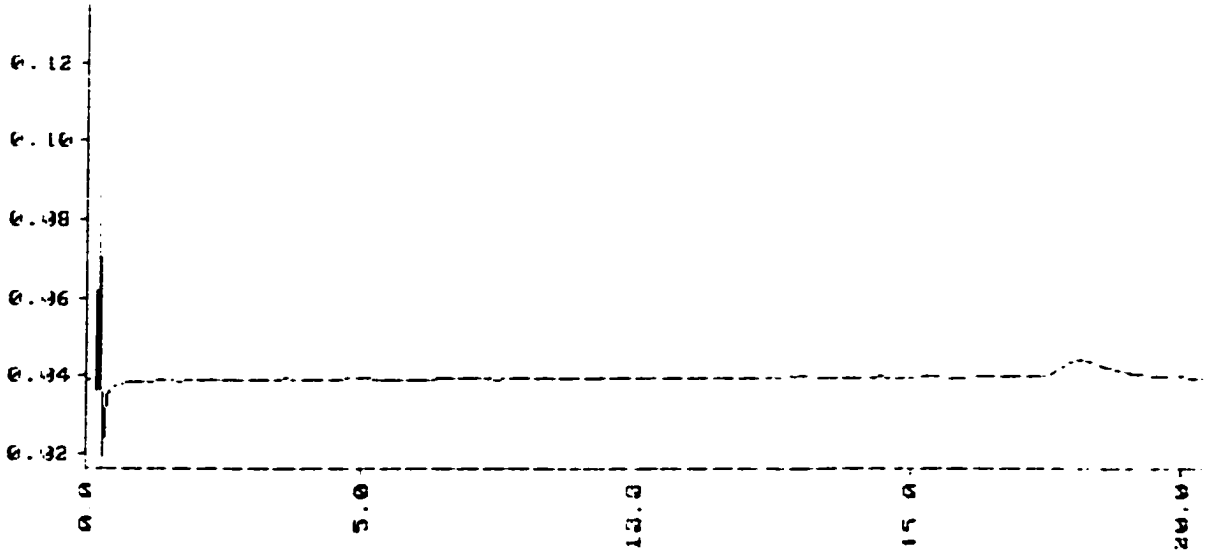

(e) C_{17}(0.5 mg/mL)

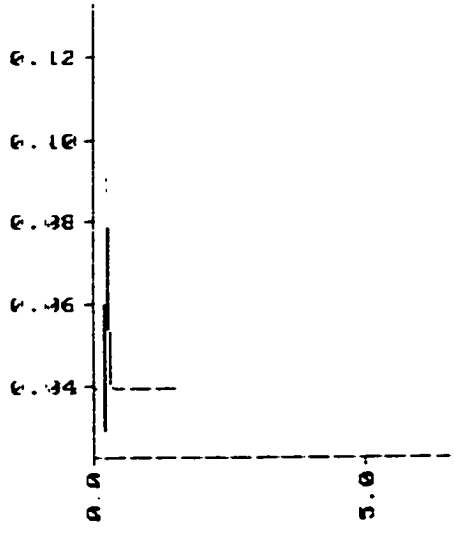

(f) DDP(0.5 mg/mL)

Figure 3-4 (Continued)

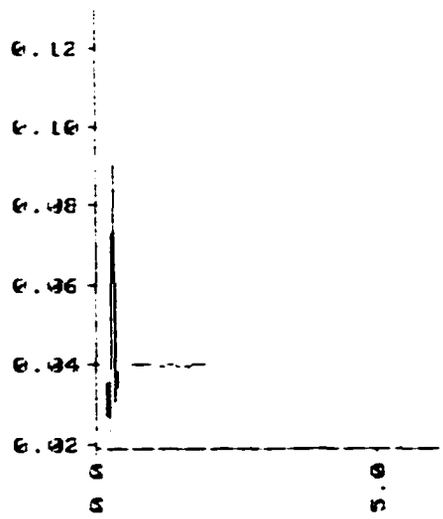

(a) C_6(0.5 mg/mL)

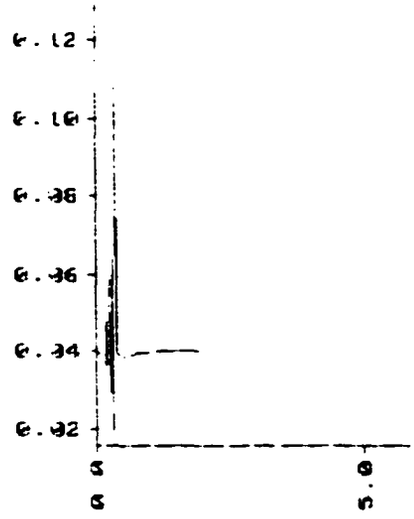

(b) C_8(0.5 mg/mL)

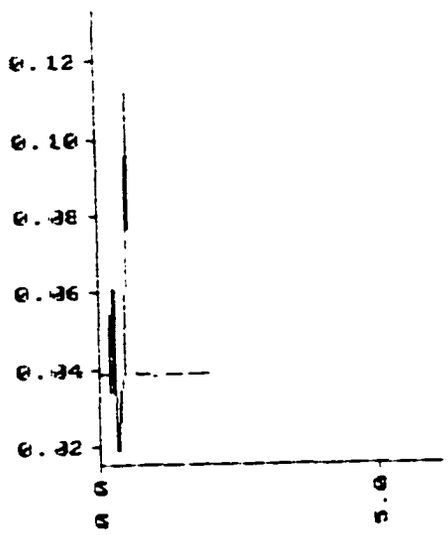

(c) C_{10}(0.5 mg/mL)

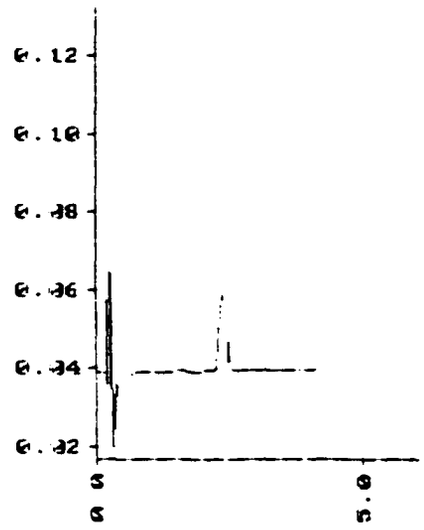

(d) C_{14}(0.5 mg/mL)

Figure 3-5 Chromatograms of alkanesulfonates with 73% CH_3OH in mobile phase

Mobile phase:	73% CH_3OH, 27% H_2O, 0.2 mM DDP
UV detection:	255 nm
Flow rate:	2.0 mL/min
Column:	3x3 C18 (33 x 4.6 mm)
Injection Volume:	2 μL
Temperature:	ambient

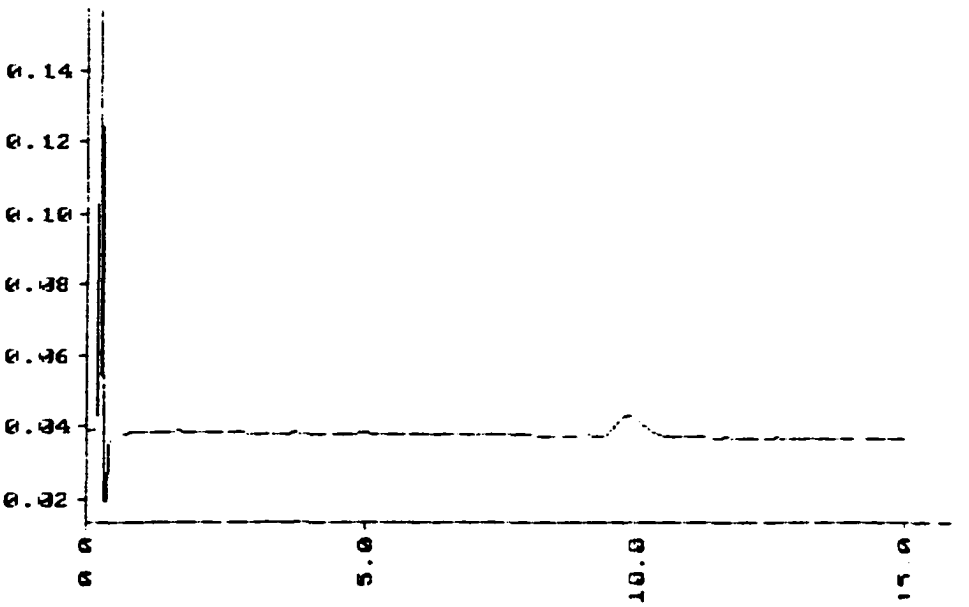

(e) C_{17}(0.25 mg/mL, 4 μL)

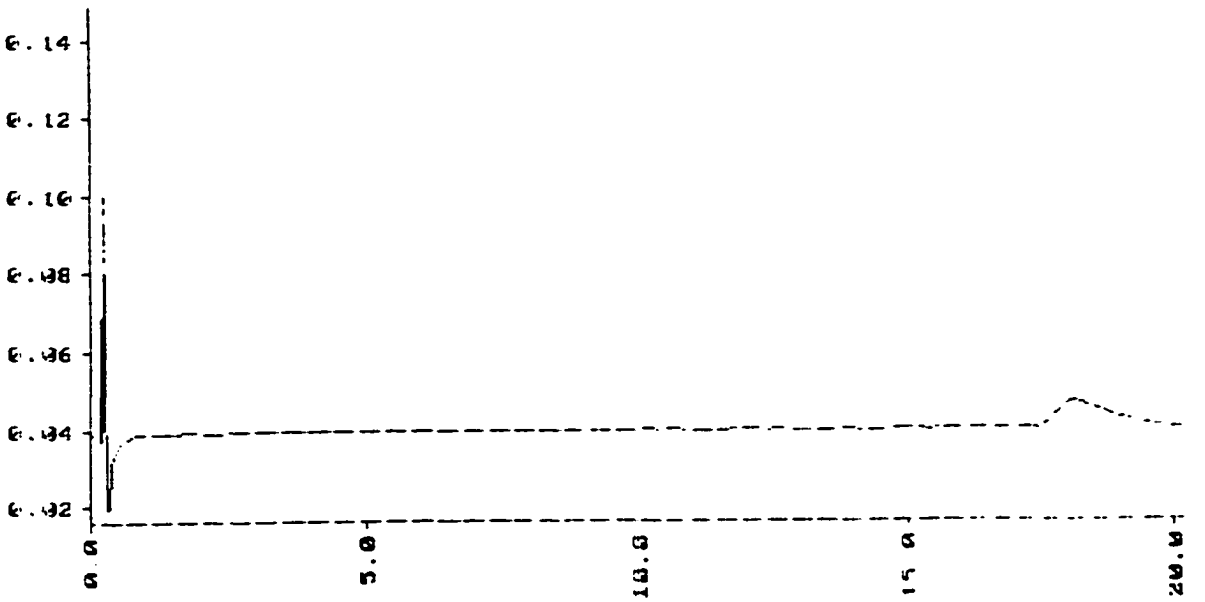

(f) C_{18}(0.50 mg/mL, 5 μL)

Figure 3-5 (Continued)

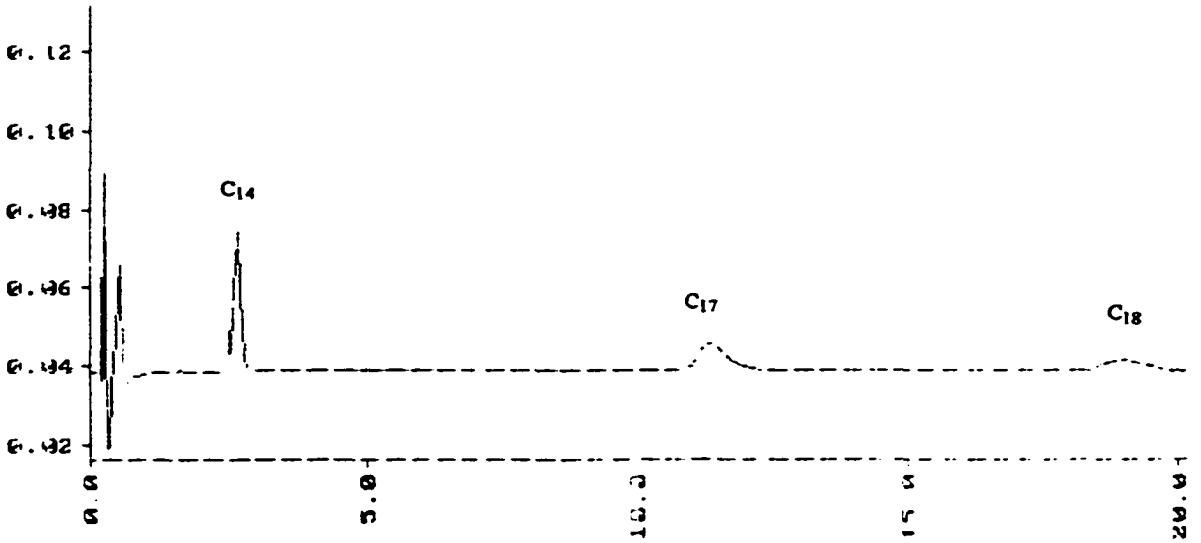

(g) C_6, C_8, C_{10}, C_{14}, C_{17}, and C_{18} Mixture (0.29 mg/mL each, 5 μL)

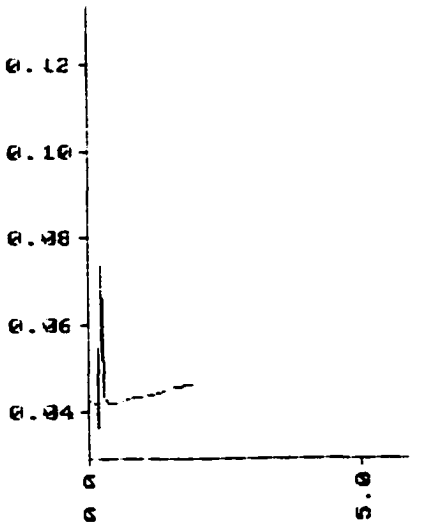

(h) DDP(0.50 mg/mL)

Figure 3-5 (Continued)

3.3.3 Column efficiency

The column efficiency is measured by the number of theoretical plates n and plate height h, or the effective plate number N and effective plate height H, which are calculated using the following equations[56][57].

$$h = \frac{L}{n} \tag{3-1}$$

$$n = 16\left(\frac{t_r}{W}\right)^2 = 5.54\left(\frac{t_r}{W_{h/2}}\right)^2 \tag{3-2}$$

$$H = \frac{L}{N} \tag{3-3}$$

$$N = 16\left(\frac{t_r'}{W}\right)^2 = 5.54\left(\frac{t_r'}{W_{h/2}}\right)^2 \tag{3-4}$$

Where L is the length of the column packing; t_r is the retention time; W is the magnitude of the base of the triangle which is formed by extending the tangents at the inflection points on the two sides of the chromatographic peak to the baseline of the chromatogram; $W_{h/2}$ is the width of the peak at half its maximum height; t_r' is the adjusted retention time. The effective plate number N has better theoretical significance for the early eluting peaks because of the large contribution to the overall retention from the void volume.

Some of n, h, N and H values in this work are listed in Table 3-3 (calculated from chromatograms in Figure 3-3 to

3-5). Data show that when t_r is approaching t_m, N is approaching zero. In the optimum chromatographic condition, the effective plate number N of 33 mm short columns can reach 2500, and the effective plate height H is approximate 0.01 mm. Compared with typical H values of 0.02 - 0.05 mm for 250 mm C18 reversed-phase column with 3 μm particles[57], the column efficiency of the 3x3 short column is pretty good in ion-interaction chromatography.

Table 3-3 *n*, *h*, *N* and *H* values of alkanesulfonate chromatography with 33 x 4.6 mm C18 column

			n	*h* (mm)	*N*	*H* (mm)
Figure 3-3	(a)	C_6	280	0.12	139	0.24
	(b)	C_8	841	0.04	646	0.05
	(c)	C_{10}	2397	0.01	2206	0.01
	(d)	DDP	287	0.21	64	0.52
Figure 3-4	(a)	C_6	355	0.09	16	2.03
	(b)	C_8	279	0.12	53	0.62
	(c)	C_{10}	496	0.07	236	0.14
	(d)	C_{14}	2822	0.01	2517	0.01
	(e)	C_{17}	2007	0.02	1958	0.02
	(f)	DDP	158	0.21	1	30.16
Figure 3-5	(a)	C_6	306	0.11	4	8.11
	(b)	C_8	316	0.10	33	1.00
	(c)	C_{10}	368	0.09	118	0.28
	(d)	C_{14}	1952	0.02	1601	0.02
	(e)	C_{17}	2654	0.01	2532	0.01
	(f)	C_{18}	1731	0.02	1688	0.02
	(h)	DDP	158	0.21	0	120.62

3.4 Separation Mechanism

3.4.1 Ion-interaction mechanism

The ion-interaction mechanism proposed by Bidlingmeyer[26] describes the retention in the column. Figure 3-6 is the schematic diagram of alkanesulfonate retention mechanism.

(1) Before injection of the sample, the surface of the stationary phase is in equilibrium with the mobile phase. The adsorption and desorption equilibria of dodecylpyridinium ions on C18 stationary phase occurs in the primary layer where the ion-interaction reagent coats the surface of the stationary phase. The driving force is the hydrophobic interaction of the alkyl chains. The counterions of the ion-interaction reagent form a secondary layer. There are electrostatic equilibria in both the primary and the secondary layer. Because of the electrostatic repulsions the surface coverage is not high. The bulk eluent contains dodecylpyridinium bromide, and the distribution equilibrium is dynamic.

(2) After injection of the sample, the previous equilibrium is disturbed locally. Alkanesulfonates go into the primary layer and adsorb onto the C18 stationary phase since the surface is not fully covered. The retention is caused by hydrophobic interactions and electrostatic interactions. The hydrophobic interaction involves the alkyl chains in alkanesulfonates, in the C18 stationary phase and in

dodecylpyridinium ions. The electrostatic interaction is due to the ionic groups in the alkanesulfonates and dodecylpyridinium ions. Addition of the negatively charged species to the positively charged primary layer has a net effect of neutralizing the positive charge at this layer. This allows more dodecylpyridinium ions to adsorb in the primary layer if there is still enough accessible surface.

In this process the adsorption of more dodecylpyridinium ions decreases its local concentration in the eluent, and results in the second negative peak in the earlier part of the chromatogram (Figure 3-3 to 3-5, where the first peak is due to the sample injection).

(3) When an alkanesulfonate ion leaves the stationary phase, an excess positive charge is left instantaneously on the surface. The partition equilibrium is disturbed again. Some of dodecylpyridinium ions will leave the surface to reestablish equilibrium. Thus, pairs of ions apparently travel through the column and reach the detector, producing positive UV signals.

The conductivity titrations, UV spectra, detector response calculations, certain chromatographic experiments, and surface coverage calculations support this mechanism. The following sections discuss these in detail.

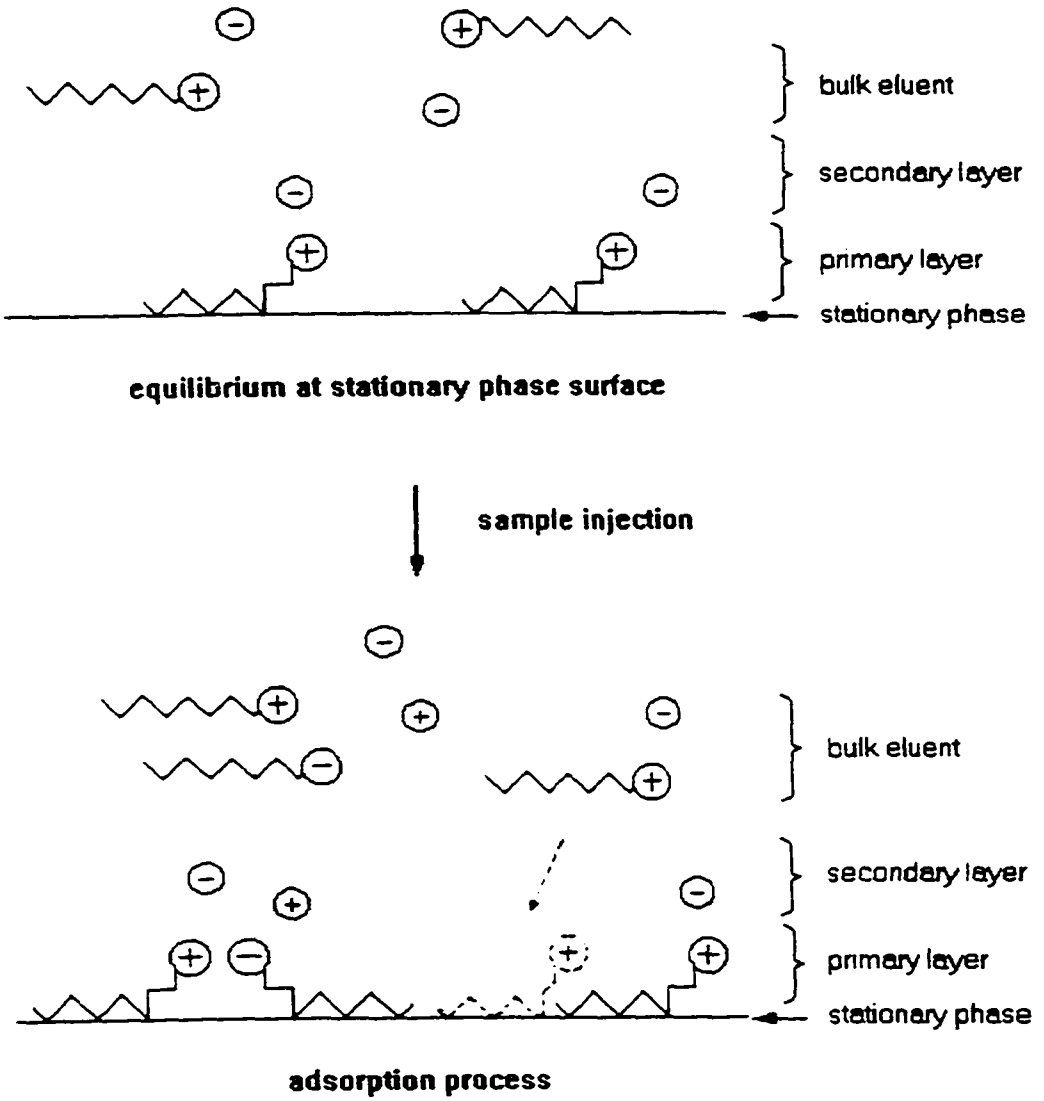

Figure 3-6 Schematic diagram of alkanesulfonate retention mechanism

3.4.2 Conductance titration

The conductance of electrolytic solutions depends on the concentration and nature of the ions (charges and mobilities)[58]. If alkanesulfonate ions and dodecylpyridinium ions formed strongly bonded ion-pairs, there would be an inflection at the equivalence point on the titration curve. Figure 3-7 shows the conductance titration curves, where 100 mL of 0.203 m*M* dodecylpyridinium bromide was titrated with 1.05 m*M* sodium dodecanesulfonate in the 65:35 CH_3OH:H_2O solvent. The equivalent point should be at about 19 mL of sodium dodecanesulfonate, 0.24 m*M* of the total concentration. The titration was carried out below the solubility limit. The curves are smooth with no inflection point.

These two compounds are expected to form strongly bonded 1:1 ion-pairs because they both have C_{12} chains but opposite charges. If ion-pairs had formed, before the equivalence point the concentration of the dodecylpyridinium ion would decrease and at the same time the concentration of Na^+ would increase. The conductance of the solution should increase due to the higher molar conductance of Na^+. After the equivalence point both the dodecanesulfonate ion and Na^+ concentration should increase. The increase of the conductance should be faster than before. However, the plot of the conductivity vs. the total molarity of two salts is a straight line. Therefore the conductance titration gives no evidence of the ion-pair formation.

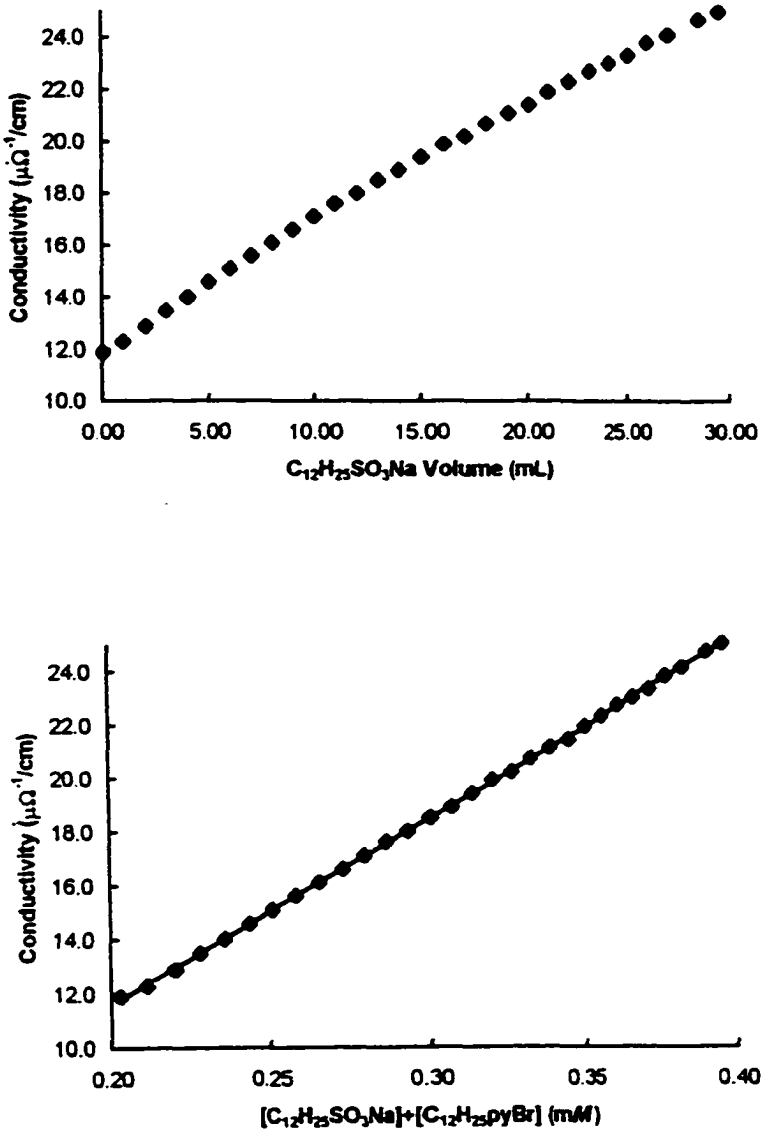

Figure 3-7 Conductance titration
100 mL of 0.203 mM dodecylpyridinium bromide titrated with 1.05 mM sodium dodecanesulfonate in 65:35 $CH_3OH:H_2O$

3.4.3 UV spectra

The electronic transition in a chromophore is affected by structural details[59] and to a lesser extent by the solvent. One would expect that the UV absorption spectrum of the dodecylpyridinium ion would change when it forms an ion-pair with an alkanesulfonate ion. The UV spectra of the following were obtained:

(a) 0.1 m*M* dodecylpyridinium;

(b) 0.1 m*M* dodecylpyridinium + 0.1 m*M* hexanesulfonate;

(c) 0.1 m*M* dodecylpyridinium + 0.1 m*M* decanesulfonate;

(d) 0.1 m*M* dodecylpyridinium + 0.1 m*M* tetradecanesulfonate,

in methanol (Figure 3-8) and water (Figure 3-9).

The results show that different solvents generate different UV spectra, but for the same solvent all UV spectra are exactly the same. Thus the addition of alkanesulfonates to the dodecylpyridinium bromide solution does not change the electronic structure of the dodecylpyridinium ion. The UV spectra suggest there are no strongly bonded ions.

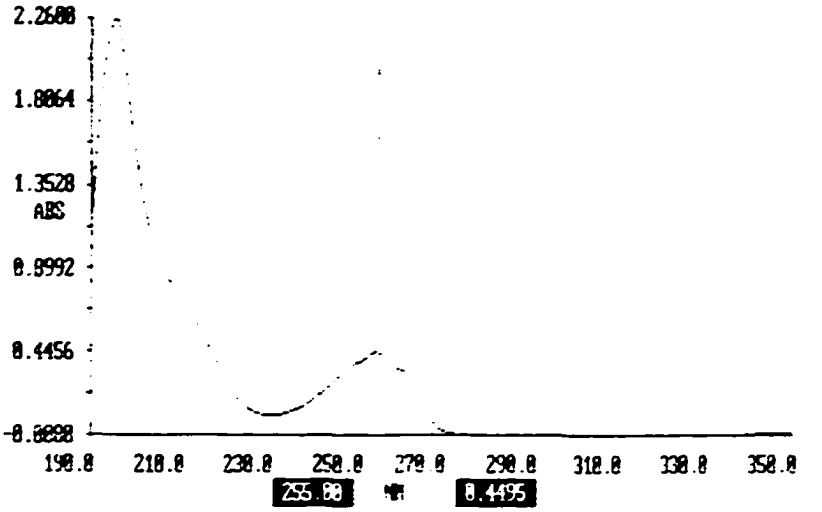

(a) 0.1 m*M* DDP

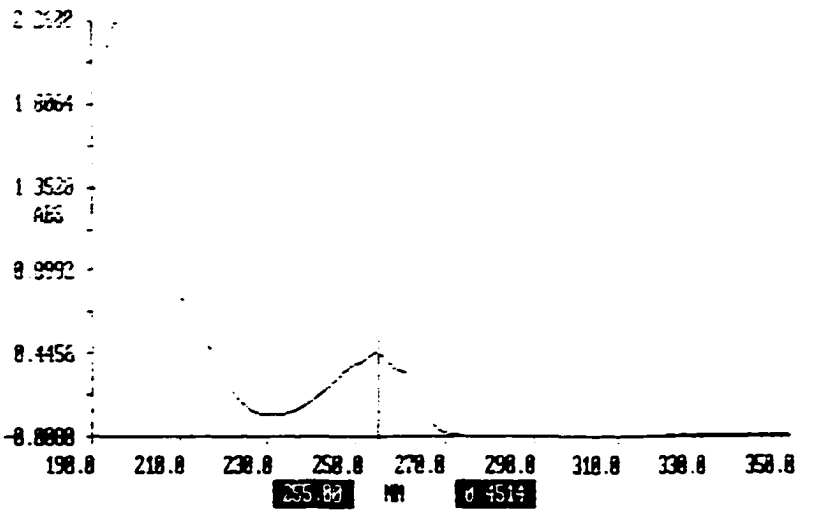

(b) 0.1 m*M* DDP + 0.1 m*M* $C_6H_{13}SO_3Na$

Figure 3-8 UV spectra of dodecylpyridinium bromide (DDP) in methanol

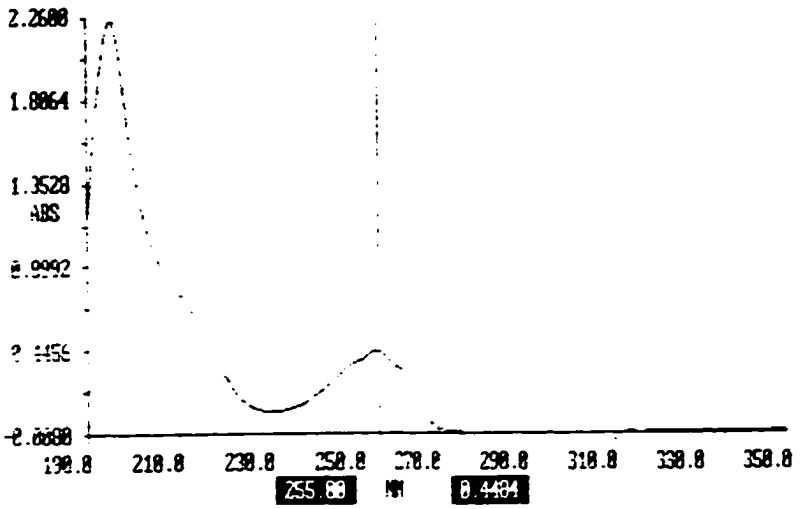

(c) 0.1 m*M* DDP + 0.1 m*M* $C_{10}H_{21}SO_3Na$

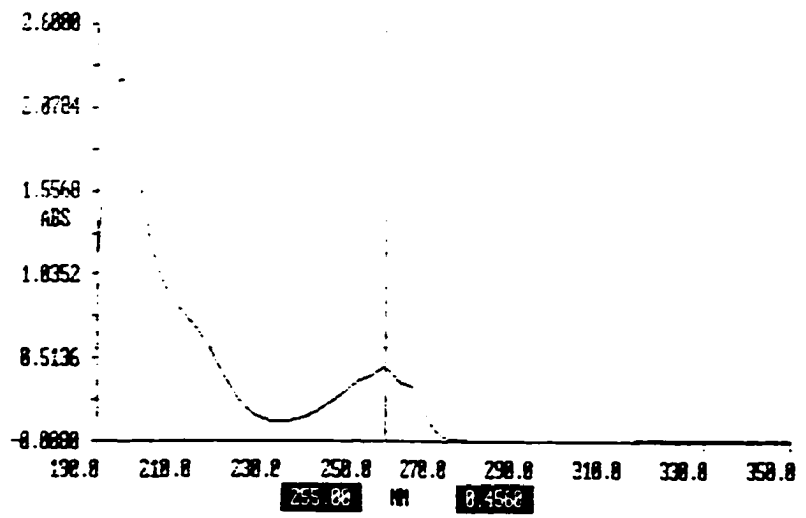

(d) 0.1 m*M* DDP + 0.1 m*M* $C_{14}H_{29}SO_3Na$

Figure 3-8 (Continued)

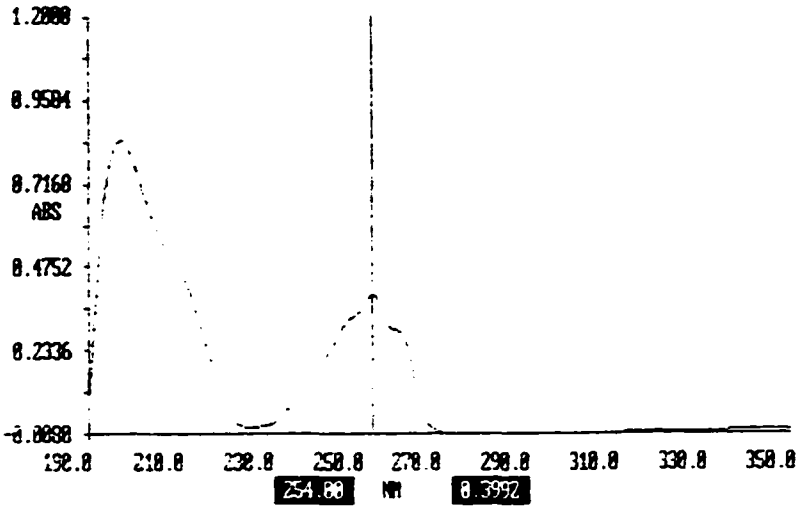

(a) 0.1 mM DDP

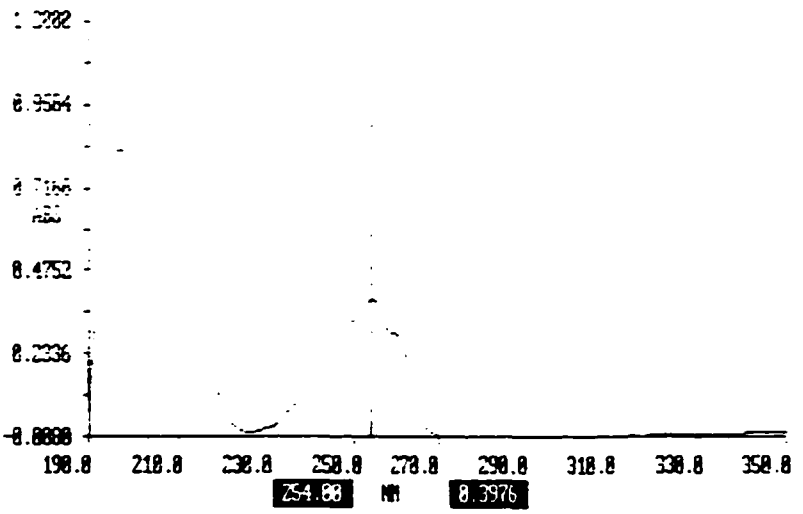

(b) 0.1 mM DDP + 0.1 mM $C_6H_{13}SO_3Na$

Figure 3-9 UV spectra of dodecylpyridinium bromide (DDP) in water

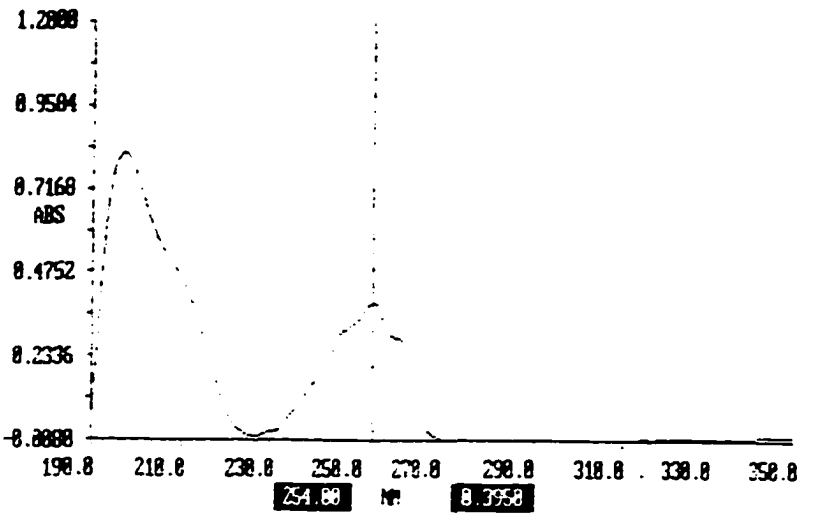

(c) 0.1 mM DDP + 0.1 mM $C_{10}H_{21}SO_3Na$

Figure 3-9 (Continued)

3.4.4 Detector response

The peaks in Figures 3-3 to 3-5 are caused by the co-elution of the UV absorbing dodecylpyridinium ion and the non-UV absorbing alkanesulfonate ion. The detector response is calculated as peak area per mole of the analyte (Table 3-4). The calculated results for alkanesulfonates are close to the value of the dodecylpyridinium ion. The data suggest the approximately equal moles of dodecylpyridinium ion and alkanesulfonate ion co-eluted. They act like pairs of ions.

Based on this factor, one can not exclude ion-pair formation. But the chromatography of alkanesulfonates under the following conditions is inconsistent with the formation of ion-pairs: the sample solutions were 0.1 m*M* alkanesulfonate, including hexanesulfonate, decanesulfonate or tetradecane-sulfonate, in combination with 0.1 m*M* dodecylpyridinium bromide; the mobile phase was a methanol and water mixture without the ion-interaction reagent. If there were ion-pairs, the retention time of each sample would be different. However all chromatograms gave one peak with the same retention time and peak area which were the same as the dodecylpyridinium ion. Therefore the conclusion is there are no tightly bonded ion-pairs.

Table 3-4 Detector response of dodecylpyridinium ion and alkanesulfonate co-elution

	Sample size mol x 10^9	Peak area cm^2	Detector response $cm^2/mol \times 10^{-7}$	Relative detector response***
C_6^*	7.97	0.74	9.25	0.99
C_8^*	6.94	0.54	7.73	0.83
C_{10}^*	6.14	0.46	7.46	0.80
DDP*	4.34	0.41	9.32	1.00
C_6^{**}	7.97	0.42	5.22	0.78
C_8^{**}	6.94	0.46	6.69	0.98
C_{10}^{**}	6.14	0.38	6.25	0.92
C_{14}^{**}	4.99	0.33	6.67	0.98
C_{17}^{**}	4.38	0.25	5.66	0.83
DDP**	4.34	0.30	6.81	1.00

* Data based on Figure 3-3.
** Data based on Figure 3-4.
*** Detector response ratio of C_n to DDP.

3.4.5 Surface coverage

As the mobile phase containing the dodecylpyridinium ion first passes through the HPLC system, the baseline sharply increases to approximately 90% of its maximum value. Then it gradually rises for about 10 minutes and reaches a stable plateau. When the baseline reaches the maximum, there should be a constant concentration (2×10^{-4} *M*) of dodecylpyridinium ion going through the detector. During the 10 minute equilibrium period, if there was no retention on the column, the amount of dodecylpyridinium ions reaching the detector would have been

$$2 \times 10^{-4}\ M \times 1 \times 10^{-3}\ \text{L/min} \times 10\ \text{min} = 2 \times 10^{-6}\ \text{mol}$$

where 2×10^{-4} *M* is the molarity of the dodecylpyridinium ions in the mobile phase and 1×10^{-3} L/min is the flow rate. Based on the change in the baseline, part of the dodecylpyridinium ions retained on the column is approximately

$$2 \times 10^{-6}\ \text{mol} \times (1.00-0.90)/2 = 1 \times 10^{-7}\ \text{mol}$$

There are no surface area data available for the 3x3 columns used in this work. However the 3 μm 80 Å pore diameter particle packing material with the C18 bonded phase typically has a surface area of 200 m^2/gram or higher[55]. An estimated surface coverage of the dodecylpyridinium ion is about 3×10^{-3} molecules/nm^2 or 300 nm^2/molecule if 0.1 g of packing is assumed. Since the surface area of one dodecylpyridinium ion is less than 10 nm^2, most of the stationary surface is not covered and is accessible to the analyte.

Chapter 4

log CMC, pC_{20} and log k' of Alkanesulfonates

4.1 Correlation between log CMC, pC_{20} and log k'

In Chapter 1 the relationships between log CMC and log k', pC_{20} and log k' were introduced.

$$\log CMC = - m\log k' + c \qquad (1\text{-}25)$$

$$pC_{20} = m'\log k' + c' \qquad (1\text{-}27)$$

These predicted linear correlations are confirmed by our experimental and calculated results for the alkanesulfonates.

Figure 4-1 is a plot of experimental log CMC values from the literature[60] vs. our log k' for C_8, C_{10}, C_{12}, C_{14} and C_{16} alkanesulfonates. A plot of pC_{20} vs. our log k' is in Figure 4-2. Because there is a very limited set of literature values for pC_{20}[61][62] obtained under identical conditions, C_{10} and C_{12} values in Figure 4-2 were taken from the literature[63], others were extrapolated from pC_{20} values of C_{10} and C_{12} alkanesulfonates. Both plots gave straight lines.

Table 4-1 lists the experimental (literature) and calculated log CMC and pC_{20} values using equations (1-25) and (1-27). The experimental CMC values for C_8 and C_{14} sulfonates

were used to define the slope and intercept of equation (1-25). The slope and intercept in equation (1-27) were calculated with the experimental pC_{20} values of C_{10} and C_{12} sulfonates. The results show good correlation between the experimental and calculated values. In addition the results demonstrate that log CMC and pC_{20} can be estimated from log k' data once two values of log CMC or pC_{20} are known in a homologous series.

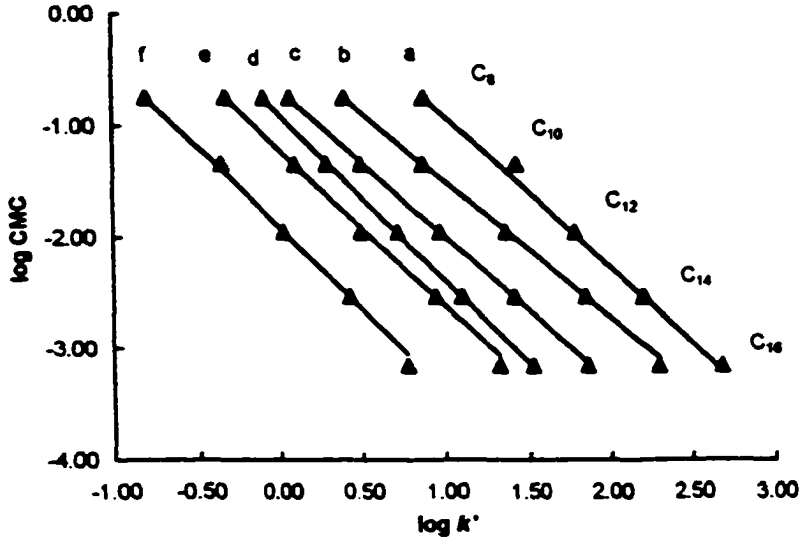

Figure 4-1 Correlation between log CMC and log k' for alkanesulfonates
log k' corresponds to a. 60%, b. 65%, c.70%, d. 73%, e. 75%, f. 80% methanol.

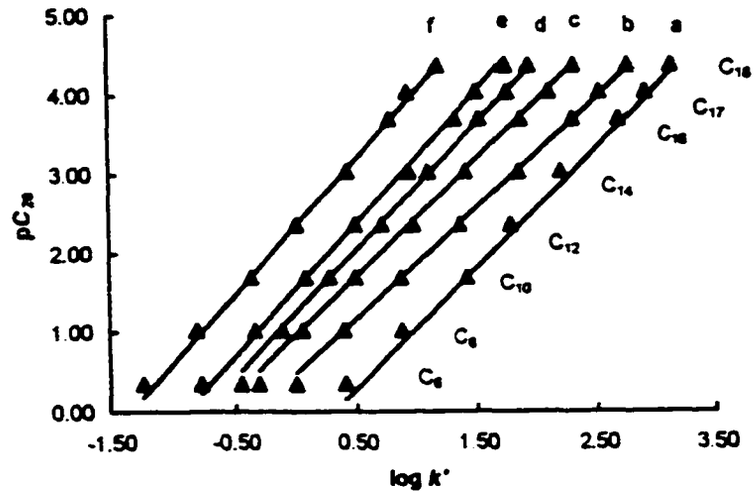

Figure 4-2 Correlation between pC_{20} and log k' for alkanesulfonates

log k' corresponds to a. 60%, b. 65%, c.70%, d. 73%, e. 75%, f. 80% methanol.

Table 4-1 log CMC and pC_{20} of alkanesulfonates

	Exp.	C_6	C_8	C_{10}	C_{12}	C_{14}	C_{16}	C_{17}	C_{18}
	log CMC*	-0.34	-0.75[#]	-1.35	-1.96	-2.54[#]	-3.15	-3.68	-3.12
	pC_{20}**	0.35	1.02	1.69[##]	2.36[##]	3.03	3.70	4.04	4.37
HPLC condition	Cal.								
60:40 $CH_3OH:H_2O$, 0.2 mM DDP	log CMC	-0.11	-	-1.49	-1.98	-	-3.20	-3.51	-3.81
	pC_{20}	0.14	0.86	-	-	2.86	3.61	3.95	4.29
65:35 $CH_3OH:H_2O$, 0.2 mM DDP	log CMC	-0.28	-	-1.34	-1.94	-	-3.08	-3.37	-3.65
	pC_{20}	0.48	1.02	-	-	3.06	3.67	4.00	4.32
70:30 $CH_3OH:H_2O$, 0.2 mM DDP	log CMC	-0.26	-	-1.32	-1.96	-	-3.13	-3.45	-3.72
	pC_{20}	0.51	1.06	-	-	3.06	3.73	4.08	4.38
73:27 $CH_3OH:H_2O$, 0.2 mM DDP	log CMC	-0.23	-	-1.32	-1.97	-	-3.16	-3.50	-3.77
	pC_{20}	0.51	1.07	-	-	3.00	3.67	4.04	4.33
75:25 $CH_3OH:H_2O$, 0.2 mM DDP	log CMC	-0.14	-	-1.35	-1.91	-	-3.06	-3.31	-3.65
	pC_{20}	0.23	0.96	-	-	3.12	3.76	4.05	4.46
80:20 $CH_3OH:H_2O$, 0.2 mM DDP	log CMC	-0.13	-	-1.39	-1.95	-	-3.05	-3.27	-3.63
	pC_{20}	0.18	0.93	-	-	3.06	3.67	3.93	4.36
Summary	log CMC	-0.19	-	-1.37	-1.95	-	-3.12	-3.40	-3.70
	stdev	0.08		0.06	0.02	-	0.06	0.10	0.07
	pC_{20}	0.34	0.98	-	-	3.03	3.69	4.01	4.36
	stdev	0.18	0.08	-	-	0.09	0.05	0.06	0.06

* CMC in H_2O; C_6 at 25 °C (ref. [64]), C_8, C_{10}, C_{12}, C_{14} and C_{16} at 50 °C (ref. [60]), C_{17} at 50 °C (ref. [65]), C_{18} at 57 °C (ref.[66]).

** pC_{20} at H_2O-air interface, 25 °C. C_{10} and C_{12} are experimental values (ref. [63]). Others are extrapolated from C_{10} and C_{12} data.

\# Used to determine parameters in equation (1-25).

\#\# Used to determine parameters in equation (1-27).

4.1.1 Calculated log CMC

The calculated log CMC values are very close to the experimental results for C_{10}, C_{12} and C_{16} (Table 4-1). For C_6, C_{17} and C_{18} there are differences between the calculated and experimental log CMC values. Presumably this is because the log CMC values were determined using different measurement conditions: refractive index at 25°C for C_8 to C_{16}[60], spectral characteristics at 25 °C for C_6[64] and at 50 °C for C_{17}[65], and Krafft point and solubility at 57 °C for C_{18}[66].

Using the CMC values of C_8 to C_{16} from reference [60], the following log CMC values are extrapolated (using equation (1-2), the number of carbon atoms):

C_6 -0.15; C_{17} -3.45; C_{18} -3.75.

These are in good agreement with our calculated log CMC values (using equation (1-25), log k'):

C_6 -0.19; C_{17} -3.40; C_{18} -3.70.

4.1.2 Calculated pC_{20}

Table 4-1 lists the calculated pC_{20} values using our chromatographic data as well. Only values for C_{10} and C_{12} are available in the literature[63]. The others are extrapolated from the C_{10} and C_{12} data assuming a linear relationship between the pC_{20} and the number of carbon atoms in the straight alkyl chain. In general, the calculated pC_{20} values from log k' compare very well with the pC_{20} values determined using surfactant properties.

4.2 Discussion

4.2.1 log CMC and log k'

The parameters of the linear regression equation (1-25) are summarized in Table 4-2.

$$\log CMC = - m\log k' + c \qquad (1\text{-}25)$$

The slopes of log CMC vs. log k' plots vary slightly from -1.2 to -1.5 within the range of mobile phase compositions. Since both log CMC and log k' change with the length of an alkyl chain, the slope here expresses the relationships between these two. In other words, the slope is a measure of different tendencies for a homologous series of surfactants to partition onto the HPLC stationary phase (the monomer adsorbing onto the interface) and to self-associate (micellization) in aqueous solution.

The intercepts of the log CMC vs. log k' plots vary from 0.4 to -1.9 over the range of mobile phase compositions. The change here is greater than the change of the slope. The data show that as the methanol percentage in the mobile phase increases, the log k' decreases and the intercept in equation (1-25) becomes more negative. Since an increase in the percentage methanol (a decrease in the percentage water) changes the HPLC environment, the change in the difference between the HPLC and the micelle environments is reflected in the intercept.

Table 4-2 Parameters in the log CMC and log k' correlation equation for alkanesulfonates

HPLC condition	Slope	Intercept
60:40 $CH_3OH:H_2O$, 0.2 mM DDP	-1.36	0.44
65:35 $CH_3OH:H_2O$, 0.2 mM DDP	-1.23	-0.27
70:30 $CH_3OH:H_2O$, 0.2 mM DDP	-1.32	-0.67
73:27 $CH_3OH:H_2O$, 0.2 mM DDP	-1.48	-0.91
75:25 $CH_3OH:H_2O$, 0.2 mM DDP	-1.39	-1.23
80:20 $CH_3OH:H_2O$, 0.2 mM DDP	-1.45	-1.92

4.2.2 pC_{20} and log k'

The parameters of the linear correlation equation (1-27) are summarized in Table 4-3.

$$pC_{20} = m' \log k' + c' \qquad (1\text{-}27)$$

The slopes of the pC_{20} vs. log k' lines vary slightly from 1.4 to 1.7 within the range of mobile phase compositions. Following the same discussion given in Section 4.2.1, the slope here is a measure of different tendencies to partition at the aqueous methanol-C_{18} interface and at the water-air interface for a homologous series of surfactants.

The intercept of the pC_{20} vs. log k' lines goes from -0.6 to 2.3 as the percentage methanol in the HPLC mobile phase increases. As mentioned previously, the change in the difference between the two environments is shown in the intercept.

Table 4-3 Parameters in the pC_{20} and log k' correlation equation for alkanesulfonates

HPLC condition	Slope	Intercept
60:40 $CH_3OH:H_2O$, 0.2 mM DDP	1.63	-0.63
65:35 $CH_3OH:H_2O$, 0.2 mM DDP	1.37	0.49
70:30 $CH_3OH:H_2O$, 0.2 mM DDP	1.39	1.01
73:27 $CH_3OH:H_2O$, 0.2 mM DDP	1.54	1.26
75:25 $CH_3OH:H_2O$, 0.2 mM DDP	1.68	1.54
80:20 $CH_3OH:H_2O$, 0.2 mM DDP	1.73	2.33

Chapter 5

Chromatography of Aromatic Quaternary Ammonium Geminis

5.1 Introduction

As reviewed in Section 2.2.2, various reversed-phase packing materials, such as CN, phenyl, C18, polystyrene-divinylbenzene, and ß-cyclodextrin have been used for RP-HPLC analysis of traditional aromatic quaternary ammonium surfactants. Mobile phases were often methanol-water or acetonitrile-water mixtures combined with organic or inorganic ion-interaction reagents. These surfactants have UV chromophores, therefore the UV detector is commonly used.

Aromatic quaternary ammonium gemini surfactants are a new type of surfactant. No work on the reversed-phase high performance liquid chromatography of these compounds has appeared in the literature. In this work RP-HPLC has been studied for the following homologous series of gemini surfactants, $(C_nN)_2Ar$:

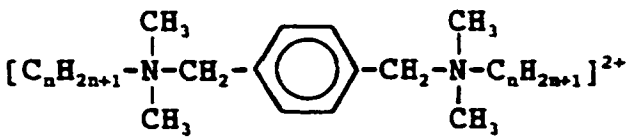

These species are too hydrophilic to be separated with a simple organic and aqueous binary solvent. Therefore ion-

interaction chromatography is needed. The experiments were undertaken with the short column used in the analysis of alkanesulfonates and a UV diode array detector. Sodium perchlorate was added to the acetonitrile-water mobile phases at pH 3. These conditions were found to give satisfactory results for the analysis of this series of surfactants based on the length of the straight alkyl chain.

Experiments designed to elucidate the ion-interaction retention mechanism were carried out. The results suggest that there are interactions between oppositely charged aromatic quaternary ammonium ions and perchlorate ions, but ions are not closely bonded.

5.2 Experimental

5.2.1 Instrumentation and reagents

The instruments and reagents were the same as those listed in Section 3.2 with the following exceptions.

A series of aromatic quaternary ammonium gemini surfactants, $(C_nN)_2Ar$ bromide salt (n = 8, 10, 12, 14, 16 and 18), were synthesized by the Surfactant Research Institute at Brooklyn College[67]. Sodium perchlorate, phosphoric acid and sodium chloride were purchased from Aldrich Chemical Co., Inc..

A Perkin-Elmer Pecosphere 5 x 15 C18 cartridge column (150 x 4.6 mm, 4 μm particles) and a Sigma-Aldrich Hypersil ODS 5 μm 150 x 4.6 mm column were used for comparison with the short column.

pH values were measured by an Orion 420A pH meter with an Orion Triode 91-57BN pH electrode.

The column temperature was controlled by a Timberline HPLC Column Heater H-500 coupled with a Data Precision 3500 DVM for temperature reading. The temperature remained stable within ±0.1 °C.

A Torsion Balance from Bethlehem Instrument company, Inc. with a ca. 5 cm perimeter platinum blade was used to measure the surface tension of the acetonitrile-water solvent mixed with sodium perchlorate and the surfactants.

5.2.2 Procedure

A homologous series of aromatic quaternary ammonium gemini ($(C_nN)_2Ar$) surfactants was chromatographed using 3x3 C18 columns. The mobile phase composition was varied from 80:20 to 95:5 (*V*:*V*) of acetonitrile:water. Only isocratic conditions were used. Sodium perchlorate was added to the mobile phases at concentration levels of 0.05 *M*, 0.10 *M*, 0.15 *M*, and 0.20 *M*. Experiments with 0.05 *M* of sodium chloride in the mobile phase were performed as well. The apparent pH of the mobile phases was adjusted to 3.0 using phosphoric acid. Samples were dissolved in the mobile phases at a concentration of 0.1 m*M* in most experiments. Before each run the column was flushed with mobile phase for several minutes until equilibrium was reached as indicated by a stable pump pressure and detector baseline. The UV detector was set to 220 nm. A column heater was used to adjust the temperature to several values in the 30 °C to 50 °C range (60 °C in some runs).

5.3 Results and Discussion

Chromatographic data were obtained for the individual surfactants and mixtures of three adjacent members in the series. However, the $(C_nN)_2Ar$ mixture of C_8, C_{10}, C_{12}, C_{14}, C_{16}, and C_{18} was analyzed as well to demonstrate the possibility of using a short column to separate them in a reasonable period of time. To explore the optimum chromatographic conditions, the mobile phases of acetonitrile, methanol, water, acetonitrile-water, and methanol-water were tested. Besides changing the mobile phase composition, various ion-interaction reagents, including sodium perchlorate, sodium chloride, sodium hexanesulfonate, and sodium dodecanesulfonate, were tried. The mobile phase of acetonitrile-water with about 0.1 *M* sodium perchlorate gave the most satisfactory results.

A summary of log k' under various chromatographic conditions for $(C_nN)_2Ar$ surfactants is given in Table 5-1, where the log k' values are the averages over the indicated number of runs (# of data). Some aspects of these data and representative chromatograms are presented in the following sections.

Table 5-1 Summary of log *k'* of aromatic quaternary ammonium geminis $(C_nN)_2Ar$

T(+-0.1°C)	Mobile phase*	# of data		C_8	C_{10}	C_{12}	C_{14}	C_{16}	C_{18}
30.3	95:5 $CH_3CN:H_2O$	>= 6	log *k'*(avg.)	-0.94	-0.49	-0.08	0.35	0.80	1.27
	0.1*M* $NaClO_4$, pH=2		stdev	0.0E+00	1.6E-02	1.2E-09	4.1E-03	1.9E-03	4.7E-03
40.2		>= 6	log *k'*(avg.)	-0.99	-0.60	-0.21	0.19	0.61	1.03
			stdev	1.3E-08	2.8E-02	7.5E-03	3.8E-03	2.7E-03	2.1E-03
50.1		>= 6	log *k'*(avg.)	-1.04	-0.72	-0.32	0.05	0.42	0.81
			stdev	0.0E+00	2.2E-02	5.0E-09	5.3E-03	2.1E-03	1.4E-03
30.3	90:10 $CH_3CN:H_2O$	>= 6	log *k'*(avg.)	-0.75	-0.29	0.16	0.65	1.17	1.70
	0.1*M* $NaClO_4$, pH=3		stdev	0.0E+00	1.6E-02	5.1E-03	3.3E-03	2.3E-03	3.8E-03
40.3		>= 6	log *k'*(avg.)	-0.77	-0.37	0.06	0.51	0.99	1.48
			stdev	0.0E+00	9.1E-03	4.2E-03	2.7E-03	1.6E-03	1.7E-03
50.1		>= 6	log *k'*(avg.)	-0.83	-0.45	-0.06	0.36	0.80	1.25
			stdev	4.1E-02	1.7E-02	5.5E-03	2.4E-03	8.5E-04	6.7E-04
30.2	85:15 $CH_3CN:H_2O$	>= 4	log *k'*(avg.)	-0.47	-0.04	0.47	1.01	1.59	-
	0.1*M* $NaClO_4$, pH=3		stdev	0.0E+00	4.2E-10	1.4E-03	4.5E-04	1.7E-04	-
40.2		>= 6	log *k'*(avg.)	-0.53	-0.12	0.34	0.85	1.38	1.93
			stdev	2.0E-02	5.5E-03	2.6E-03	1.2E-03	1.2E-03	1.1E-03
50.1		>= 6	log *k'*(avg.)	-0.57	-0.19	0.23	0.70	1.20	1.71
			stdev	9.4E-09	9.6E-03	3.5E-03	1.2E-03	1.0E-03	1.0E-03

Table 5-1 (Continued)

T(+-0.1°C)	Mobile phase*	# of data		C_8	C_{10}	C_{12}	C_{14}	C_{16}	C_{18}
30.3	80:20 $CH_3CN:H_2O$	>= 4	log *k*'(avg.)	-0.26	0.23	0.78	1.38	2.01	-
	0.1*M* $NaClO_4$, pH=3		stdev	0.0E+00	2.8E-03	3.6E-03	4.5E-03	1.0E-02	-
40.2		>= 4	log *k*'(avg.)	-0.33	-0.13	0.65	1.21	1.81	-
			stdev	0.0E+00	4.5E-03	1.7E-03	1.2E-03	1.6E-03	-
50.1		>= 4	log *k*'(avg.)	-0.42	0.02	0.51	1.04	1.60	-
			stdev	0.0E+00	0.0E+00	6.1E-03	6.7E-03	7.3E-03	-
30.3	85:15 $CH_3CN:H_2O$	>= 4	log *k*'(avg.)	-0.46	-0.01	0.48	1.03	1.61	-
	0.05*M* $NaClO_4$, pH=3		stdev	1.6E-02	1.4E-02	9.6E-03	1.2E-02	2.0E-02	-
40.2		>= 4	log *k*'(avg.)	-0.54	-0.11	0.35	0.86	1.40	1.95
			stdev	2.0E-02	1.1E-02	9.8E-03	7.5E-03	1.0E-02	1.1E-02
50.1		>= 6	log *k*'(avg.)	-0.58	-0.20	0.22	0.69	1.19	1.71
			stdev	2.2E-02	8.4E-03	2.0E-02	2.9E-02	3.6E-02	4.9E-02
30.3	85:15 $CH_3CN:H_2O$	>= 4	log *k*'(avg.)	-0.45	0.00	0.52	1.07	1.65	-
	0.15*M* $NaClO_4$, pH=3		stdev	1.9E-02	5.8E-03	1.6E-03	2.1E-03	3.9E-03	-
40.2		>= 4	log *k*'(avg.)	-0.55	-0.10	0.38	0.89	1.43	1.99
			stdev	1.6E-02	7.5E-03	8.8E-03	8.8E-03	9.3E-03	8.8E-03
50.1		>= 6	log *k*'(avg.)	-0.55	-0.17	0.26	0.73	1.23	1.74
			stdev	3.6E-02	0.0E+00	3.4E-03	3.7E-03	5.3E-03	5.7E-03

Table 5-1 (Continued)

T(+-0.1°C)	Mobile phase*	# of data		C_8	C_{10}	C_{12}	C_{14}	C_{16}	C_{18}
30.3	85:15 $CH_3CN:H_2O$	>= 4	log *k*'(avg.)	-0.45	0.01	0.53	1.08	1.67	-
	0.2*M* $NaClO_4$, pH=3		stdev	1.4E-02	4.5E-03	2.3E-03	4.9E-03	6.4E-03	-
40.2		>= 3	log *k*'(avg.)	-0.52	-0.07	0.41	0.92	1.47	2.02
			stdev	1.7E-02	1.1E-02	6.1E-03	4.0E-03	5.5E-03	6.2E-03
50.1		>= 6	log *k*'(avg.)	-0.57	-0.16	0.29	0.77	1.28	1.80
			stdev	1.6E-02	8.7E-03	5.4E-03	5.8E-03	7.0E-03	8.8E-03
30.3	80:20 $CH_3CN:H_2O$	>= 4	log *k*'(avg.)	-0.23	0.25	0.79	1.39	2.03	-
	0.05*M* $NaClO_4$, pH=3		stdev	1.1E-02	4.1E-03	3.8E-03	3.2E-03	6.4E-03	-
40.2		>= 4	log *k*'(avg.)	-0.30	0.15	0.67	1.23	1.83	-
			stdev	1.1E-02	0.0E+00	3.7E-03	3.0E-03	5.1E-03	-
50.1		>= 4	log *k*'(avg.)	-0.36	0.08	0.56	1.08	1.64	-
			stdev	1.3E-02	0.0E+00	2.4E-03	2.0E-03	2.9E-03	-
60.0		>= 2	log *k*'(avg.)	-0.38	0.00	0.44	0.92	1.44	-
			stdev	0.0E+00	0.0E+00	2.1E-03	4.0E-03	5.6E-03	-
40.2	**80:20 $CH_3CN:H_2O$	>= 2	log *k*'(avg.)	-0.19	0.29	0.83	1.41	-	-
	0.05*M* $NaClO_4$, pH=3		stdev	0.0E+00	6.3E-03	1.2E-02	1.4E-02	-	-
40.2	***80:20 $CH_3CN:H_2O$	>= 2	log *k*'(avg.)	0.02	0.39	0.92	-	-	-
	0.05*M* $NaClO_4$, pH=3		stdev	5.2E-02	1.9E-03	1.3E-02	-	-	-

Table 5-1 (Continued)

T(+-0.1°C)	Mobile phase*	# of data		C_8	C_{10}	C_{12}	C_{14}	C_{16}	C_{18}
30.3	80:20 $CH_3CN:H_2O$	>= 4	log *k'*(avg.)	-0.35	0.13	0.69	1.28		-
	0.05*M* NaCl,pH=3		stdev	3.5E-02	3.1E-02	4.2E-02	4.4E-02	-	-
40.2		>= 2	log *k'*(avg.)	-0.43	-0.01	0.50	1.05	1.65	-
			stdev	2.2E-02	6.8E-03	1.2E-02	2.1E-02	1.9E-02	-
50.1		>= 2	log *k'*(avg.)	-0.49	-0.08	0.38	0.89	1.45	-
			stdev	0.0E+00	1.4E-02	7.0E-03	1.7E-02	1.7E-02	-
60.0		>= 2	log *k'*(avg.)	-0.58	-0.20	0.27	0.74	1.25	-
			stdev	0.0E+00	1.8E-02	2.5E-02	1.2E-02	9.1E-03	-

* *V*:*V* for $CH_3CN:H_2O$; pH was adjusted using H_3PO_4.

** 150 x 4.6 C18 Perkin-Elmer column.

*** 150 x 4.6 C18 Sigma-Aldrich column.

5.3.1 log *k'*, the number of carbon atoms, the mobile phase composition, and temperature

The log *k'* increases linearly with the number of carbon atoms in the straight chain as expected. Figure 5-1 illustrates this relationship in four different mobile phases with 0.1 *M* of sodium perchlorate. The slopes are in the range of 0.19 to 0.28 under these chromatographic conditions. The slopes decrease about 0.02 with each 5% increase of the acetonitrile volume percentage.

Figure 5-1 also shows the effect of temperature on log *k'*. The log *k'* decreases with increasing temperature.

The log *k'* of each surfactant decreases linearly with increasing volume percentage of acetonitrile over the experimental range (Figure 5-2).

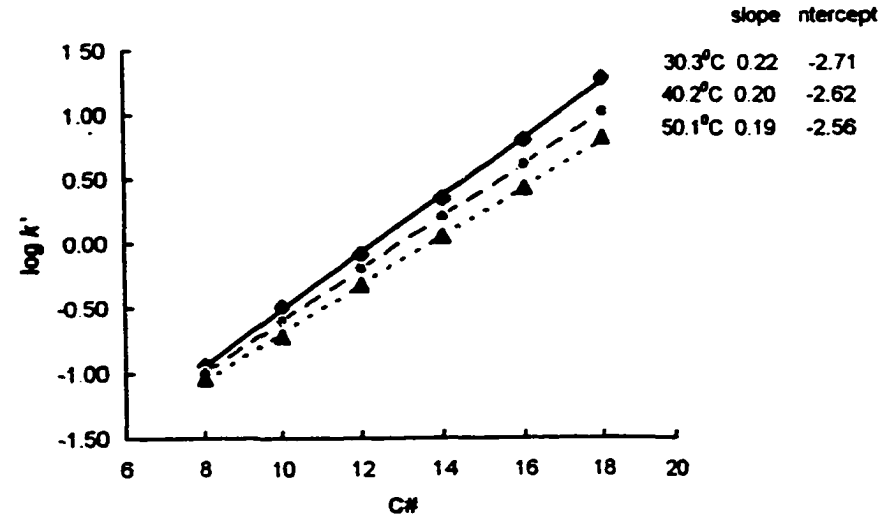

(a) 95:5 $CH_3CN:H_2O$

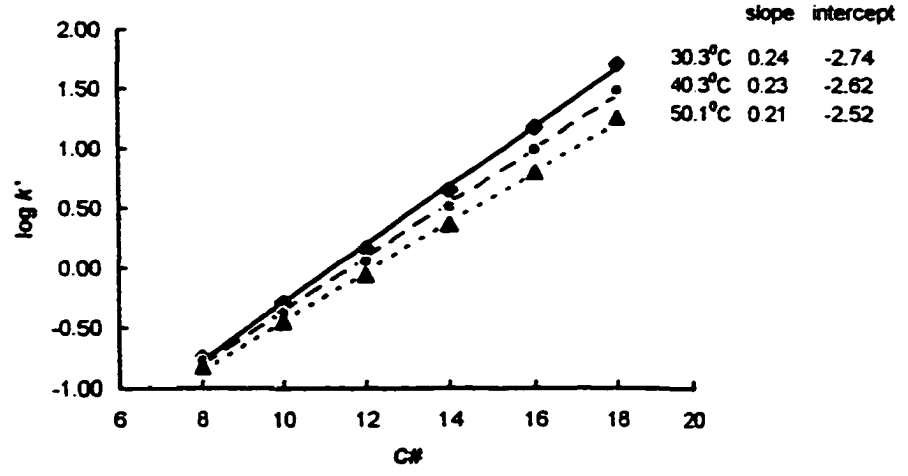

(b) 90:10 $CH_3CN:H_2O$

Figure 5-1 log k' vs. carbon number of $(C_nN)_2Ar$ (CH_3CN/H_2O + 0.1 *M* sodium perchlorate)

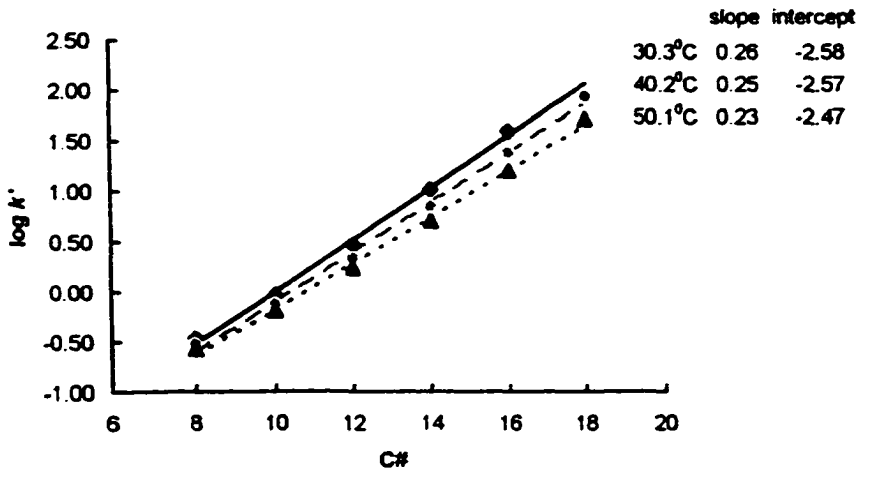

(c) 85:15 $CH_3CN:H_2O$

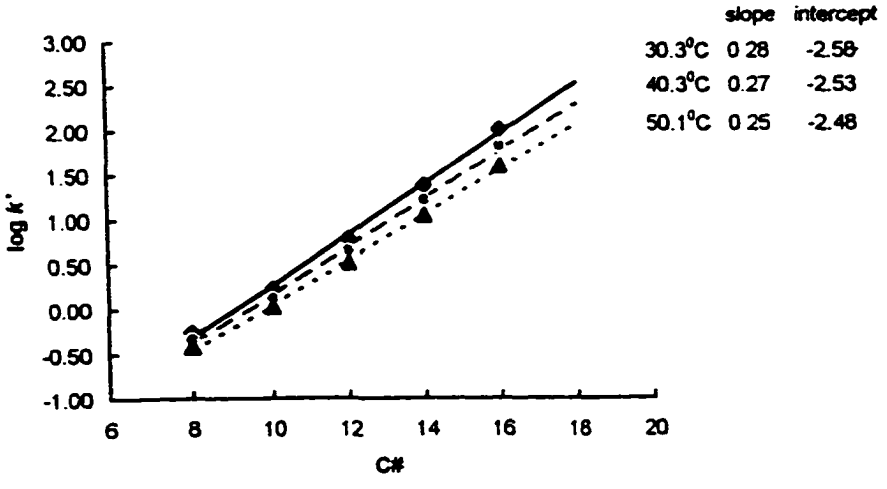

(b) 80:20 $CH_3CN:H_2O$

Figure 5-1 (Continued)

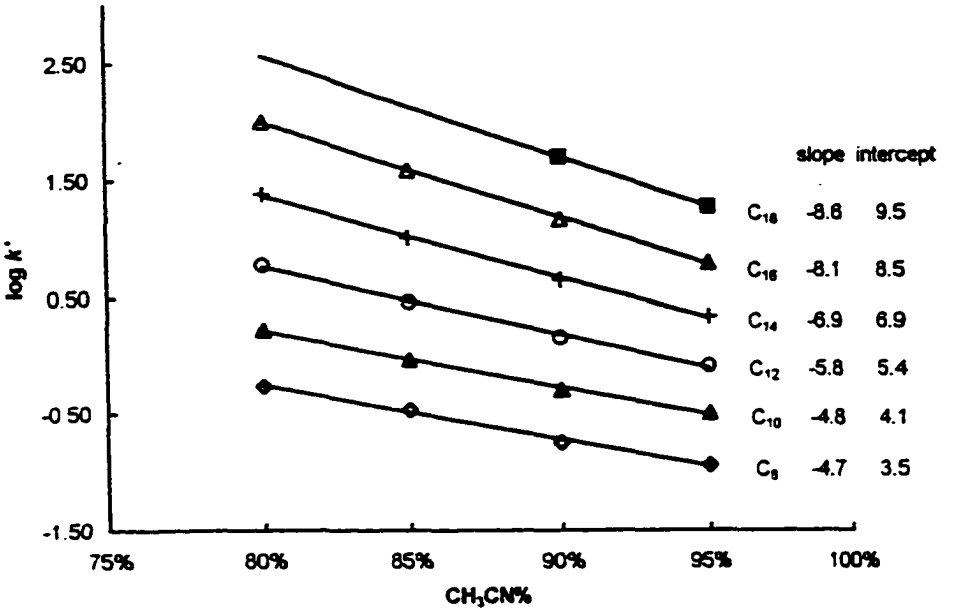

Figure 5-2 log k' vs. CH_3CN volume fraction in chromatography of $(C_nN)_2Ar$ (CH_3CN/H_2O + 0.1 *M* sodium perchlorate, 30°C)

5.3.2 Separation of $(C_nN)_2Ar$

Figure 5-3 presents the chromatograms of $(C_nN)_2Ar$ surfactant mixtures:

(a) C_8, C_{10} and C_{12}, (b) C_{10}, C_{12} and C_{14},

(c) C_{12}, C_{14} and C_{16}, (d) C_{14}, C_{16} and C_{18},

(e) C_8, C_{10}, C_{12}, C_{14}, C_{16} and C_{18}.

These chromatograms show that at 30 °C separation of C_8 to C_{12} mixture can be accomplished using 80% or 85% (V/V) acetonitrile with sodium perchlorate as an ion-interaction reagent; 85% acetonitrile is good for a C_{10} to C_{12} mixture; 90% acetonitrile can be used for a C_{12} to C_{16} mixture; and 95% for a C_{14} to C_{18} mixture. The first peak in the chromatograms is induced by a disturbance upon injection. This also appears when the solvent is injected in the absence of the ion-interaction reagent.

The chromatographic experiments were undertaken under isocratic conditions in this work. However, the gradient chromatography would work with those mobile phases.

An impurity peak appears between C_{16} and C_{18} surfactants (Figure 5-3 (d), (e)). Its retention time is the same as the predicted value for $(C_{17}N)_2Ar$ (Figure 5-4). However, heptadecyl-*N*,*N*-dimethylamine is not in the raw materials[68], but there is 1% to 2% of C_{16} in C_{18} or 1% to 2% of C_{18} in C_{16}. Therefore it is believed to be a gemini surfactant with one C_{16} and one C_{18} chain. The impurity in the mixtures is about 10%

of $(C_{16}N)_2Ar$ or $(C_{18}N)_2Ar$, which is higher than the expected value and also higher than in the individual samples. This might be attributable to the sample preparation method used for the chromatographic experiments. Since the longer chain sample solutions were sonicated for dissolution, an exchange reaction could occur.

The limit of quantitative measurement and the linear range were not studied. The lowest concentration used in our experiments is approximately 0.01 mM (5×10^{-11} moles of sample with 5 μL injection). The detection limit can be much lower than this value. The upper concentration limit of chromatography is restricted by the low solubility in the presence of the high concentration of sodium perchlorate and the high volume percentage of acetonitrile.

The variations in the peak areas between each replicated run are less than 3%. Thus quantitative measurements can be made using this method.

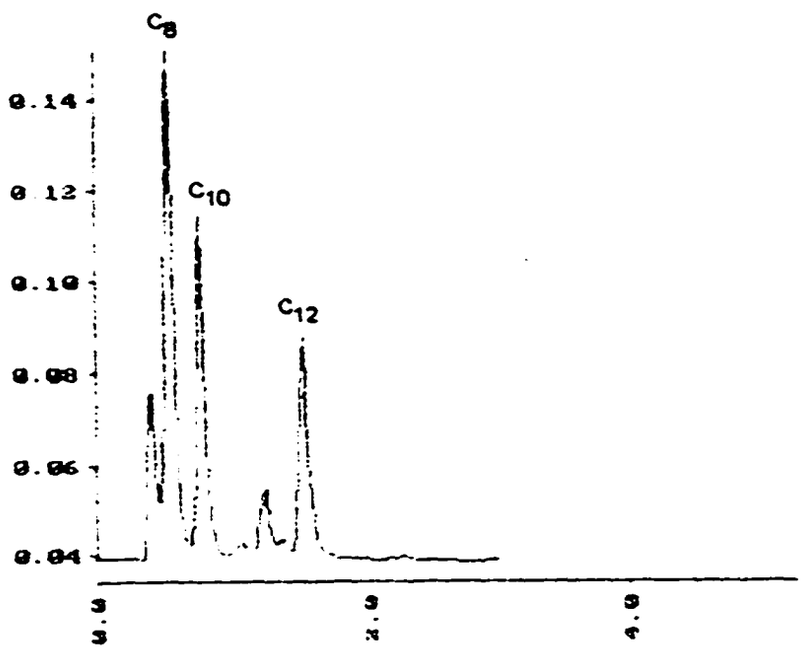

(a) C_8, C_{10}, C_{12} mixture (85% CH_3CN)

Figure 5-3 Chromatograms of $(C_nN)_2Ar$ gemini surfactants (0.1 m*M* each dissolved in mobile phase)

Mobile phase:	CH_3CN, H_2O, 0.1 *M* $NaClO_4$, pH=3 (H_3PO_4)
UV detection:	220 nm
Flow rate:	1.0 ml/min
Column:	3x3 C18 (33 x 4.6 mm)
Injection volume:	5 μl
Temperature:	30.2 °C

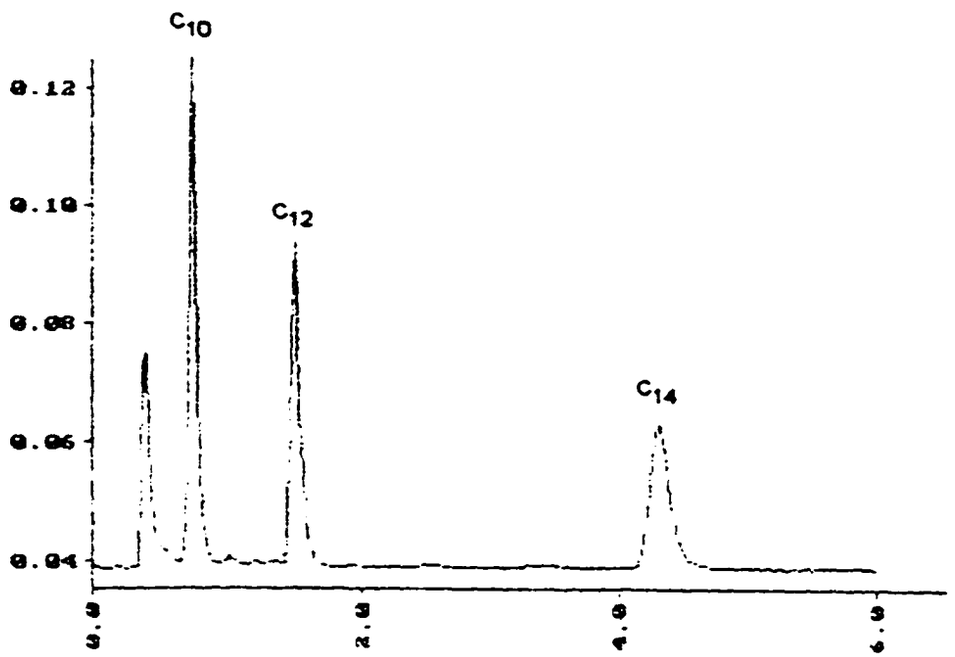

(b) C_{10}, C_{12}, C_{14} mixture (85% CH_3CN)

Figure 5-3 (Continued)

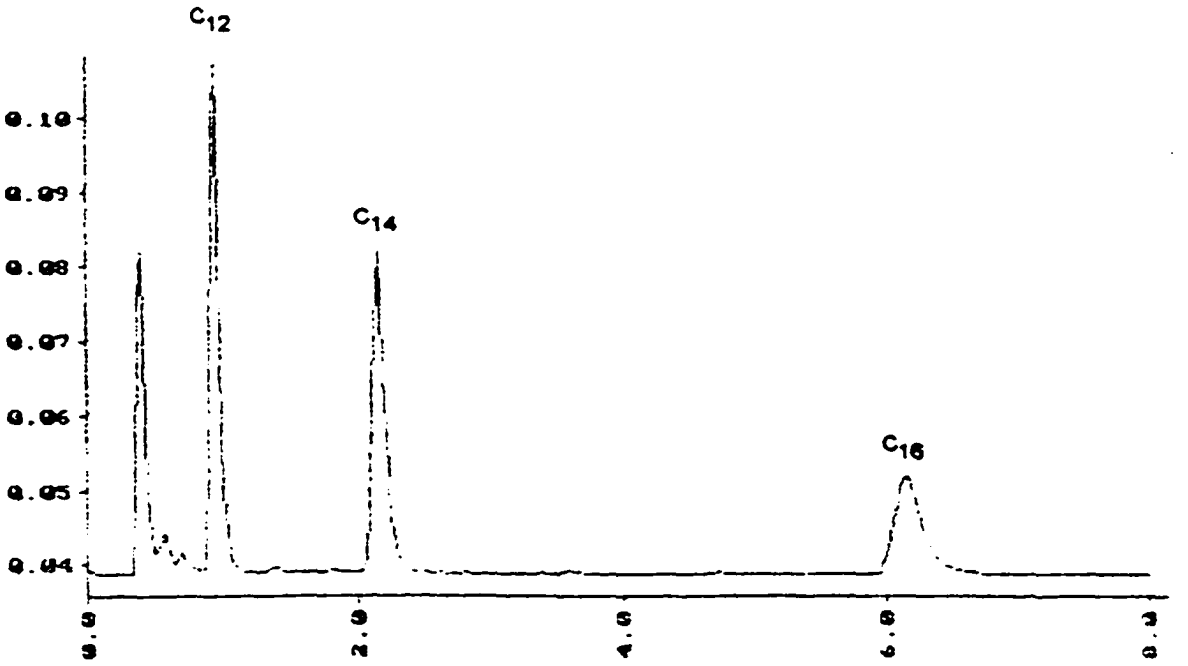

(c) C_{12}, C_{14}, C_{16} mixture (90% CH_3CN)

Figure 5-3 (Continued)

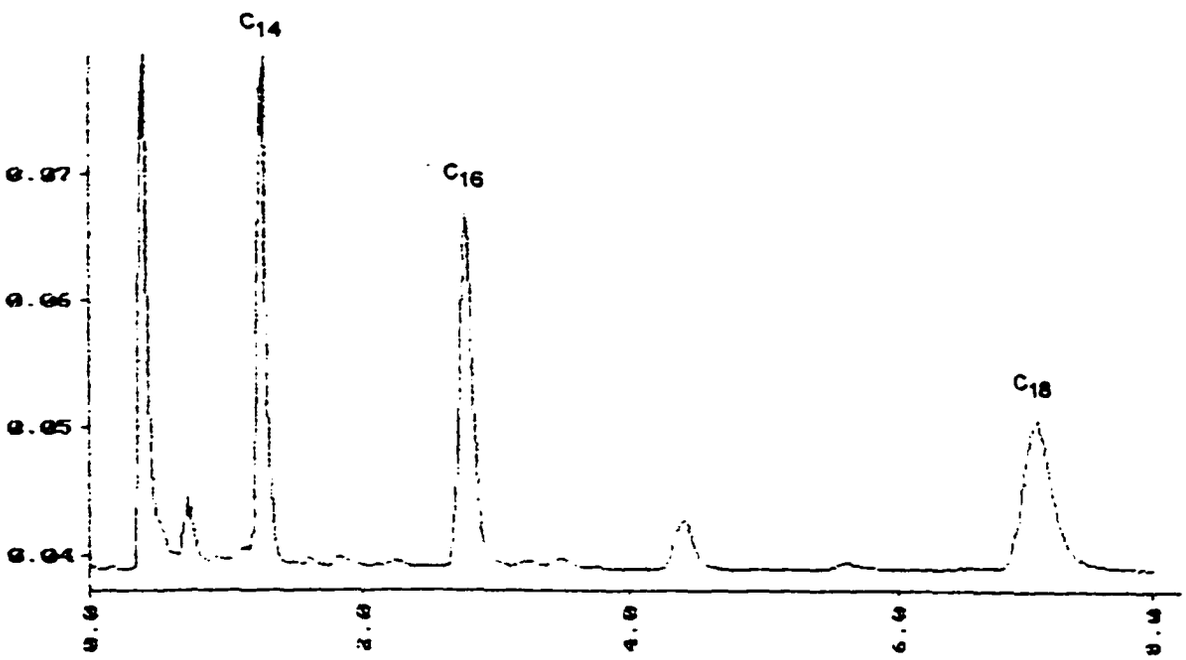

(d) C_{14}, C_{16}, C_{18} mixture (90% CH_3CN)
(0.04 m*M* each, injection volume 10 μl)

Figure 5-3 (Continued)

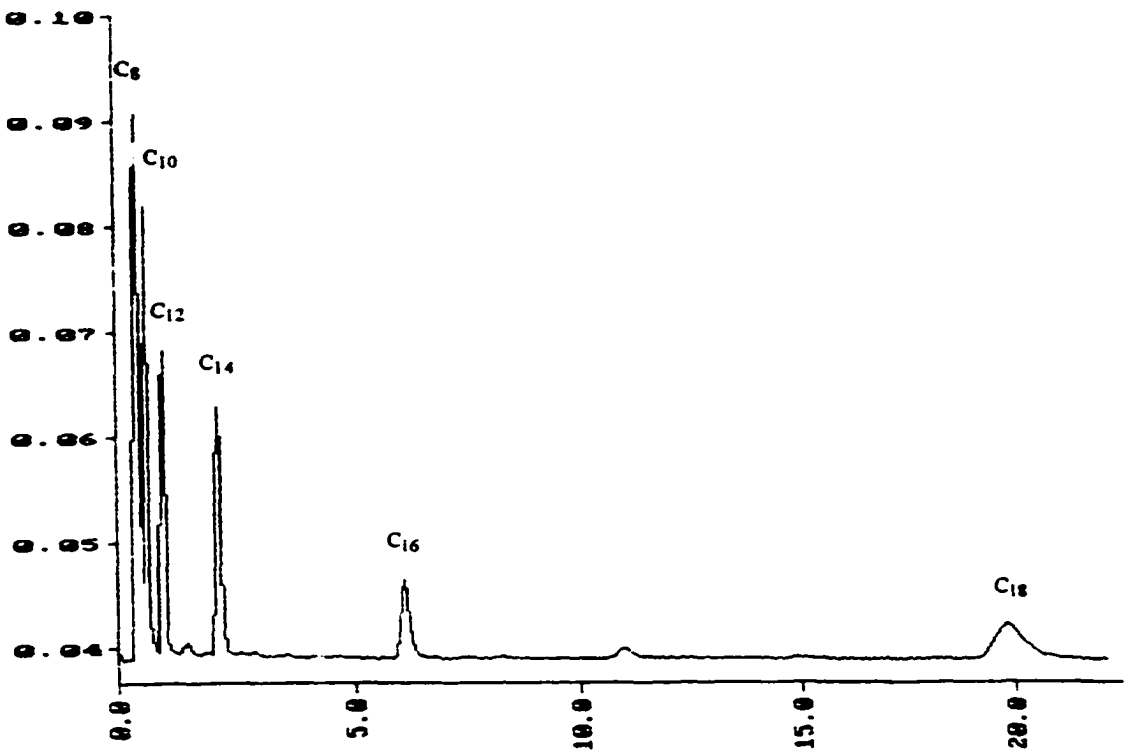

(e) C_8 to C_{18} mixture (90% CH_3CN)
(0.04 mM each, injection volume 10 μl)

Figure 5-3 (Continued)

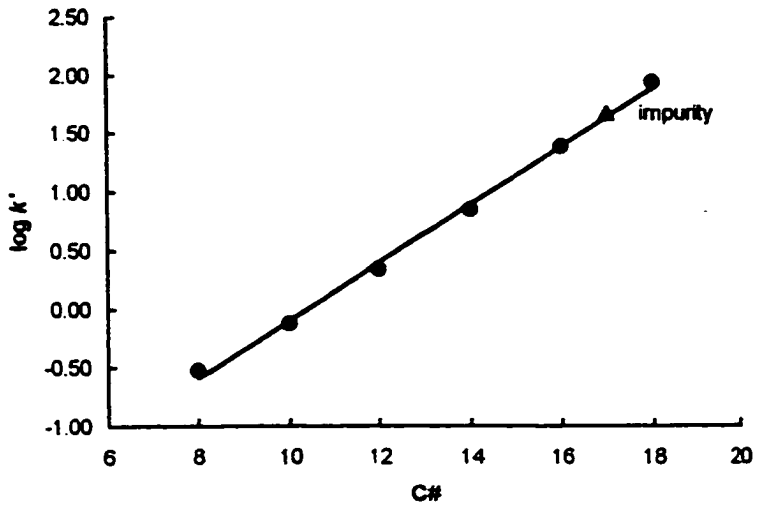

Figure 5-4 Impurity between $(C_{16}N)_2Ar$ and $(C_{18}N)_2Ar$ (85:15 $CH_3CN:H_2O$, 0.1 *M* $NaClO_4$, pH=3, 40°C)

5.3.3 Sodium perchlorate as an ion-interaction reagent

Several organic or inorganic salts, including sodium perchlorate, sodium chloride, sodium hexanesulfonate, and sodium dodecanesulfonate, were added to the mobile phase in order to find the best ion-interaction reagent. The mobile phases containing 1 mM of sodium hexanesulfonate or 0.1 mM of sodium dodecanesulfonate did not give good separation. Sodium chloride gave separation, but sodium perchlorate produced better results. Figure 5-5 provides a comparison of sodium perchlorate and sodium chloride as ion-interaction reagents in the separation of $(C_nN)_2Ar$ surfactants.

There are two differences between chromatograms using sodium perchlorate and sodium chloride. The column efficiency is worse (peak tailing) when sodium chloride is the ion-interaction reagent and retention times are slightly shorter with sodium chloride.

Tailing problems are common for ammonium compounds in RP-HPLC. This is due to the electrostatic interaction between ammonium groups and residual silanol groups on packing materials. One method used to reduce tailing is to cover the residual silanol groups; the other is to cover the amine groups. The ClO_4^- and Cl^- are unlikely to get into the C18 stationary phase to cover the -OH groups. The reason for better peak shape with ClO_4^- is probably that the ammonium group is better covered by ClO_4^-. This fact suggests that

there is a stronger interaction between ammonium groups and ClO_4^-.

The concentration of sodium perchlorate cannot be too low or too high. Insufficient concentration results in poor performance. Excessive concentration can cause solubility problems and column blockage. The optimum concentration is about 0.1 *M*. Figure 5-6 shows that log *k'* is nearly independent of the concentration of sodium perchlorate in the range of 0.05 *M* to 0.2 *M*.

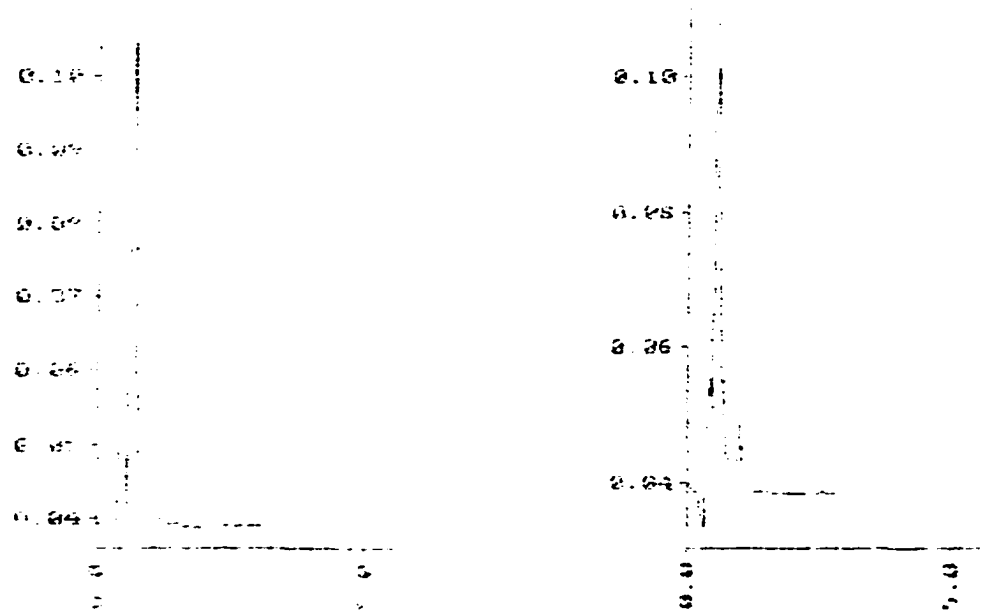

0.05 *M* $NaClO_4$ 0.05 *M* NaCl

C_8

Figure 5-5 Comparison of ion-interaction reagents for chromatography of $(C_nN)_2Ar$ (0.1 m*M*)

Mobile phase:	80:20 $CH_3CN:H_2O$, pH = 3 (H_3PO_4) 0.05 *M* $NaClO_4$ or 0.05 *M* NaCl
Flow rate:	1.0 ml/min
Column:	3x3 C18 (33 x 4.6 mm)
Detection:	220 nm
Injection volume:	5 μl
Temperature:	30.3 °C

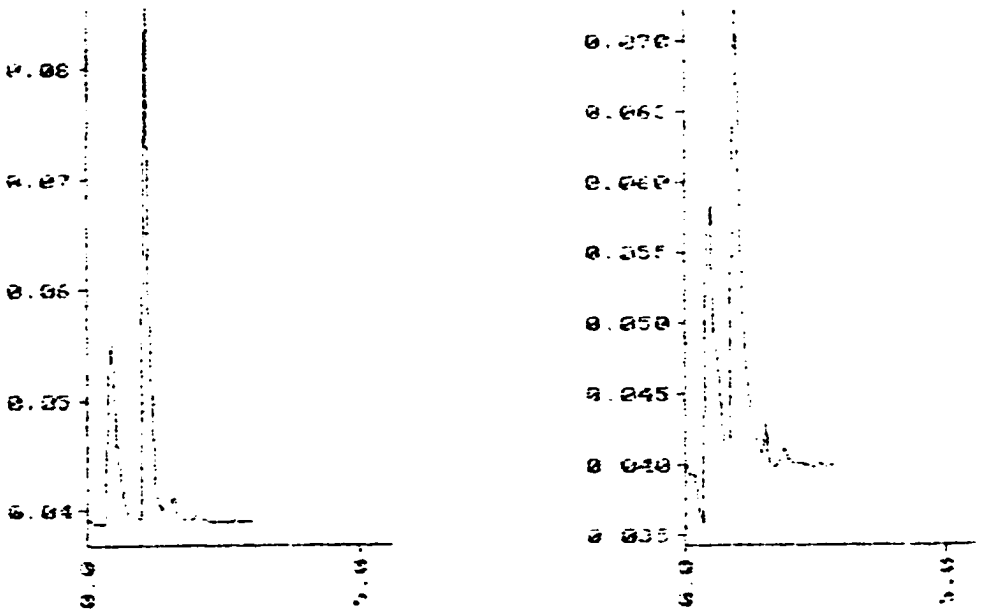

0.05 *M* $NaClO_4$ 0.05 *M* NaCl

C_{10}

Figure 5-5 (Continued)

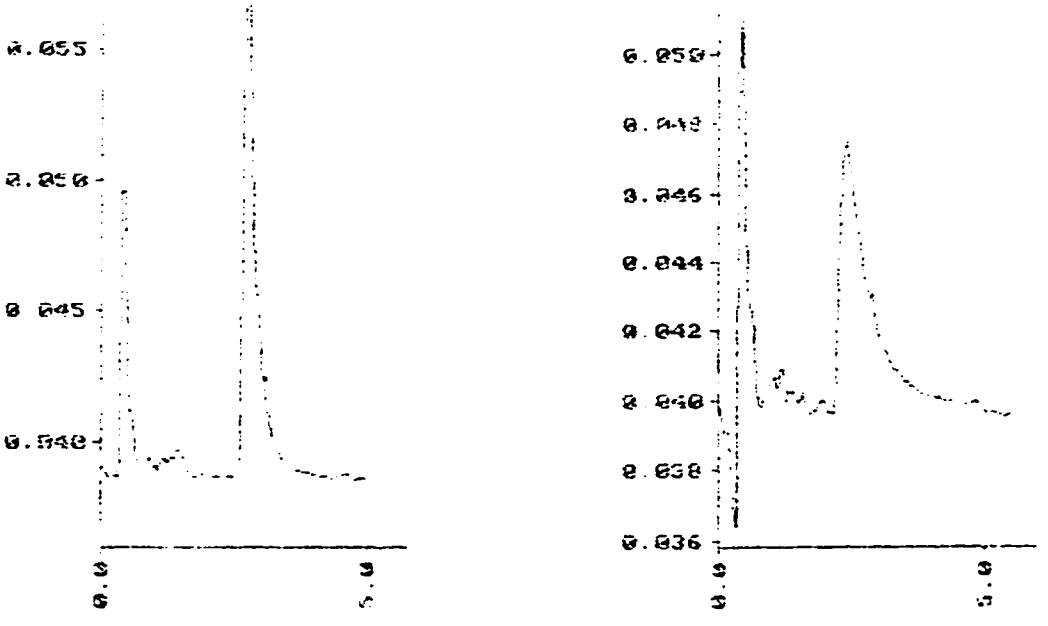

0.05 *M* $NaClO_4$ 0.05 *M* NaCl

C_{12}

Figure 5-5 (Continued)

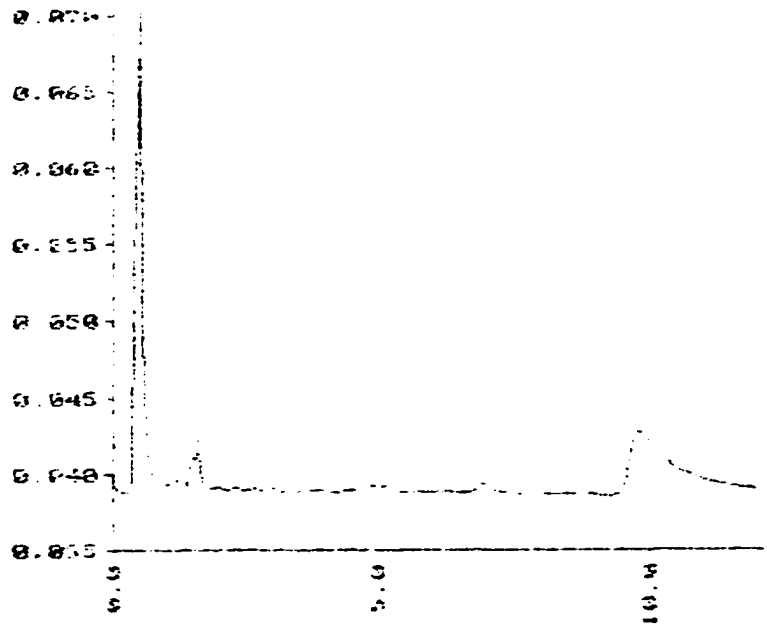

0.05 *M* $NaClO_4$

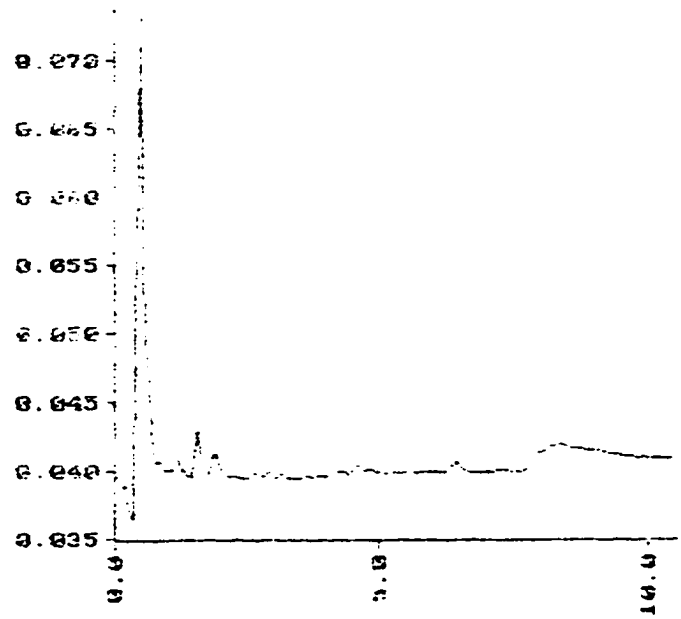

0.05 *M* NaCl

C_{14}

Figure 5-5 (Continued)

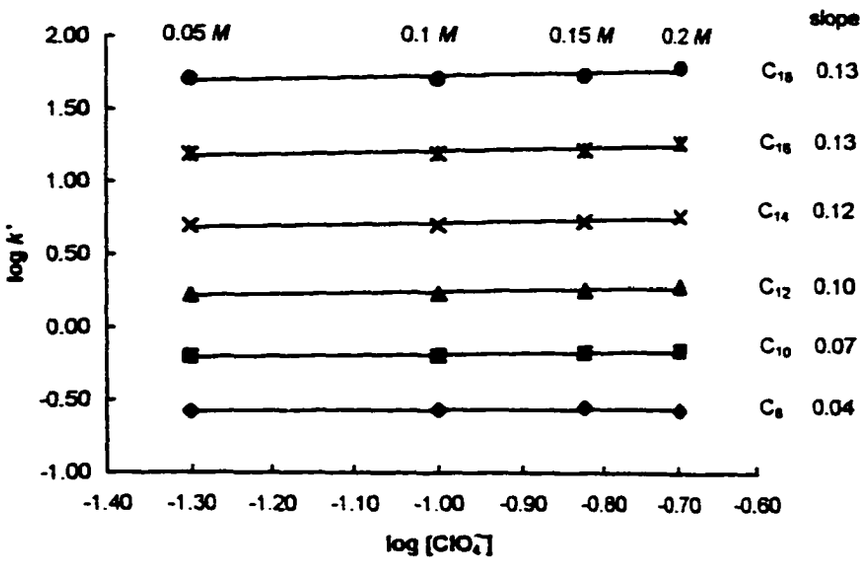

Figure 5-6 log k' vs. log $[ClO_4^-]$ for $(C_nN)_2Ar$ (85:15 $CH_3CN:H_2O$, pH=3, 50.1°C)

5.3.4 33 x 4.6 mm and 150 x 4.6 mm column

Two new 150 x 4.6 columns (C18, 5 μm particle) were used for comparison with the short column. The 150 x 4.6 mm Perkin-Elmer column gave better peak shape than the 33 x 4.6 mm column, but needed much more time. A 150 x 4.6 mm Sigma-Aldrich column did not produce satisfactory results. Under the conditions of 80:20 $CH_3CN:H_2O$ with 0.05 *M* $NaClO_4$ at 40 °C, $(C_{12}N)_2Ar$ retention time is about 2.2 min with the 33 x 4.6 mm column, 9.8 min for the 150 x 4.6 mm Perkin-Elmer column, and 13 min using a 150 x 4.6 mm Sigma-Aldrich column (Figure 5-8). Clearly the advantage of the 33 x 4.6 mm column is quicker separation and less solvent consumption. The drawback is lower column efficiency, however in many cases the separation on the short column is still excellent.

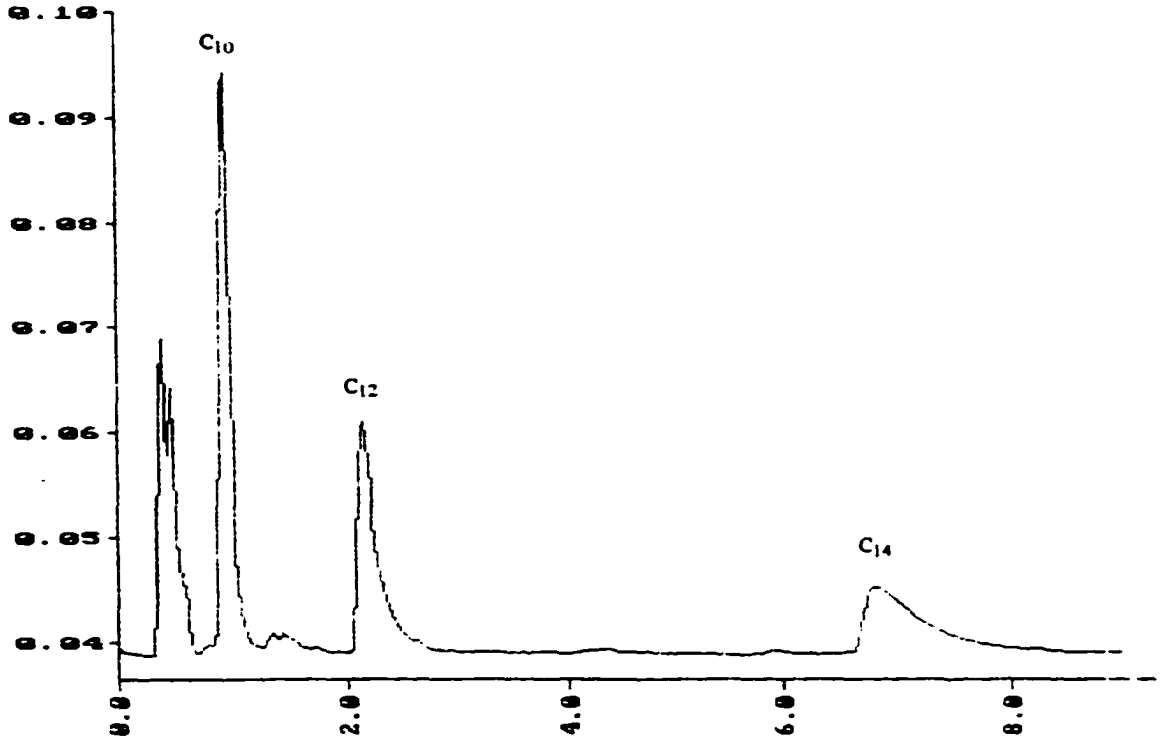

C_{10}, C_{12}, C_{14} mixture with 33 x 4.6 mm (3 μm) column

Figure 5-7 Comparison of 33 x 4.6 mm and 150 x 4.6 mm columns for chromatography of $(C_nN)_2Ar$ (0.1 m*M*)

Mobile phase:	80:20 CH_3CN:H_2O, 0.05 *M* $NaClO_4$, pH = 3 (H_3PO_4)
Flow rate:	1.0 ml/min
Column:	C18
Detection:	220 nm
Injection volume:	5 μl
Temperature:	40.2 °C

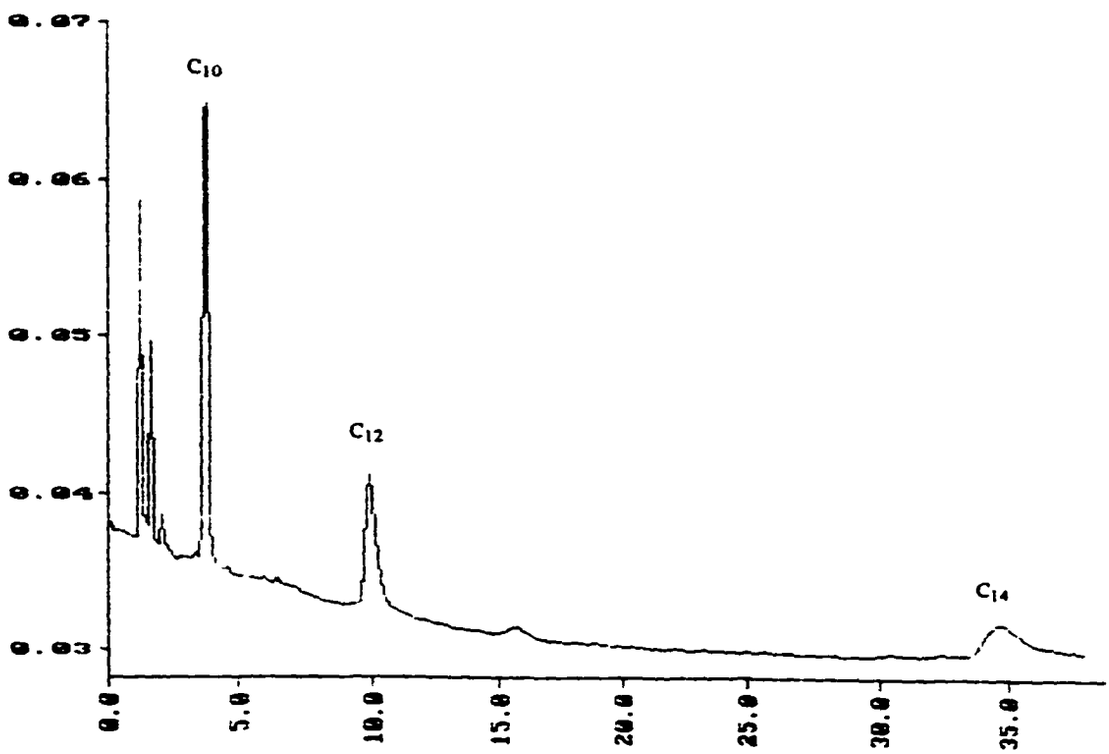

C_{10}, C_{12}, C_{14} mixture with 150 x 4.6 mm (5 μm) Perkin-Elmer column

Figure 5-7 (Continued)

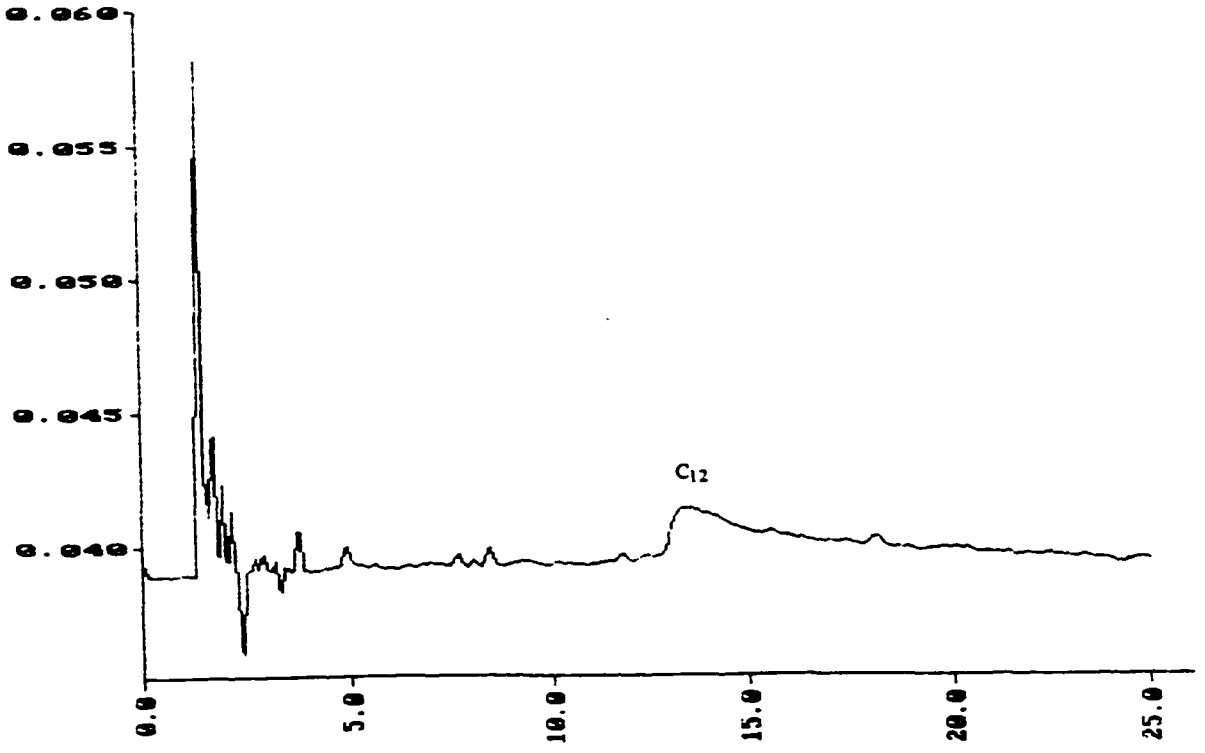

C_{12} with 150 x 4.6 mm (5 μm) Sigma-Aldrich column

Figure 5-7 (Continued)

5.3.5 Surface tension of the solutions in HPLC experiments

The surface tension of a series of $(C_{12}N)_2Ar$ solutions was measured in order to find out the CMC and pC_{20} of the surfactants under the chromatographic condition. The results are in Table 5-2. The surface tension of acetonitrile (HPLC grade) is very low, 28.4 dyne/cm at 30 °C (a literature value[69] is 19.1 dyne/cm). The surface tension of a 80:20 $CH_3CN:H_2O$ solvent is 31.3 dyne/cm at 30 °C. Addition of the ion-interaction reagent and the $(C_{12}N)_2Ar$ surfactant to this solvent does not change the surface tension. Apparently, these surfactants do not form micelles in the chromatographic mobile phases used in our work. The log k' values result from individual surfactants, and are directly proportional to the number of carbon atoms in the alkyl chain.

Table 5-2 Surface tension of solutions in HPLC at 30 °C

Solution	surface tension (dyne/cm)
100% CH_3CN (HPLC grade)	28.4
100% H_2O (distilled and filtered)	71.8
80:20 CH_3CN:H_2O, 0.1 *M* $NaClO_4$, pH = 3 (H_3PO_4) Mobile phase	31.3
12 $(C_{12}N)_2Ar$ solutions with concentrations between 2.6 x 10^{-6} *M* to 1.8 x 10^{-3} *M* in 80:20 CH_3CN:H_2O, 0.1 *M* $NaClO_4$, pH=3 (H_3PO_4) mobile phase	31.3 - 31.5

5.4 Separation Mechanism

5.4.1 Proposed mechanism

The proposed ion-interaction mechanism for $(C_nN)_2Ar$ gemini surfactants is illustrated in Figure 5-8 and 5-9. Figure 5-8 is the retention mechanism with the ion-interaction reagent sodium perchlorate. Figure 5-9 shows a mechanism with sodium chloride. When these inorganic salts are used as ion-interaction reagents in RP-HPLC, the C18 stationary phase surface is not coated by the ion-interaction reagent.

The proposed mechanism suggests that the oppositely charged ions attract each other in the mobile phase. They are separated by solvent molecules and are not tightly bonded. In a polar solvent all ions will be surrounded by polar solvent molecules. The larger and more polarizable ions have a less organized surrounding solvent, whereas the smaller and less polarizable ions have a well organized surrounding solvent. This difference is shown in Figures 5-8 and 5-9. Since perchlorate ions are larger with a diffuse charge, the solvent molecules are not well surrounded compared with chloride. The surfactant ions can stay closer to perchlorate ions than chloride ions. Therefore there is a stronger interaction between ammonium groups on the surfactants and perchlorate ions as discussed in Section 5.3.3, and perchlorate ions give better chromatograms.

The analyte ions of $(C_nN)_2Ar$ move through the column and undergo adsorption and desorption along with some oppositely charged ions from the ion-interaction reagents, even though they are not tightly bonded. The conductance titration results and theoretical considerations discussed in the following sections support this mechanism.

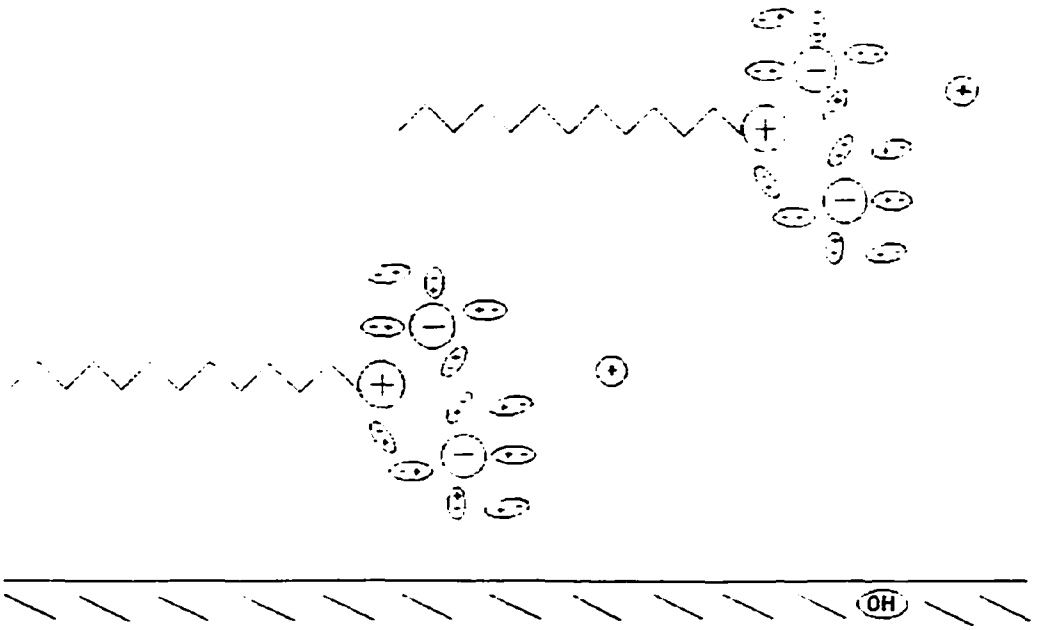

Ion-pairs in the mobile phase

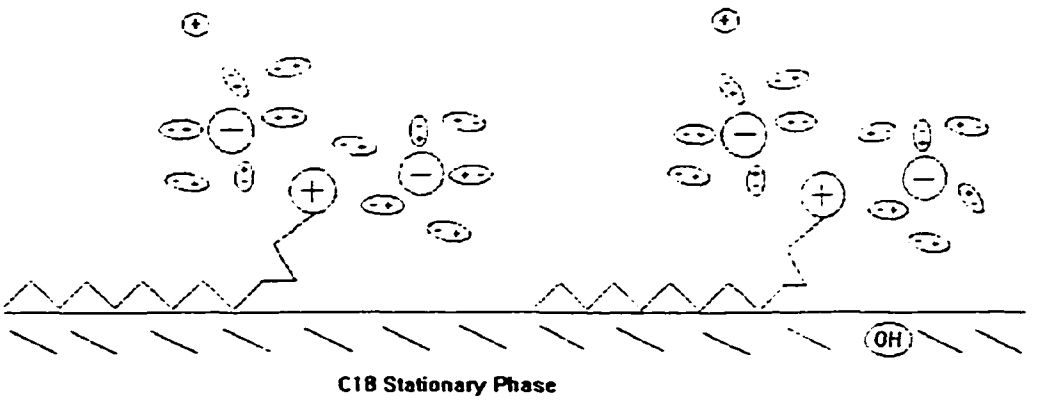

Adsorption on the stationary phase

Figure 5-8 Schematic diagram of $(C_nN)_2Ar$ retention mechanism with ion-interaction reagent $NaClO_4$

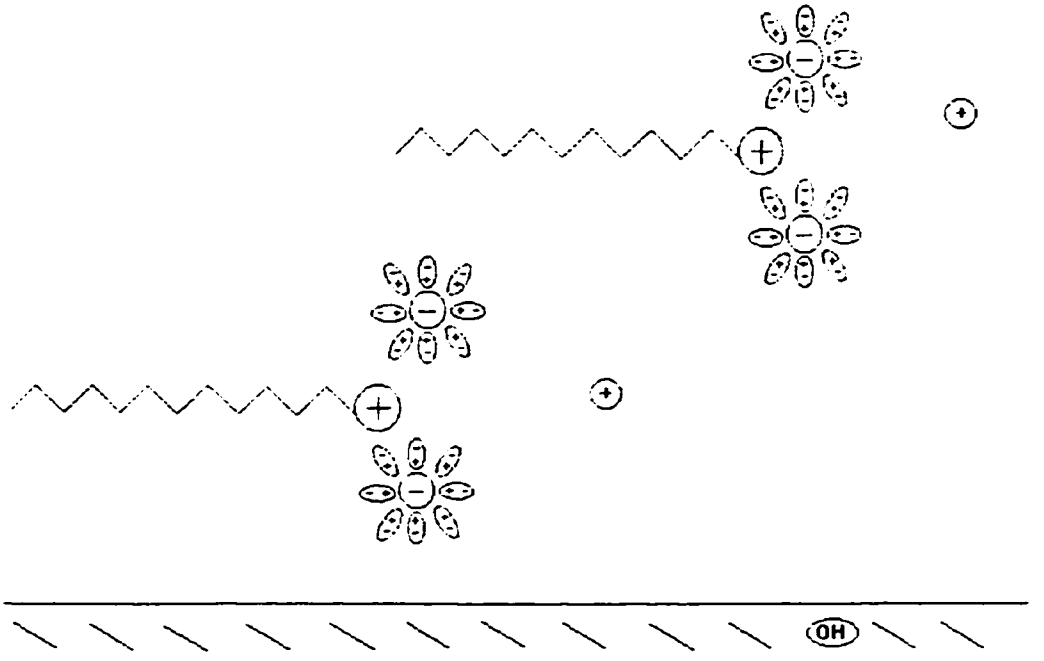

Ion-pairs in the mobile phase

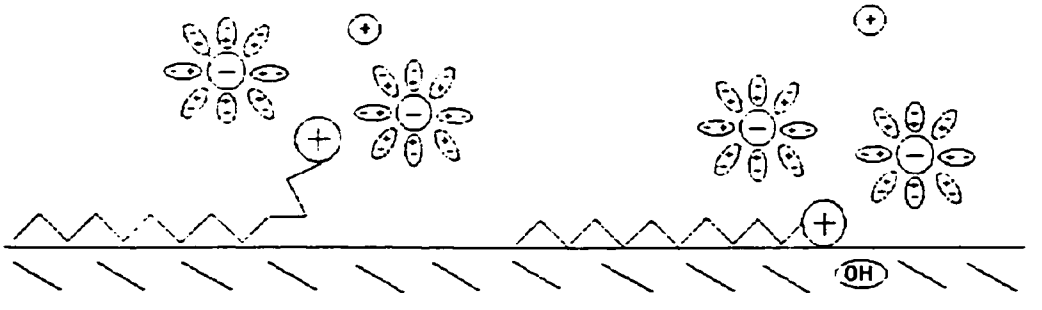

Adsorption on the stationary phase

Figure 5-9 Schematic diagram of $(C_nN)_2Ar$ retention mechanism with ion-interaction reagent NaCl

5.4.2 Conductance titration

Conductance titrations were undertaken for $(C_{12}N)_2Ar$ and $(C_{18}N)_2Ar$ gemini surfactants. Figures 5-10 and 5-11 are the results of the titration of $(C_{12}N)_2ArBr_2$ or $(C_{18}N)_2ArBr_2$ with sodium perchlorate in the 80:20 $CH_3CN:H_2O$ solvent. As discussed in Section 3.4.2, if strongly bonded ion-pairs had formed, before and after the equivalence point the change in the conductance with the same increment of the total salt concentration would be different, and a titration curve would have an inflection point at the equivalence point (approximately 9 mL of sodium perchlorate, 0.27 mM of the total concentration). However, these titration curves are smooth. Plotting the conductivity vs. the total molarity of $(C_nN)_2ArBr_2$ and sodium perchlorate gives straight lines.

The mobilities of $(C_{12}N)_2Ar$ and $(C_{18}N)_2Ar$ cations are different due to their different molecular size. Smaller $(C_{12}N)_2Ar$ ions have a higher mobility and will have a larger conductivity compared with $(C_{18}N)_2Ar$ ions when titration conditions are the same. This difference can be observed from Figures 5-10 and 5-11. The entire titration curve for $(C_{12}N)_2Ar$ is at a conductivity level of about 5 $\mu\Omega^{-1}$/cm higher than for $(C_{18}N)_2Ar$.

The conductance titration results provide additional evidence that tight ion-pairs are not found in these mixtures.

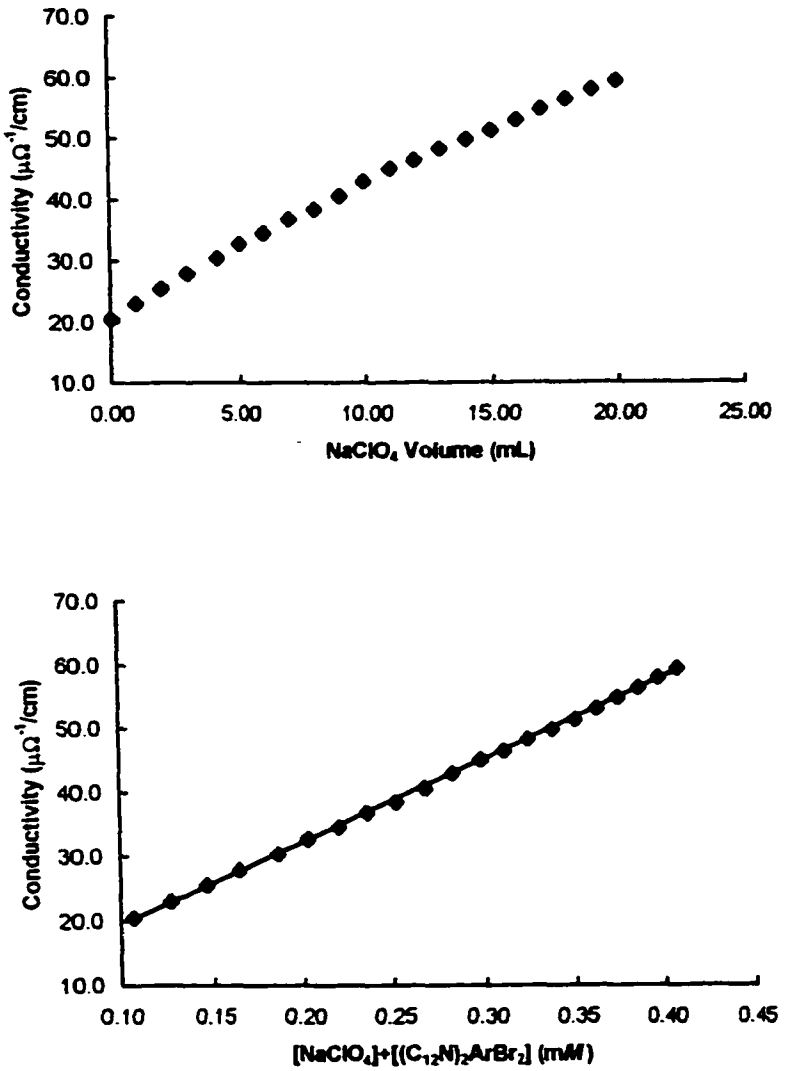

Figure 5-10 Conductance titration 50 mL of 0.107 mM $(C_{12}N)_2ArBr_2$ titrated with 1.16 mM $NaClO_4$ in 80:20 $CH_3CN:H_2O$

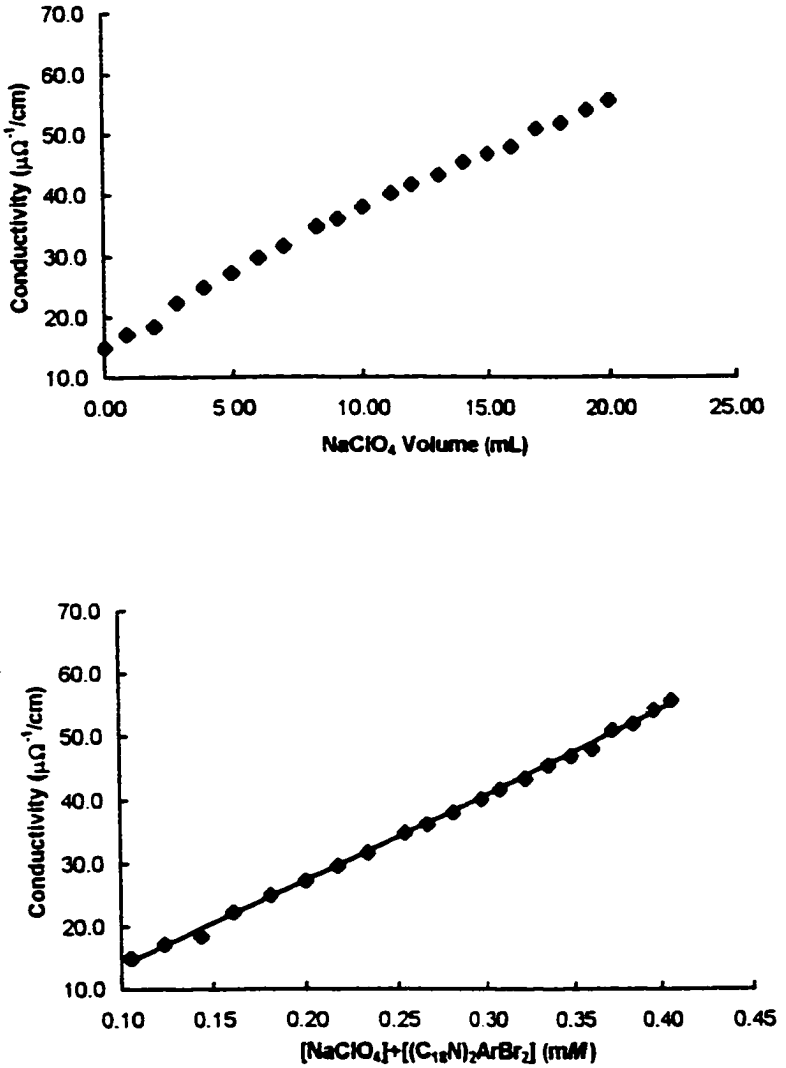

Figure 5-11 Conductance titration 50 mL of 0.105 m*M* $(C_{18}N)_2ArBr_2$ titrated with 1.16 m*M* $NaClO_4$ in 80:20 $CH_3CN:H_2O$

5.4.3 Thermodynamic parameters of chromatography

Combining equations (1-5) and (1-15) with the ΔG, ΔH, and ΔS relationship,

$$K = k' \frac{V_m}{V_s} \qquad (1\text{-}5)$$

$$\Delta G^\circ_{LC} = -2.3RT \log K \qquad (1\text{-}15)$$

$$\Delta G^\circ = \Delta H^\circ - T\Delta S^\circ \qquad (5\text{-}1)$$

the following equation is obtained

$$\Delta H^\circ - T\Delta S^\circ = -RT \ln k' - RT \ln \frac{V_m}{V_s} \qquad (5\text{-}2)$$

The ΔG°, ΔH°, and ΔS° are thermodynamic parameters for the transfer of the surfactant from the mobile phase to the stationary phase.

Then $\ln k'$ can be written as

$$\ln k' = -\frac{\Delta H^\circ}{RT} + \frac{\Delta S^\circ}{R} - \ln \frac{V_m}{V_s} \qquad (5\text{-}3)$$

Assuming ΔH° and ΔS° do not change with the temperature in the range studied, a plot of $\ln k'$ vs. $1/T$ should be a straight line with

$$\text{slope} = -\frac{\Delta H^\circ}{R} \qquad (5\text{-}4)$$

$$\text{intercept} = \frac{\Delta S^\circ}{R} - \ln \frac{V_m}{V_s} \qquad (5\text{-}5)$$

The ΔH° value can be calculated from the slope. Even though the absolute ΔS° value cannot be obtained, relative values can be compared using the intercepts. Figure 5-12 is a plot of log k' vs. $1/T$ for $(C_{18}N)_2Ar$ with sodium perchlorate and sodium chloride as ion-interaction reagents. The values of ΔH° and $\Delta S^\circ - R\ln (V_m/V_s)$ listed in Figure 5-12 are calculated using equations (5-4) and (5-5), where R = 8.314 J/K·mol.

(a) ΔH°, ΔS° and the length of the alkyl chain

The ΔH° values are negative and become more negative with increase in the number of carbon atoms in the alkyl chain for the $(C_nN)_2Ar$ series. The data suggest that the retention process is energetically favored. The longer hydrocarbon chain has a larger London dispersion force and a stronger interaction with the C18 stationary phase. Therefore the ΔH° is more negative for a larger surfactant in the homologous series.

The ΔS° values become more negative or less positive with increase in the length of the alkyl chain, since the $R\ln (V_m/V_s)$ term (Figure 5-12) is approximately a constant. The difference in the randomness of the solvent structure in the presence and absence of alkyl chains will result in this ΔS° difference. The surfactants could affect the entropy of the mobile phase in two ways. The solvent molecules (mainly CH_3CN) are dipoles and have a tendency to arrange themselves

in a certain orientation based on the dipole-dipole interaction. The alkyl chains of the surfactant can disrupt this solvent structure and increase the disorder of the solvent. Solvent molecules can also form cavities for the alkyl chains. In this case the entropy of the solution may decrease, if solvent molecules are more ordered around the alkyl chain. Since there is no ΔS° value, we can not make conclusion. The difference in the entropy change is also associated with the interaction of the alkyl chain with the stationary phase. When retention occurs the configurational entropy of the larger surfactant will be largely reduced because of a stronger interaction between the longer alkyl chain and the C18 phase. This can be part of the less favorable ΔS° for a larger surfactant.

The ΔG° is a combination of ΔH° and ΔS°. Here the more favorable ΔH° values of the larger surfactants compensate their less favorable ΔS° values. Hence ΔG° is more negative and retention is favored for larger homologs.

(b) ΔH°, ΔS° and perchlorate vs. chloride ions

The ΔH° values are more negative when sodium chloride is used as an ion-interaction reagent. This can be explained with the model of solvent separated ions. As discussed in Section 5.4.1, the perchlorate ion does not form a well-oriented surrounding solvent layer as does sodium chloride. The ammonium group and the ClO_4^- ion can remain closer. Thus, the quaternary ammonium surfactants interact more strongly

with perchlorate ion than chloride ion. The mobile phase with perchlorate ion has a lower energy. When the surfactants transfer to the stationary phase, it is primarily the surfactant alkyl chains that interact with the C18 stationary phase, and the enthalpies will be similar or slightly lower with the perchlorate system. Therefore the enthalpy change of the transfer is less negative for the sodium perchlorate system.

The ΔS° values are more negative or less positive when sodium chloride mobile phase is used. The difference in the surrounding solvent structures of the ion-interaction reagents can cause an entropy difference between two mobile phases. In addition, the data suggest that the entropy changes of the retention process in two mobile phases are different. However, there is no enough information about the direction of the entropy change. The entropies of the stationary phases in two systems should be similar initially. When the retention occurs, the entropy of the chloride system can be slightly lower because of a stronger interaction between the quaternary ammonium groups and silanol groups on the stationary phase. This can contribute to less favorable ΔS° values for the retention process in the chloride system.

Since ΔG° is given by

$$\Delta G^\circ = \Delta H^\circ - T\Delta S^\circ \qquad (5\text{-}8)$$

The mobile phase with sodium perchlorate has a slightly more negative ΔG°, which leads to longer retention times.

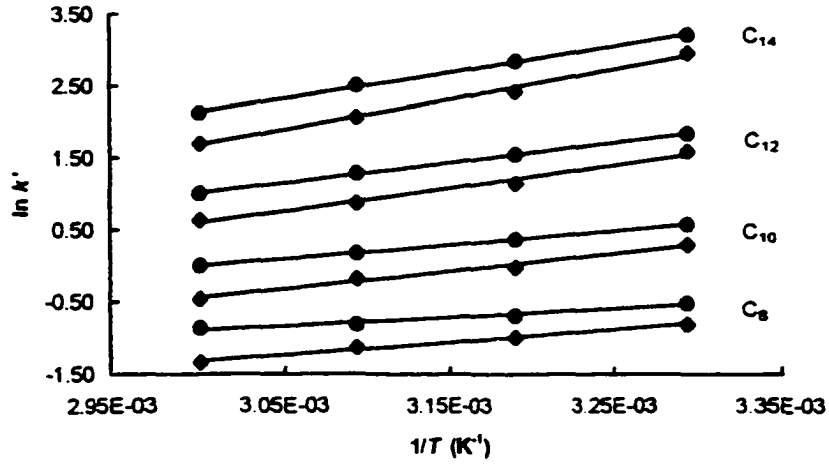

● 0.05 *M* $NaClO_4$ in 80/20 CH_3CN/H_2O, pH=3
◆ 0.05 *M* NaCl in 80/20 CH_3CN/H_2O, pH=3

	ΔH° (kJ/mol)		$\Delta S^\circ - R\ln(V_m/V_s)$ (J/mol)	
	$NaClO_4$	NaCl	$NaClO_4$	NaCl
C_8	-9.8	-14.7	-36.9	-55.0
C_{10}	-16.1	-20.5	-48.5	-65.2
C_{12}	-23.4	-26.8	-61.9	-75.6
C_{14}	-30.4	-35.0	-73.4	-91.0

Figure 5-12 ln *k'* vs. 1/*T* for $(C_nN)_2Ar$

5.4.4 Equilibrium considerations

The chromatographic experiments and the thermodynamic parameters show that there are interactions between the surfactants and the ion-interaction reagent. Since the oppositely charged ions are separated by solvent molecules and are not tight ion-pairs, they behave independently as evidenced by the conductance titrations.

Even though the ions are separated by the solvent molecules, the following chemical equilibria should be still applicable to the retention process.

$$(C_nN)_2Ar^{2+}(m) + 2ClO_4^-(m) \overset{K_1}{\rightleftharpoons} (C_nN)_2Ar(ClO_4)_2(m)$$

$$(C_nN)_2Ar(ClO_4)_2(m) \overset{K_2}{\rightleftharpoons} (C_nN)_2Ar(ClO_4)_2(s)$$

Where m represents the mobile phase and s the stationary phase. The coefficient for ClO_4^- could be any number, *n*. The overall equilibrium expression is

$$K_1K_2 = \frac{[(C_nN)_2Ar(ClO_4)_2(s)]}{[(C_nN)_2Ar^{2+}(m)]\,[ClO_4^-(m)]^2} \qquad (5\text{-}6)$$

This equation can be rearranged to express the ratio of the analyte ion concentration in the two phases:

$$\frac{[(C_nN)_2Ar(ClO_4)_2(s)]}{[(C_nN)_2Ar^{2+}(m)] + [(C_nN)_2Ar(ClO_4)_2(m)]} = \frac{[(C_nN)_2Ar^{2+}(m)][ClO_4^-(m)]^2K_1K_2}{[(C_nN)_2Ar^{2+}(m)] + [(C_nN)_2Ar(ClO_4)_2(m)]} \quad (5\text{-}7)$$

The capacity factor, k', equals the ratio of moles of solute in the stationary phase to that in the mobile phase at equilibrium.

$$k' = \frac{[(C_nN)_2Ar(ClO_4)_2(s)]V_s}{([(C_nN)_2Ar^{2+}(m)] + [(C_nN)_2Ar(ClO_4)_2(m)])V_m} \quad (5\text{-}8)$$

where V_s is the volume of the stationary phase, and V_m is the column void volume. Combining equation (5-8) with equation (5-7) gives

$$k' = K_1K_2\frac{[(C_nN)_2Ar^{2+}(m)][ClO_4^-(m)]^2V_s}{([(C_nN)_2Ar^{2+}(m)] + [(C_nN)_2Ar(ClO_4)_2(m)])V_m} \quad (5\text{-}9)$$

Then,

$$\log k' = \log K_1K_2\frac{V_s}{V_m} - \log \frac{[(C_nN)_2Ar^{2+}(m)] + [(C_nN)_2Ar(ClO_4)_2(m)]}{[(C_nN)_2Ar^{2+}(m)][ClO_4^-(m)]^2} \quad (5\text{-}10)$$

where all concentrations refer to the mobile phase species. The log k' value changes with log $[ClO_4^-](m)$. But if there are solvent separated paired ions, $[(C_nN)_2Ar^{2+}]$ will be much less

than $[(C_nN)_2Ar(ClO_4)_2]$ in the presence of excess ClO_4^-. Then the second term in the equation (5-10) becomes the equilibrium expression of K_1.

$$K_1 = \frac{[(C_nN)_2Ar(ClO_4)_2(m)]}{[(C_nN)_2Ar^{2+}(m)]\,[ClO_4^-(m)]^2} \qquad (5\text{-}11)$$

Thus, log k' is unaffected by the change of log $[ClO_4^-]$. This is observed in our experiment (Figure 5-6).

Chapter 6

log CMC, pC_{20} and log k' of Aromatic Quaternary Ammonium Geminis

6.1 Correlation between log CMC, pC_{20} and log k'

This series of aromatic quaternary ammonium gemini surfactants, $(C_nN)_2Ar$, has unusual surface and micellar properties in water. The surface tension measurement results[70] showed that their log CMC and pC_{20} values deviate from the linear relation with the alkyl chain length for the larger homologs. The C_{14}, C_{16} and C_{18} surfactants in this series have higher CMC values and lower pC_{20} values than they are expected to have. This unusual property is also reflected in the log CMC and log k', pC_{20} and log k' correlations. Since there is no micelle formation in the chromatographic mobile phases used in our work, log k' vs. carbon number is almost linear. Therefore, equations (1-25) and (1-27) only apply to the lower members, C_8, C_{10} and C_{12}.

$$\log CMC = - m\log k' + c \qquad (1\text{-}25)$$

$$pC_{20} = m'\log k' + c' \qquad (1\text{-}27)$$

Plotting the literature log CMC and pC_{20} values[70] vs. our

experimental log k' gives straight lines for C_8, C_{10} and C_{12} as showed in Figures 6-1 and 6-2. The deviations of C_{14}, C_{16} and C_{18} from linearity will be discussed in the next section.

Table 6-1 lists the literature[70] and calculated log CMC and pC_{20} values, where the summary is the average over all calculated values. The calculated values were obtained using our log k' values and equations (1-25) and (1-27). The slopes and intercepts in the equations were defined with the C_8 and C_{12} data.

The results show a good agreement between experimental and calculated values for $(C_{10}N)_2Ar$. The standard deviation over all calculated values is small. But the calculated log CMC values of C_{14}, C_{16} and C_{18} are smaller than experimental data, and the pC_{20} values are larger. These deviations are similar to the surface tension measurement results (see Section 6-2). The results suggest that the prediction of log CMC and pC_{20} using log k' is applicable for the normal behaved surfactants.

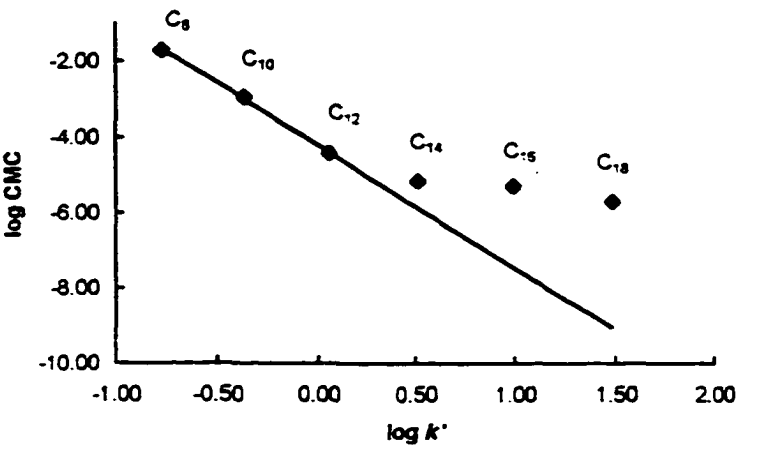

(a)

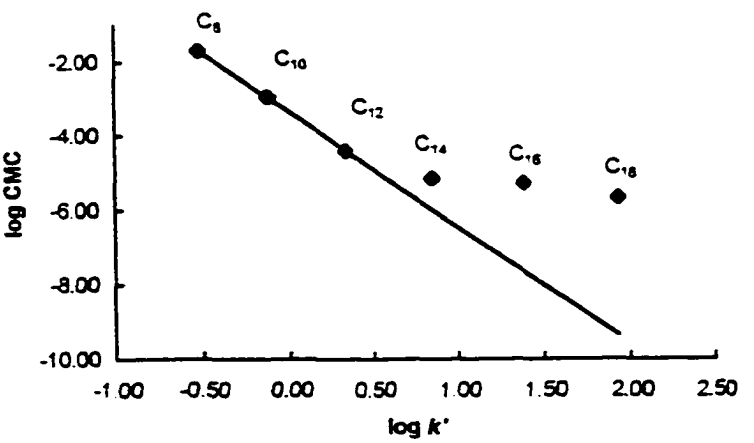

(b)

Figure 6-1 Correlation between log CMC and log k' for $(C_nN)_2Ar$

(a) log k': 90:10 $CH_3CN:H_2O$, 0.1 M $NaClO_4$, 40°C
(b) log k': 85:15 $CH_3CN:H_2O$, 0.1 M $NaClO_4$, 40°C

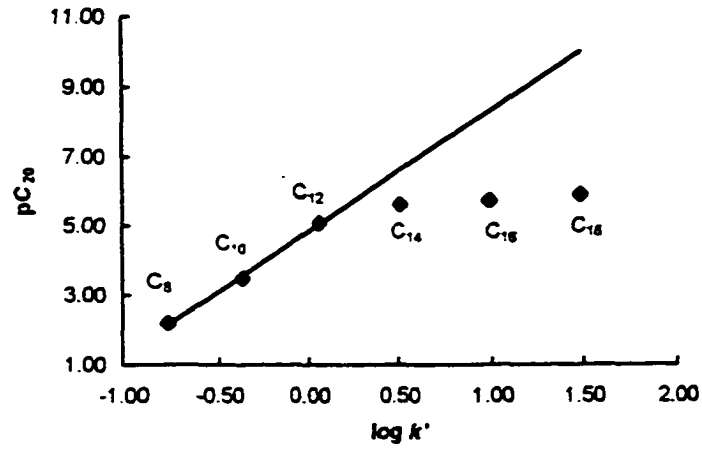

(a)

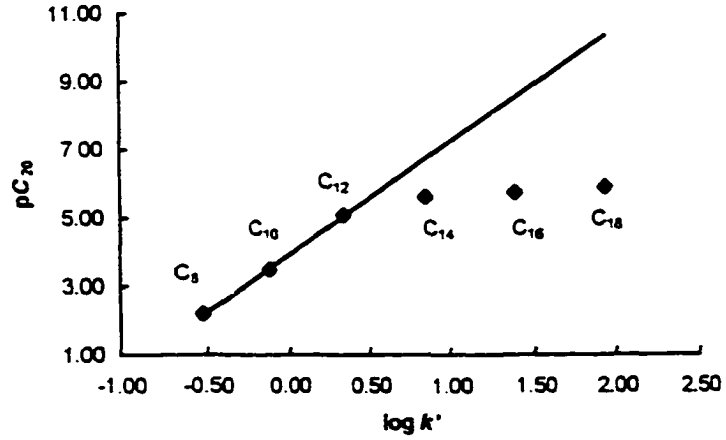

(b)

Figure 6-2 Correlation between pC_{20} and log k' for $(C_nN)_2Ar$

(a) log k': 90:10 $CH_3CN:H_2O$, 0.1 M $NaClO_4$, 40°C
(b) log k': 85:15 $CH_3CN:H_2O$, 0.1 M $NaClO_4$, 40°C

Table 6-1 log CMC and pC_{20} of aromatic quaternary ammonium geminis surfactants $(C_nN)_2Ar$

		Exp.*	C_8**	C_{10}	C_{12}**	C_{14}	C_{16}	C_{18}
		log CMC	-1.70	-2.94	-4.40	-5.14	-5.27	-5.68
		pC_{20}	2.20	3.48	5.08	5.62	5.74	5.90
HPLC condition	T(+-0.1°C)	Cal.						
95:5 $CH_3CN:H_2O$, 0.1*M* $NaClO_4$	30.3	log CMC	-	-3.11	-	-5.75	-7.16	-8.64
pH=2(H_3PO_4)		pC_{20}	-	3.71	-	6.52	8.03	9.60
	40.2	log CMC	-	-3.05	-	-5.79	-7.24	-8.69
		pC_{20}	-	3.64	-	6.56	8.11	9.66
	50.1	log CMC	-	-2.90	-	-5.79	-7.18	-8.64
		pC_{20}	-	3.48	-	6.56	8.04	9.60
90:10 $CH_3CN:H_2O$, 0.1*M* $NaClO_4$	30.3	log CMC	-	-3.06	-	-5.85	-7.40	-8.97
pH=3(H_3PO_4)		pC_{20}	-	3.66	-	6.63	8.28	9.95
	40.3	log CMC	-	-3.00	-	-5.86	-7.43	-9.02
		pC_{20}	-	3.59	-	6.64	8.31	10.01
	50.1	log CMC	-	-3.03	-	-5.87	-7.42	9.00
		pC_{20}	-	3.62	-	6.65	8.30	9.98
85:15 $CH_3CN:H_2O$, 0.1*M* $NaClO_4$	30.2	log CMC	-	-2.93		-5.95	-7.62	-8.98
pH=3(H_3PO_4)		pC_{20}	-	3.52	-	6.73	8.51	9.96
	40.2	log CMC	-	-2.97	-	-5.98	-7.63	-9.34
		pC_{20}	-	3.56	-	6.77	8.52	10.34
	50.1	log CMC	-	-2.98	-	-5.99	-7.68	-9.40
		pC_{20}	-	3.57	-	6.77	8.57	10.41

Table 6-1 (Continued)

		Exp.*	C_8**	C_{10}	C_{12}**	C_{14}	C_{16}	C_{18}
		log CMC	-1.70	-2.94	-4.40	-5.14	-5.27	-5.68
		pC_{20}	2.20	3.48	5.08	5.62	5.74	5.90
HPLC condition	T(+-0.1°C)	Cal.						
80:20 $CH_3CN:H_2O$, 0.1*M* $NaClO_4$	30.3	log CMC	-	-2.97	-	-5.96	-7.59	-8.96
pH=3(H_3PO_4)		pC_{20}	-	3.56	-	6.74	8.49	9.94
	40.2	log CMC	-	-2.25	-	-5.94	-7.60	-9.03
		pC_{20}	-	2.79	-	6.73	8.49	10.01
	50.1	log CMC	-	-2.98	-	-5.94	-7.57	-8.93
		pC_{20}	-	3.56	-	6.72	8.46	9.90
85:15 $CH_3CN:H_2O$, 0.05*M* $NaClO_4$	30.3	log CMC	-	-2.99	-	-5.98	-7.65	-9.01
pH=3(H_3PO_4)		pC_{20}	-	3.58	-	6.77	8.54	9.99
	40.2	log CMC	-	-3.00	-	-5.95	-7.59	-9.26
		pC_{20}	-	3.59	-	6.73	8.48	10.26
	50.1	log CMC	-	-2.98	-	-5.97	-7.64	-9.37
		pC_{20}	-	3.56	-	6.76	8.53	10.38
85:15 $CH_3CN:H_2O$, 0.15*M* $NaClO_4$	30.3	log CMC	-	-2.97	-	-5.95	-7.58	-8.94
pH=3(H_3PO_4)		pC_{20}	-	3.55	-	6.73	8.47	9.92
	40.2	log CMC	-	-3.02	-	-5.91	-7.49	-9.11
		pC_{20}	-	3.61	-	6.69	8.37	10.10
	50.1	log CMC	-	-2.97	-	-5.99	-7.66	-9.38
		pC_{20}	-	3.55	-	6.78	8.56	10.39

Table 6-1 (Continued)

		Exp.*	C_8**	C_{10}	C_{12}**	C_{14}	C_{16}	C_{18}
		log CMC	-1.70	-2.94	-4.40	-5.14	-5.27	-5.68
		pC_{20}	2.20	3.48	5.08	5.62	5.74	5.90
HPLC condition	T(+-0.1°C)	Cal.						
85:15 $CH_3CN:H_2O$, 0.2*M* $NaClO_4$	30.3	log CMC	-	-2.97	-	-5.94	-7.55	-8.91
pH=3(H_3PO_4)		pC_{20}	-	3.56	-	6.72	8.44	9.89
	40.2	log CMC	-	-3.00	-	-5.91	-7.50	-9.12
		pC_{20}	-	3.59	-	6.69	8.38	10.11
	50.1	log CMC	-	-3.00	-	-5.92	-7.51	-9.15
		pC_{20}	-	3.58	-	6.70	8.40	10.14
80:20 $CH_3CN:H_2O$, 0.05*M* $NaClO_4$	30.3	log CMC	-	-2.95	-	-5.98	-7.67	-9.03
pH=3(H_3PO_4)		pC_{20}	-	3.54	-	6.76	8.56	10.01
	40.2	log CMC	-	-2.96	-	-5.96	-7.62	-8.98
		pC_{20}	-	3.55	-	6.74	8.52	9.97
	50.1	log CMC	-	-2.98	-	-5.96	-7.61	-8.97
		pC_{20}	-	3.56	-	6.74	8.51	9.96
	60.0	log CMC	-	-2.95	-	-6.01	-7.72	-9.09
		pC_{20}	-	3.53	-	6.79	8.62	10.08
' 80:20 $CH_3CN:H_2O$, 0.05*M* $NaClO_4$	40.2	log CMC	-	-2.96	-	-5.96	-7.31	-8.74
pH=3(H_3PO_4)		pC_{20}	-	3.54	-	6.75	8.19	9.70
"80:20 $CH_3CN:H_2O$, 0.05*M* $NaClO_4$	40.2	log CMC	-	-2.80	-	-5.67	-7.02	-8.37
pH=3(H_3PO_4)		pC_{20}	-	3.37	-	6.43	7.87	9.31

Table 6-1 (Continued)

		Exp.*	C_8**	C_{10}	C_{12}**	C_{14}	C_{16}	C_{18}
		log CMC	-1.70	-2.94	-4.40	-5.14	-5.27	-5.68
		pC_{20}	2.20	3.48	5.08	5.62	5.74	5.90
HPLC condition	T(+-0.1°C)	Cal.						
80:20 $CH_3CN:H_2O$, 0.05*M* NaCl	30.3	log CMC	-	-2.94	-	-5.94	-7.29	-8.71
pH=3(H_3PO_4)		pC_{20}	-	3.52	-	6.72	8.16	9.67
	40.2	log CMC	-	-2.93	-	-6.03	-7.77	-9.14
		pC_{20}	-	3.51	-	6.81	8.67	10.13
	50.1	log CMC	-	-2.99	-	-6.02	-7.75	-9.11
		pC_{20}	-	3.57	-	6.81	8.65	10.10
	60.0	log CMC	-	-2.90	-	-5.87	-7.48	-8.83
		pC_{20}	-	3.48	-	6.65	8.36	9.80
Summary		log CMC	-	-2.96	-	-5.92	-7.51	-8.99
		stdev	-	1.4E-01	-	6.9E-02	1.6E-01	2.1E-01
		pC_{20}	-	3.53	-	6.70	8.39	9.97
		stdev	-	7.0E-02	-	5.6E-02	1.4E-01	1.7E-01

* CMC and pC_{20} were measured in 0.1 *M* NaCl, at 50 °C[70].

** Used to determine parameters in equations (1-25) and (1-27).

' 150 x 4.6 C18 Perkin-Elmer column.

'' 150 x 4.6 C18 Sigma-Aldrich column.

6.2 Discussion

6.2.1 Irregularity of C_{14}, C_{16} and C_{18}

The study of the aromatic quaternary ammonium gemini surfactants at the Surfactant Research Institute of Brooklyn College shows a regular change of log CMC and pC_{20} with increase in the alkyl chain length for the shorter homologs, but an unexpected deviation from the regularity for C_{14}, C_{16} and C_{18} in water (Figure 6-3)[70]. The proposed reason is the formation of premicellar aggregates which have little or no surface activity before the micelle formation. The premicellar aggregates change the surface property of these surfactants. Therefore surface tension measurement gives the unexpected CMC and pC_{20} values for C_{14}, C_{16}, and C_{18}.

Because the premicellar aggregation occurs in the aqueous solution but not in the chromatographic mobile phases used in our work, the measured CMC and pC_{20} values of C_{14}, C_{16}, and C_{18} from surface properties cannot be used to calculate the slopes and intercepts in equations (1-25) and (1-27). However one can use equations (1-25) and (1-27) to estimate what the CMC and pC_{20} would be if there were no premicellar aggregates. The calculated log CMC and pC_{20} values of $(C_{14}N)_2Ar$, $(C_{16}N)_2Ar$, and $(C_{18}N)_2Ar$ listed in Table 6-1 are the expected values. These results correspond well with the expected values extrapolated from the linear relationship between the log CMC, pC_{20} and the alkyl chain length (see Table 6-2).

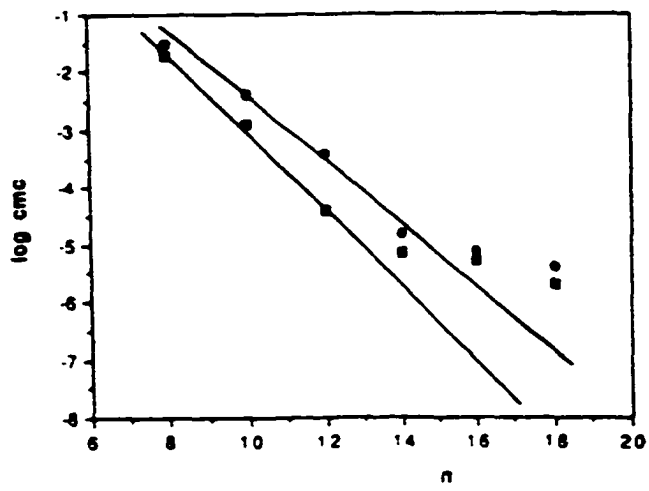

log CMC vs. carbon number

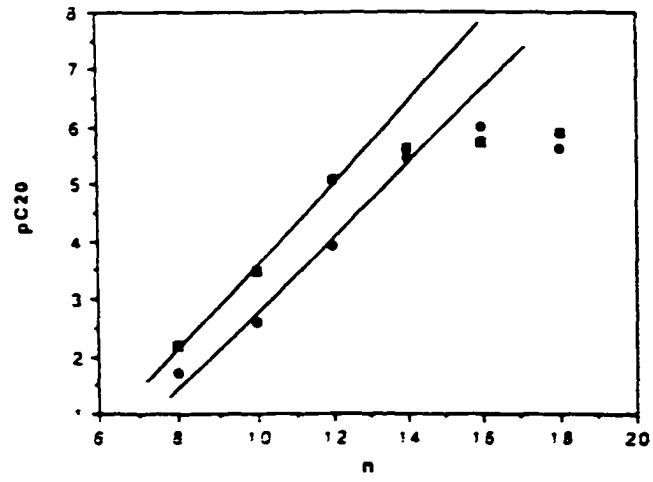

pC_{20} vs. carbon number

Figure 6-3 Unexpected surface properties of aromatic quaternary ammonium gemini surfactants[70] ● in 0.01 *M* NaCl; ■ in 0.1 *M* NaCl.

Table 6-2 Expected log CMC and pC_{20} of $(C_{14}N)_2Ar$, $(C_{16}N)_2Ar$, and $(C_{18}N)_2Ar$

Method	C_{14}	C_{16}	C_{18}
log CMC			
log CMC vs. carbon atom number*	-5.75	-7.10	-8.45
log CMC vs. log k'**	-5.92	-7.51	-8.99
pC_{20}			
pC_{20} vs. carbon atom number*	6.52	7.96	9.40
pC_{20} vs. log k'**	6.70	8.39	9.97

* Ref. [70].
** The summary values in Table 6-1.

6.2.2 log CMC and log k'

The values of the slope and intercept from equation (1-25) are listed in Table 6-3.

$$\log CMC = - m \log k' + c \qquad (1\text{-}25)$$

These values are calculated using C_8 and C_{12} data. The log k' values are averages over various sets of chromatographic experiments.

The slope varies from -2.6 to -3.8. It becomes more negative with increase in the acetonitrile percentage and temperature in HPLC experiments. As discussed in Section 4.2.1, the slope is a measure of different tendencies for a homologous series of surfactants to partition onto the HPLC stationary phase (the monomer adsorbing onto the interface) and to self-associate (micellization) in aqueous solution

The intercept is between -2.3 to -5.6. It is more negative when the acetonitrile percentage and temperature increase in HPLC experiments. The change of the intercept is greater than the slope change. Therefore the change in the difference between the HPLC and micelle environments has a larger effect on the intercept than the slope.

Table 6-3 Parameters in the log CMC and log *k'* correlation equation for $(C_nN)_2Ar$ surfactants

HPLC condition	T(+-0.1°C)	Slope	Intercept
95:5 $CH_3CN:H_2O$, 0.1 *M* $NaClO_4$	30.3	-3.14	-4.65
pH=2(H_3PO_4)	40.2	-3.46	-5.13
	50.1	-3.75	-5.60
90:10 $CH_3CN:H_2O$, 0.1 *M* $NaClO_4$	30.3	-2.97	-3.93
pH=3(H_3PO_4)	40.3	-3.25	-4.20
	50.1	-3.51	-4.61
85:15 $CH_3CN:H_2O$, 0.1 *M* $NaClO_4$	30.2	-2.87	-3.05
pH=3(H_3PO_4)	40.2	-3.10	-3.34
	50.1	-3.38	-3.62
80:20 $CH_3CN:H_2O$, 0.1 *M* $NaClO_4$	30.3	-2.60	-2.37
pH=3(H_3PO_4)	40.2	-2.76	-2.61
	50.1	-2.90	-2.92
85:15 $CH_3CN:H_2O$, 0.05 *M* $NaClO_4$	30.3	-2.87	-3.02
pH=3(H_3PO_4)	40.2	-3.03	-3.34
	50.1	-3.35	-3.65
85:15 $CH_3CN:H_2O$, 0.15 *M* $NaClO_4$	30.3	-2.80	-2.96
pH=3(H_3PO_4)	40.2	-2.93	-3.30
	50.1	-3.36	-3.54

Table 6-3 (Continued)

HPLC condition	T(+-0.1°C)	Slope	Intercept
85:15 $CH_3CN:H_2O$, 0.2 *M* $NaClO_4$	30.3	-2.76	-2.95
pH=3(H_3PO_4)	40.2	-2.92	-3.22
	50.1	-3.15	-3.49
80:20 $CH_3CN:H_2O$, 0.05 *M* $NaClO_4$	30.3	-2.65	-2.30
pH=3(H_3PO_4)	40.2	-2.78	-2.54
	50.1	-2.95	-2.76
	60.0	-3.33	-2.95
*80:20 $CH_3CN:H_2O$, 0.05 *M* $NaClO_4$	40.2	-2.67	-2.20
**80:20 $CH_3CN:H_2O$, 0.05 *M* $NaClO_4$	40.2	-3.00	-1.64
80:20 $CH_3CN:H_2O$, 0.05 *M* NaCl	30.3	-2.60	-2.61
pH=3(H_3PO_4)	40.2	-2.92	-2.95
	50.1	-3.12	-3.23
	60.0	-3.16	-3.53

* 150 x 4.6 C18 Perkin-Elmer column.
** 150 x 4.6 C18 Sigma-Aldrich column.

6.2.3 pC_{20} and log k'

The values of the slope and intercept from equation (1-27) are listed in Table 6-4.

$$pC_{20} = m' \log k' + c' \qquad (1\text{-}27)$$

They are obtained using C_8 and C_{12} data. The log k' values are averages over various sets of chromatographic experiments.

The slope is in the range of 2.8 to 4.0, which increases with increase in the acetonitrile percentage and temperature in the HPLC experiments. This slope is a measure of the different tendencies for partitioning between the aqueous methanol-C_{18} interface and the water-air interface for a homologous series of surfactants.

The intercept becomes more positive as the acetonitrile percentage and temperature are increased because of the decrease in log k'. Its value is between 2.7 to 6.4, and the change is greater than the slope change. As mentioned previously, the change in the difference between the two environments has a larger effect on the intercept.

The slope and intercept from equations (1-25) and (1-27) vary among different sets of chromatographic data. If two series of surfactants are chromatographed under the same conditions, these parameters can be compared. The comparison will be made in Chapter 8 for two series of nonaromatic quaternary ammonium gemini surfactants.

Table 6-4 Parameters in the pC_{20} and log k' correlation equation for $(C_nN)_2Ar$ surfactants

HPLC condition	T(+-0.1°C)	Slope	Intercept
95:5 $CH_3CN:H_2O$, 0.1 *M* $NaClO_4$	30.3	3.35	5.35
pH=2(H_3PO_4)	40.2	3.69	5.86
	50.1	4.00	6.36
90:10 $CH_3CN:H_2O$, 0.1 *M* $NaClO_4$	30.3	3.16	4.57
pH=3(H_3PO_4)	40.3	3.47	4.87
	50.1	3.74	5.30
85:15 $CH_3CN:H_2O$, 0.1 *M* $NaClO_4$	30.2	3.06	3.64
pH=3(H_3PO_4)	40.2	3.31	3.95
	50.1	3.60	4.25
80:20 $CH_3CN:H_2O$, 0.1 *M* $NaClO_4$	30.3	2.77	2.92
pH=3(H_3PO_4)	40.2	2.94	3.17
	50.1	3.10	3.50
85:15 $CH_3CN:H_2O$, 0.05 *M* $NaClO_4$	30.3	3.06	3.61
pH=3(H_3PO_4)	40.2	3.24	3.95
	50.1	3.58	4.28
85:15 $CH_3CN:H_2O$, 0.15 *M* $NaClO_4$	30.3	2.98	3.54
pH=3(H_3PO_4)	40.2	3.12	3.90
	50.1	3.58	4.17

Table 6-4 (Continued)

HPLC condition	T(+-0.1°C)	Slope	Intercept
85:15 $CH_3CN:H_2O$, 0.2 *M* $NaClO_4$	30.3	2.94	3.53
pH=3(H_3PO_4)	40.2	3.11	3.82
	50.1	3.36	4.11
80:20 $CH_3CN:H_2O$, 0.05 *M* $NaClO_4$	30.3	2.82	2.84
pH=3(H_3PO_4)	40.2	2.96	3.09
	50.1	3.15	3.33
	60.0	3.55	3.53
*80:20 $CH_3CN:H_2O$, 0.05 *M* $NaClO_4$	40.2	2.84	2.73
**80:20 $CH_3CN:H_2O$, 0.05 *M* $NaClO_4$	40.2	3.20	2.13
80:20 $CH_3CN:H_2O$, 0.05 *M* NaCl	30.3	2.77	3.17
pH=3(H_3PO_4)	40.2	3.12	3.53
	50.1	3.33	3.83
	60.0	3.37	4.16

* 150 x 4.6 C18 Perkin-Elmer column.
** 150 x 4.6 C18 Sigma-Aldrich column.

Chapter 7

Chromatography of Nonaromatic Quaternary Ammonium Geminis

7.1 Introduction

As mentioned in Section 2.2.3, RP-HPLC analysis of traditional fatty quaternary ammonium salts has been undertaken using various columns, including CN, phenyl, C8, C18, and polystyrene-divinylbenzene. Mobile phases are often methanol-water or acetonitrile-water mixtures in combination with organic or inorganic ion-interaction reagents. Because of the lack of a UV absorbing chromophore, indirect UV, refractive index, and postcolumn reaction have been used for detection.

Nonaromatic quaternary ammonium gemini surfactants are a new type of surfactant. No chromatographic study of these surfactants has been appeared in the literature. In our work reversed-phase high performance liquid chromatography has been studied for the following two homologous series of gemini surfactants.

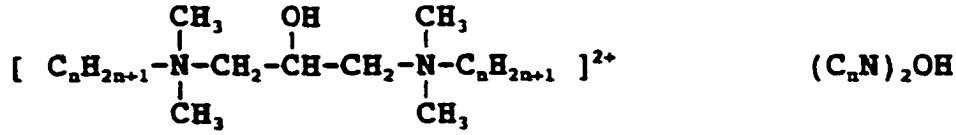

$$[\ C_nH_{2n+1}\text{-}N^{+}(CH_3)_2\text{-}CH_2\text{-}CH(OH)\text{-}CH_2\text{-}N^{+}(CH_3)_2\text{-}C_nH_{2n+1}\ ]^{2+} \qquad (C_nN)_2OH$$

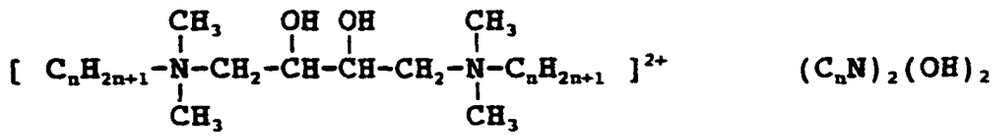

Since these two series of surfactants have similar structures, their chromatographic behavior is similar. Reversed-phase ion-interaction chromatography with an indirect UV detection was used for analysis of these surfactants (Section 7.3).

The retention mechanism has been studied as well (Section 7-4). The ion-interaction reagent was a mixture of sodium *p*-toluenesulfonate and *p*-toluenesulfonic acid. A co-elution of nonaromatic quaternary ammonium gemini surfactants and *p*-toluenesulfonate with approximately 1:2 molar ratio would be expected, specially if they would form tightly bonded ion-pairs. However, the results show that there is no 1:2 ratio of $(C_nN)_2OH$ and *p*-toluenesulfonate or $(C_nN)_2(OH)_2$ and *p*-toluenesulfonate co-elution.

7.2 Experimental

7.2.1 Instrumentation and reagents

The instruments and reagents were the same as those listed in Section 3.2 with the following exceptions.

Two series of nonaromatic quaternary ammonium gemini surfactants, $(C_nN)_2OH$ chloride and $(C_nN)_2(OH)_2$ bromide salt (n = 8, 10, 12, 14, 16 and 18), were synthesized by the Surfactant Research Institute at Brooklyn College[67,71]. Sodium *p*-toluenesulfonate (*p*-TSNa) and *p*-toluenesulfonic acid (*p*-TSA) used as ion-interaction reagents were purchased from Aldrich Chemical Co., Inc..

The column temperature was controlled by a YSI Model 74 THERMISTEMP® Temperature Controller or by a Timberline HPLC Column Heater H-500 coupled with a Data Precision 3500 DVM for temperature reading.

7.2.2 Procedure

Two homologous series of nonaromatic quaternary ammonium gemini surfactants $(C_nN)_2OH$ and $(C_nN)_2(OH)_2$ were chromatographed using the 3x3 C18 column. The mobile phases were methanol-acetonitrile-water mixtures with the volume ratios of 80:20:0, 78:19.5:2.5, and 76:19:5. Only isocratic conditions were used. Sodium *p*-toluenesulfonate and *p*-toluenesulfonic acid were added to the mobile phases each at a concentration of

5 mM. They served as ion-interaction reagents and provided indirect UV detection as well. Samples were dissolved in the mobile phases at 0.1 mM in most experiments. Before each run the column was flushed with the mobile phase until equilibrium was reached as indicated by stable pump pressure and detector baseline. The UV detector was set at 255 nm. The column temperature was controlled in the range of 25 °C to 50 °C by a thermostat or a column heater.

7.3 Results and Discussion

Chromatographic data were obtained for the individual surfactants and C_8, C_{10}, C_{12}, C_{14}, C_{16} and C_{18} mixtures. Acetonitrile-methanol-water mixtures with 5 m*M* sodium *p*-toluenesulfonate and 5 m*M* *p*-toluenesulfonic acid gave the best result. The summary of log *k'* for $(C_nN)_2OH$ and $(C_nN)_2(OH)_2$ surfactants under these chromatographic conditions are given in Table 7-1 and 7-2, where the log *k'* values are the averages over the indicated number of runs (# of data). Some aspects of these data and representative chromatograms are presented in the following sections.

Table 7-1 Summary of log k' of nonaromatic quaternary ammonium geminis $(C_nN)_2OH$

T(+-1°C)	Mobile phase	# of data		C_8	C_{10}	C_{12}	C_{14}	C_{16}	C_{18}
24.0	80:20:0 $CH_3OH:CH_3CN:H_2O$	8	log k'(avg.)	-0.75	-0.37	-0.12	0.17	0.49	0.82
	5m*M* *p*-TSA, 5m*M* *p*-TSNa		stdev	0.03	0.05	0.02	0.02	0.02	0.02
27.0		16	log k'(avg.)	-0.75	-0.38	-0.14	0.13	0.44	0.76
			stdev	0.05	0.04	0.02	0.02	0.03	0.03
41.0		10	log k'(avg.)	-0.80	-0.44	-0.30	-0.09	0.15	0.39
			stdev	0.04	0.01	0.01	0.01	0.01	0.01
51.0		12	log k'(avg.)	-0.89	-0.55	-0.39	-0.19	0.03	0.26
			stdev	0.14	0.05	0.04	0.05	0.05	0.05
25.4	78:19.5:2.5 $CH_3OH:CH_3CN:H_2O$	14	log k'(avg.)	-0.56	-0.27	0.03	0.35	0.70	1.07
	5m*M* *p*-TSA, 5m*M* *p*-TSNa		stdev	0.03	0.03	0.02	0.02	0.02	0.03
31.0		10	log k'(avg.)	-0.60	-0.32	-0.06	0.23	0.55	0.90
			stdev	0.04	0.02	0.03	0.02	0.02	0.01
41.0		10	log k'(avg.)	-0.66	-0.40	-0.14	0.14	0.43	0.75
			stdev	0.02	0.02	0.03	0.03	0.04	0.04
51.0		10	log k'(avg.)	-0.65	-0.40	-0.17	0.08	0.36	0.65
			stdev	0.04	0.03	0.03	0.03	0.03	0.03
24.0	76:19:5 $CH_3OH:CH_3CN:H_2O$	13	log k'(avg.)	-0.43	-0.16	0.18	0.54	0.95	1.38
	5m*M* *p*-TSA, 5m*M* *p*-TSNa		stdev	0.03	0.02	0.02	0.02	0.02	0.03
31.0		10	log k'(avg.)	-0.48	-0.22	0.10	0.44	0.81	1.21
			stdev	0.03	0.03	0.02	0.02	0.03	0.03
41.0		10	log k'(avg.)	-0.47	-0.28	0.03	0.32	0.65	1.00
			stdev	0.04	0.07	0.03	0.02	0.03	0.04
51.0		10	log k'(avg.)	-0.56	-0.34	-0.10	0.18	0.47	0.78
			stdev	0.04	0.03	0.02	0.02	0.02	0.02

Table 7-2 Summary of log k' of nonaromatic quaternary ammonium geminis $(C_nN)_2(OH)_2$

T(+-1°C)	Mobile phase	# of data		C_8	C_{10}	C_{12}	C_{14}	C_{16}	C_{18}
25.6	80:20:0 CH_3OH:CH_3CN:H_2O	12	log k'(avg.)	-0.68	-0.47	-0.20	0.08	0.38	0.70
	5m*M* *p*-TSA, 5m*M* *p*-TSNa		stdev	0.03	0.06	0.03	0.02	0.03	0.03
29.0		8	log k'(avg.)	-0.69	-0.46	-0.22	0.04	0.34	0.65
			stdev	0.00	0.00	0.02	0.00	0.01	0.01
41.0		10	log k'(avg.)	-0.71	-0.51	-0.34	-0.13	0.11	0.34
			stdev	0.02	0.00	0.01	0.02	0.01	0.01
51.0		12	log k'(avg.)	-0.79	-0.59	-0.41	-0.22	0.00	0.22
			stdev	0.07	0.06	0.05	0.05	0.05	0.04
25.4	78:19.5:2.5 CH_3OH:CH_3CN:H_2O	14	log k'(avg.)	-0.57	-0.32	-0.02	0.30	0.65	1.01
	5m*M* *p*-TSA, 5m*M* *p*-TSNa		stdev	0.06	0.03	0.02	0.02	0.02	0.03
31.0		10	log k'(avg.)	-0.57	-0.34	-0.12	0.18	0.51	0.85
			stdev	0.02	0.00	0.02	0.02	0.02	0.02
41.0		10	log k'(avg.)	-0.66	-0.44	-0.20	0.09	0.38	0.69
			stdev	0.02	0.02	0.03	0.03	0.03	0.04
51.0		10	log k'(avg.)	-0.62	-0.44	-0.22	0.04	0.32	0.61
			stdev	0.02	0.03	0.03	0.02	0.03	0.03
24.0	76:19:5 CH_3OH:CH_3CN:H_2O	12	log k'(avg.)	-0.50	-0.22	0.12	0.49	0.89	1.31
	5m*M* *p*-TSA, 5m*M* *p*-TSNa		stdev	0.05	0.03	0.02	0.02	0.02	0.03
31.0		10	log k'(avg.)	-0.55	-0.28	0.04	0.39	0.76	1.16
			stdev	0.04	0.04	0.02	0.02	0.02	0.02
41.0		10	log k'(avg.)	-0.49	-0.31	-0.02	0.28	0.61	0.96
			stdev	0.03	0.06	0.03	0.02	0.01	0.02
51.0		10	log k'(avg.)	-0.60	-0.39	-0.14	0.14	0.43	0.75
			stdev	0.02	0.01	0.02	0.01	0.02	0.02

7.3.1 log k', the number of carbon atoms, the mobile phase composition, and temperature

Log k' increases linearly with the number of carbon atoms in the straight chain. Figures 7-1 and 7-2 show this relationship in various mobile phases. The slopes are in the range of 0.055 to 0.091 for $(C_nN)_2OH$ and 0.050 to 0.091 for $(C_nN)_2(OH)_2$ under these chromatographic conditions. The slope increases slightly with increasing water percentage in the mobile phase and decreasing temperature.

The log k' value also increases with increasing the volume percentage of water and decreasing temperature. A certain percentage of acetonitrile is needed in the mobile phase. Without acetonitrile peak tailing occurs; too much acetonitrile causes co-elution of the homologs and poor separation. The low viscosity of acetonitrile plays an important role in the separation.

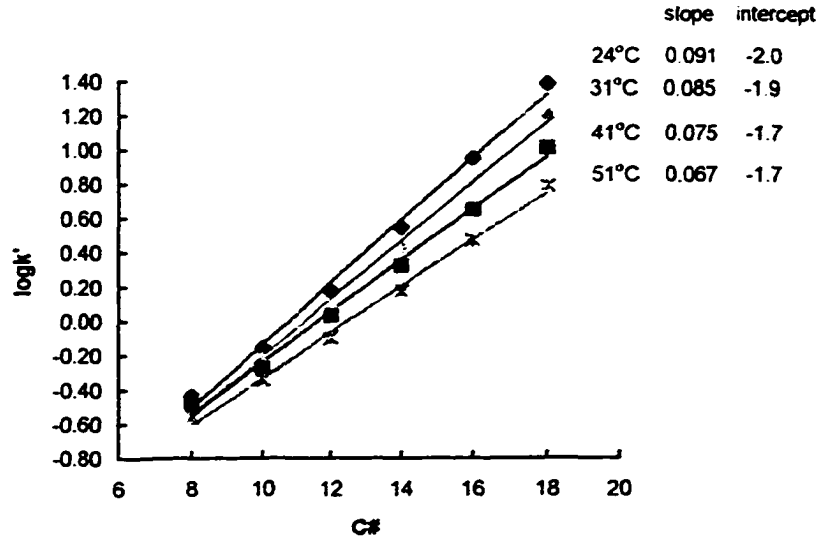

(a) 76:19:5 CH_3OH:CH_3CN:H_2O, 5 m*M* *p*-TSNa, 5 m*M* *p*-TSA

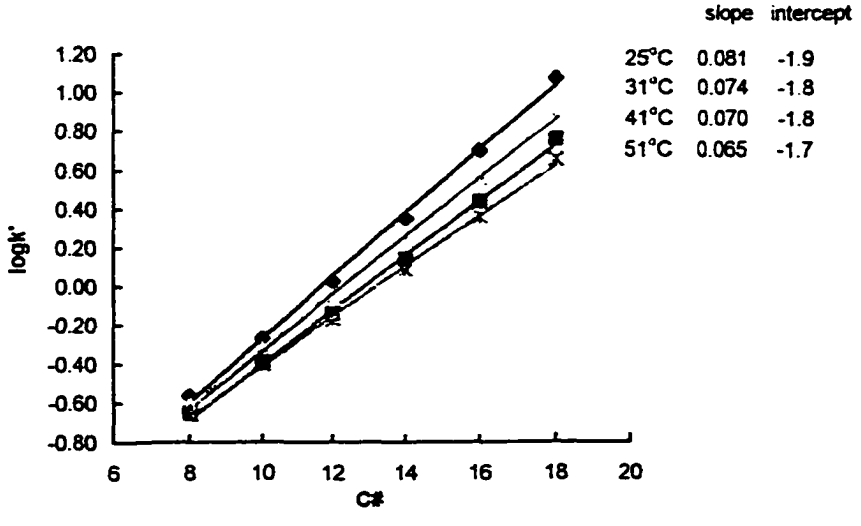

(b) 78:19.5:2.5 CH_3OH:CH_3CN:H_2O, 5 m*M* *p*-TSNa, 5 m*M* *p*-TSA

Figure 7-1 log *k'* vs. carbon number of $(C_nN)_2OH$

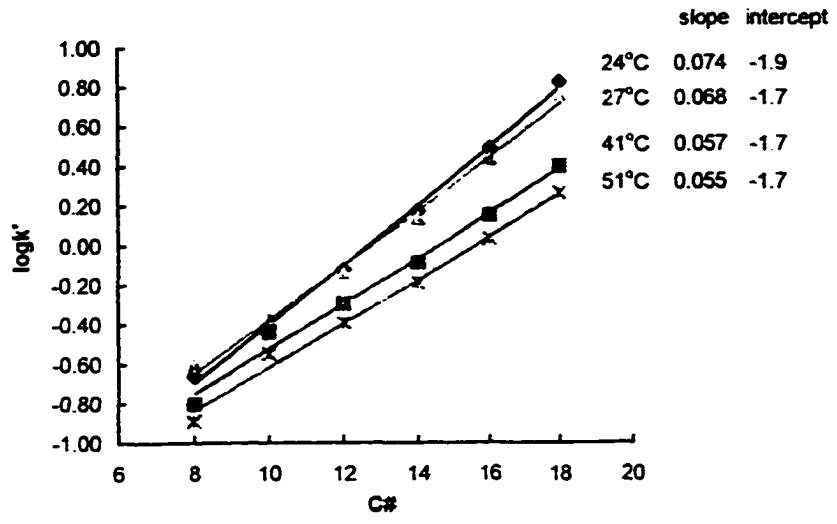

(c) 80:20:0 CH_3OH:CH_3CN:H_2O, 5 m*M* *p*-TSNa, 5 m*M* *p*-TSA

Figure 7-1 (Continued)

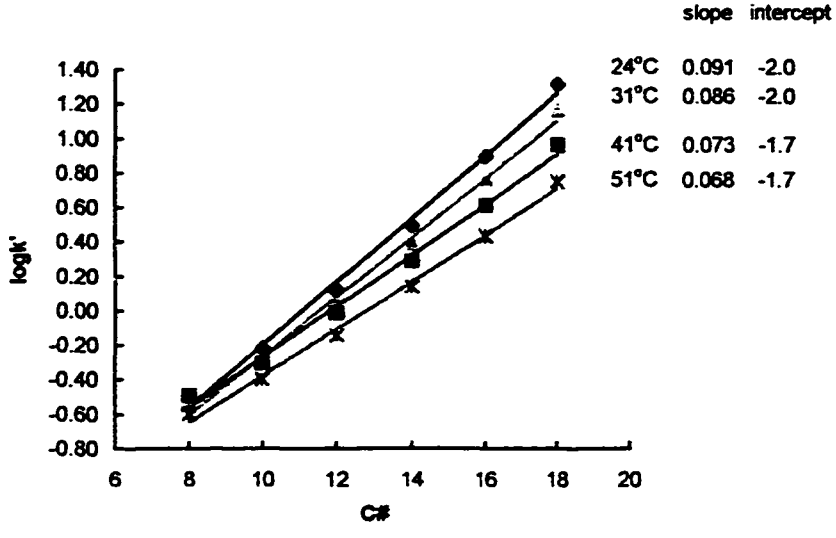

(a) 76:19:5 CH_3OH:CH_3CN:H_2O, 5 m*M* *p*-TSNa, 5 m*M* *p*-TSA

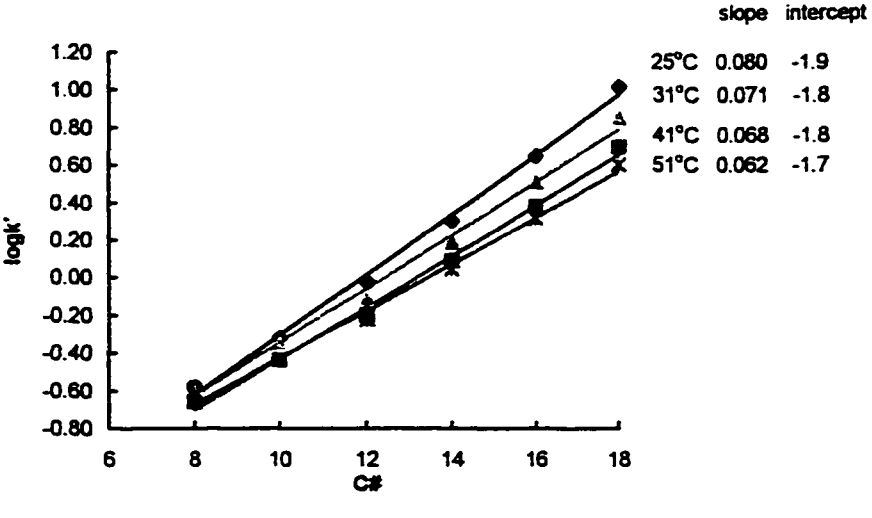

(b) 78:19.5:2.5 CH_3OH:CH_3CN:H_2O, 5 m*M* *p*-TSNa, 5 m*M* *p*-TSA

Figure 7-2 log *k'* vs. carbon number of $(C_nN)_2(OH)_2$

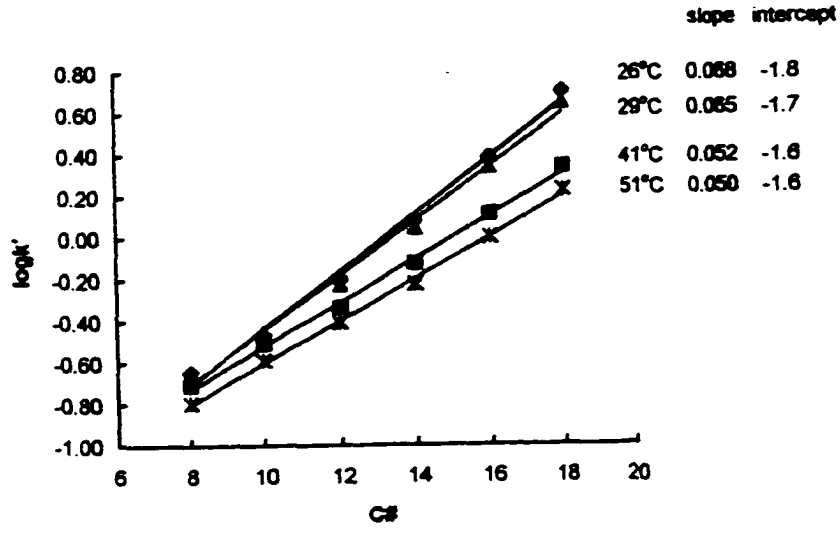

(c) 80:20:0 CH_3OH:CH_3CN:H_2O, 5 m*M* *p*-TSNa, 5 m*M* *p*-TSA

Figure 7-2 (Continued)

7.3.2 Separation of $(C_nN)_2OH$ and $(C_nN)_2(OH)_2$

Figure 7-3 to 7-8 are some representative chromatograms of $(C_nN)_2OH$ and $(C_nN)_2(OH)_2$ surfactants. At 25 °C, the C_8 to C_{14} mixture can be separated using a mobile phase of 76:19:5 CH_3OH:CH_3CN:H_2O with 5 m*M* *p*-TSNa and 5 m*M* *p*-TSA; the mobile phase of 78:19.5:2.5 CH_3OH:CH_3CN:H_2O with 5 m*M* *p*-TSNa and 5 m*M* *p*-TSA is good for the C_{12} to C_{16} mixture; the mobile phase of 80:20:0 CH_3OH:CH_3CN:H_2O with 5 m*M* *p*-TSNa and 5 m*M* *p*-TSA can be used for the C_{14} to C_{18} mixture.

There is a negative peak in the early part of these chromatograms. Its retention time is the same as the peak retention time when the 0.5 m*M* *p*-TSNa and 0.5 m*M* *p*-TSA mixture is injected (Figure 7-3). Injection of a mobile phase mixture without the ion-interaction reagents gives the same negative peak which has the same retention time (Figure 7-6). Therefore the negative peak is due to the lower concentration of *p*-TSNa and *p*-TSA in the eluent (discussed in Section 7-4). The retention time of this negative peak is used as t_m for the capacity factor, k', calculations.

These two series of surfactants give similar chromatograms. Retention time of $(C_nN)_2OH$ is sightly longer than $(C_nN)_2(OH)_2$. This is attributable to the structure difference. With two -OH groups, $(C_nN)_2(OH)_2$ is more hydrophilic which reduces its retention time.

The limit of quantitative measurement and the linear

range were not studied. The concentration used in most experiments is 1 mM (1 x 10^{-8} moles of sample for injection of 10 μL). The detection limit is lower than this concentration. The upper concentration limit is restricted by the solubility in the presence of the high concentration of ion-interaction reagents.

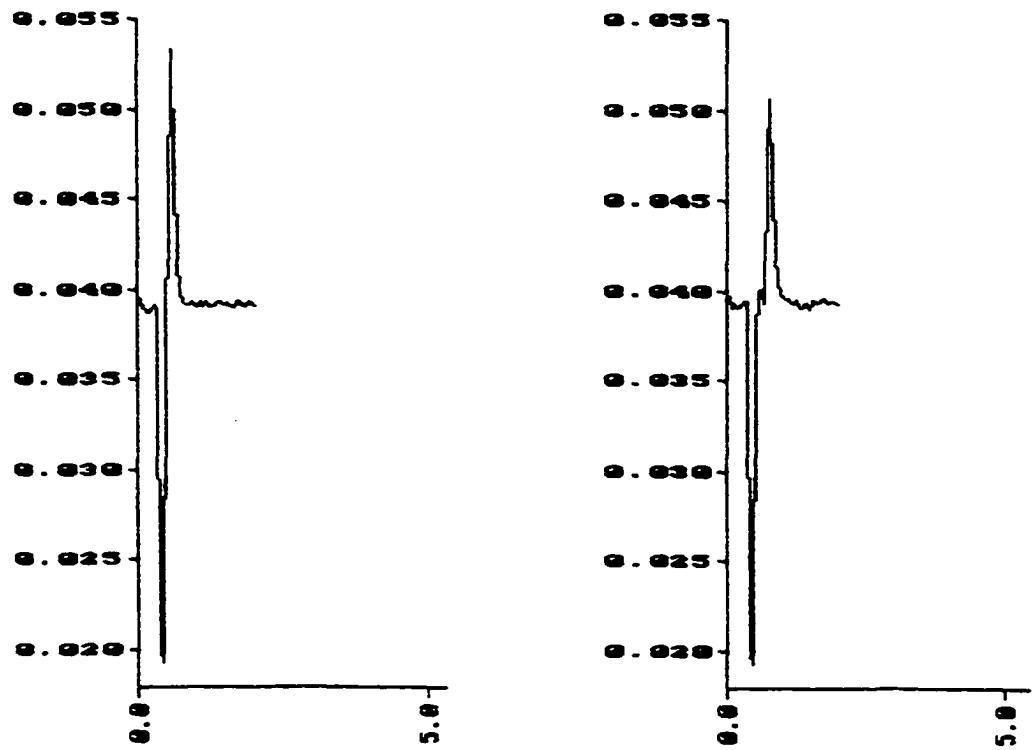

Figure 7-3 Chromatograms of $(C_nN)_2OH$ surfactants (1 m*M* each) with 5% H_2O in mobile phase

Mobile phase:	76:19:5 CH_3OH:CH_3CN:H_2O, 5 m*M* *p*-TSA and 5 m*M* *p*-TSNa
UV detection:	255 nm
Flow rate:	1.0 mL/min
Column:	3x3 C18 (33 x 4.6 mm)
Injection volume:	10 μl
Temperature:	25 °C

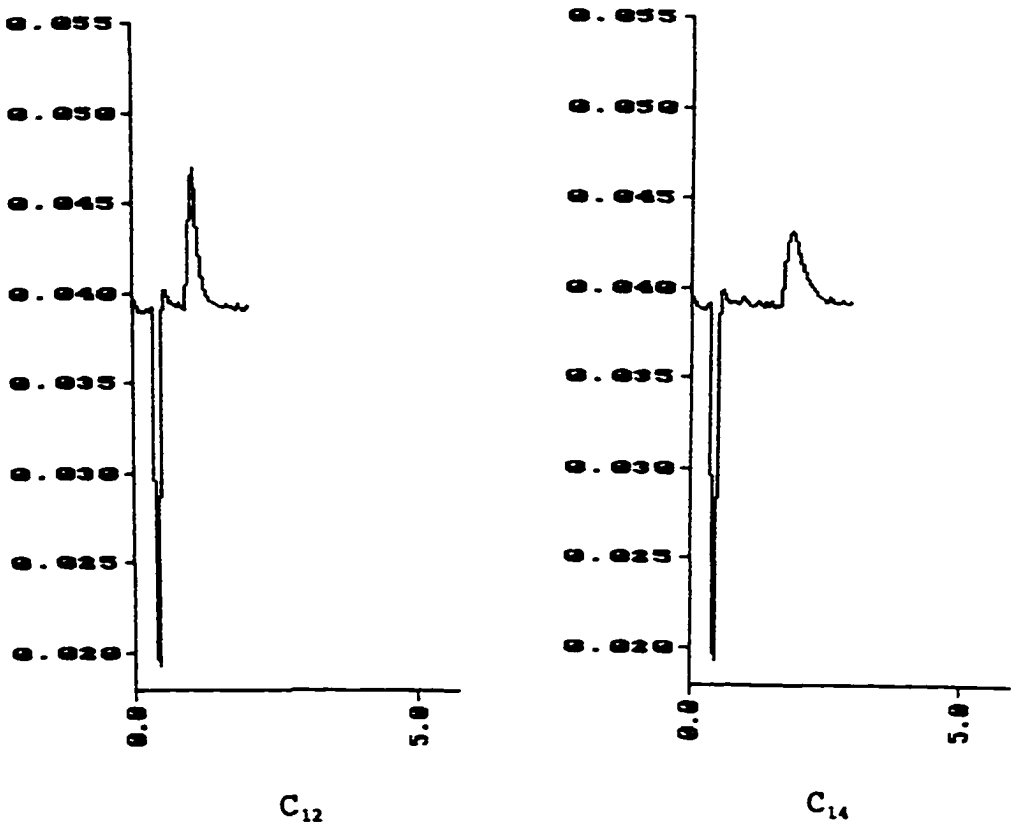

Figure 7-3 (Continued)

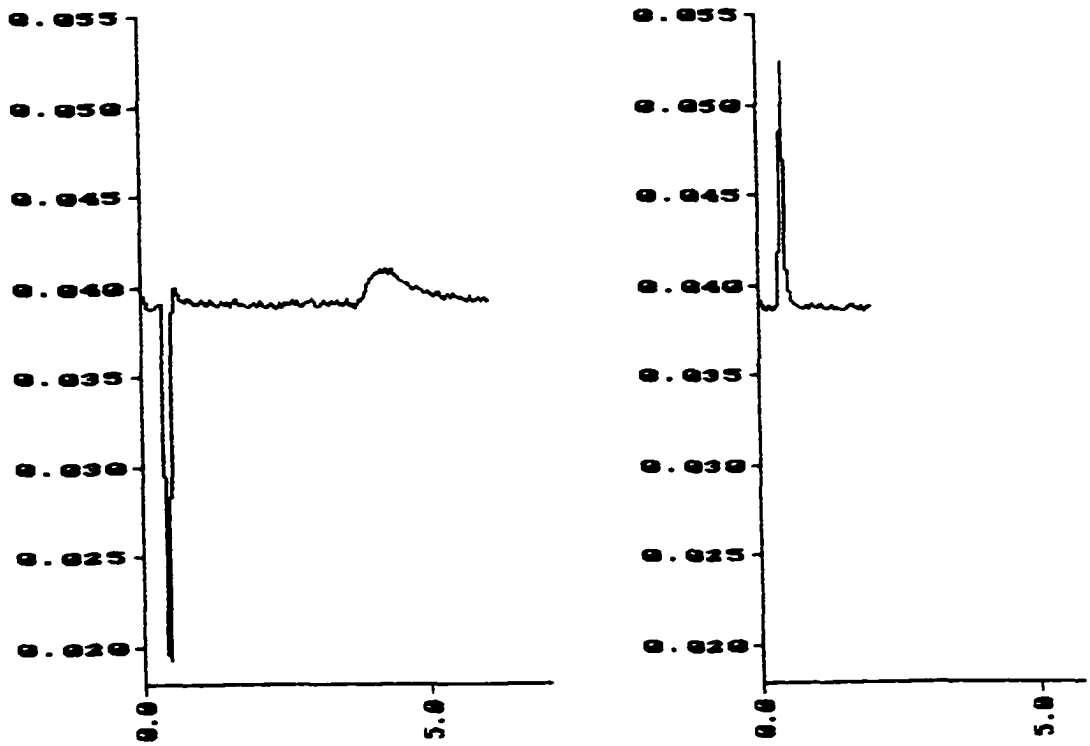

C_{16}

0.5 mM *p*-TSA
0.5 mM *p*-TSNa

Figure 7-3 (Continued)

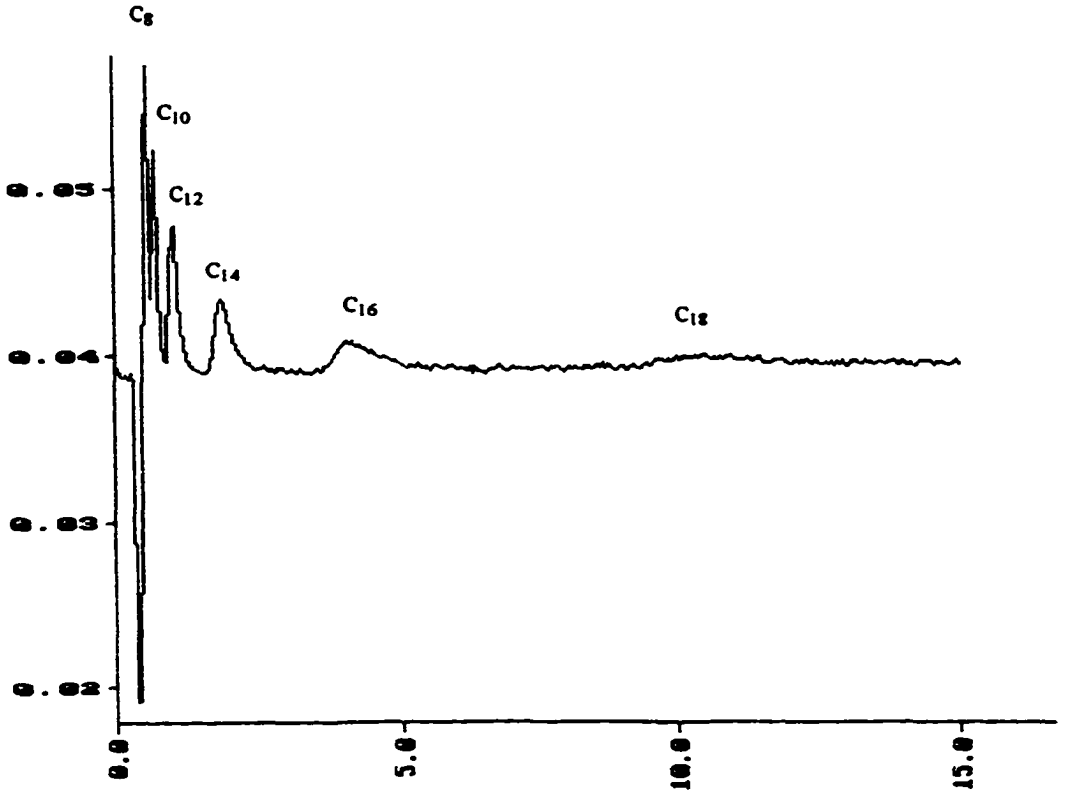

C_8, C_{10}, C_{12}, C_{14}, C_{16} and C_{18} mixture

Figure 7-3 (Continued)

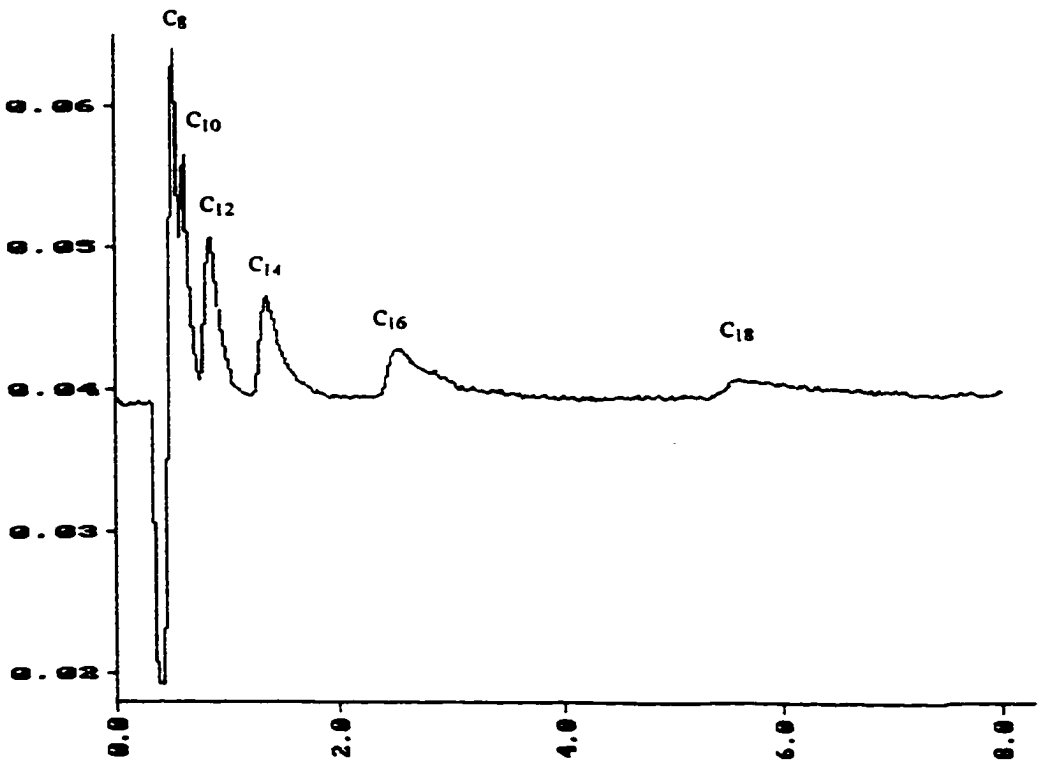

C_8, C_{10}, C_{12}, C_{14}, C_{16} and C_{18} mixture

Figure 7-4 Chromatogram of $(C_nN)_2OH$ surfactants (1 m*M* each) with 2.5% H_2O in mobile phase

Mobile phase:	78:19.5:2.5 CH_3OH:CH_3CN:H_2O, 5 m*M* *p*-TSA and 5 m*M* *p*-TSNa
UV detection:	255 nm
Flow rate:	1.0 mL/min
Column:	3x3 C18 (33 x 4.6 mm)
Injection volume:	10 μl
Temperature:	25 °C

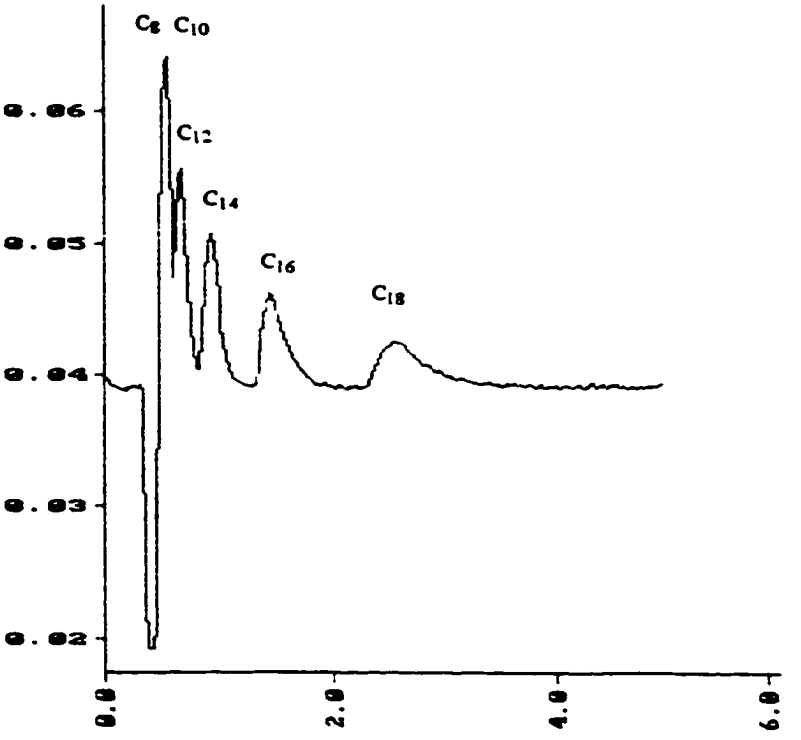

C_8, C_{10}, C_{12}, C_{14}, C_{16} and C_{18} mixture

Figure 7-5 Chromatogram of $(C_nN)_2OH$ surfactants (1 m*M* each) with 0% H_2O

Mobile phase:	80:20:0 CH_3OH:CH_3CN:H_2O, 5 m*M* *p*-TSA and 5 m*M* *p*-TSNa
UV detection:	255 nm
Flow rate:	1.0 mL/min
Column:	3x3 C18 (33 x 4.6 mm)
Injection volume:	10 μl
Temperature:	26 °C

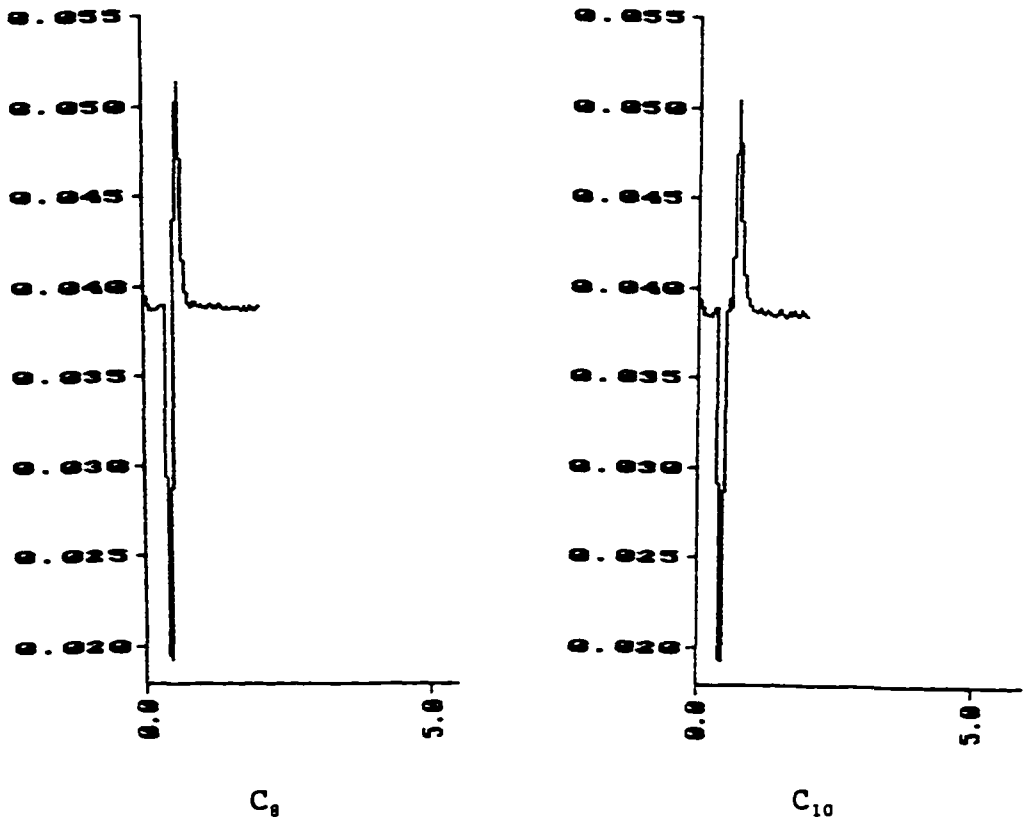

Figure 7-6 Chromatograms of $(C_nN)_2(OH)_2$ surfactants (1 m*M* each) with 5% H_2O in mobile phase

Mobile phase:	76:19:5 CH_3OH:CH_3CN:H_2O, 5 m*M* *p*-TSA and 5 m*M* *p*-TSNa
UV detection:	255 nm
Flow rate:	1.0 mL/min
Column:	3x3 C18 (33 x 4.6 mm)
Injection volume:	10 μl
Temperature:	25 °C

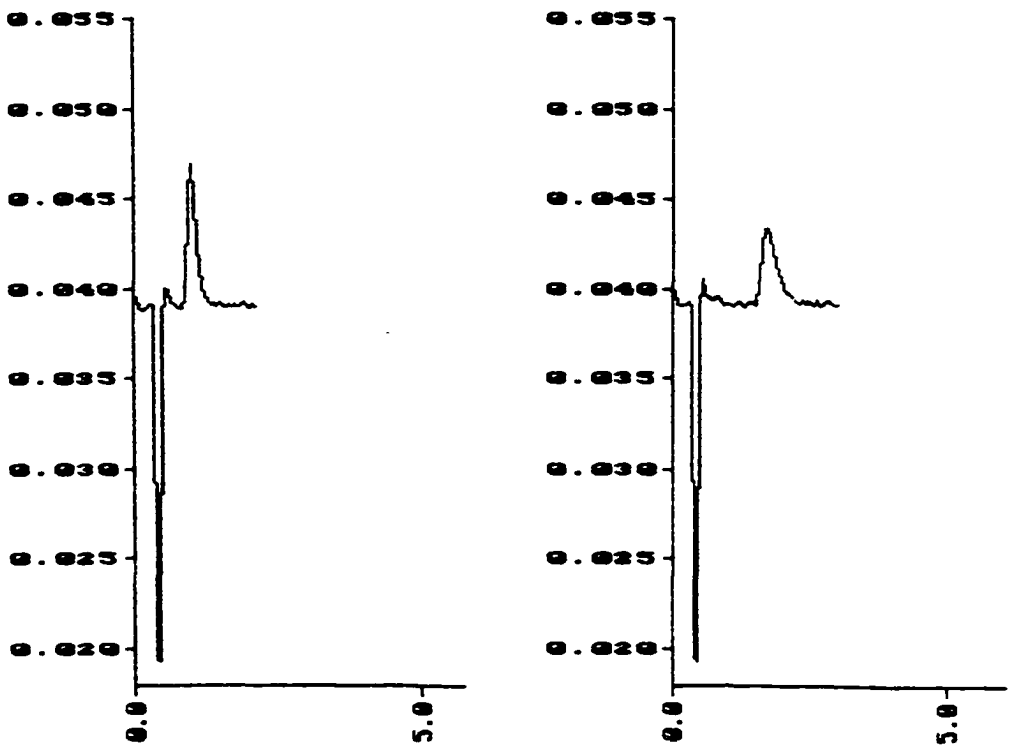

C_{12} C_{14}

Figure 7-6 (Continued)

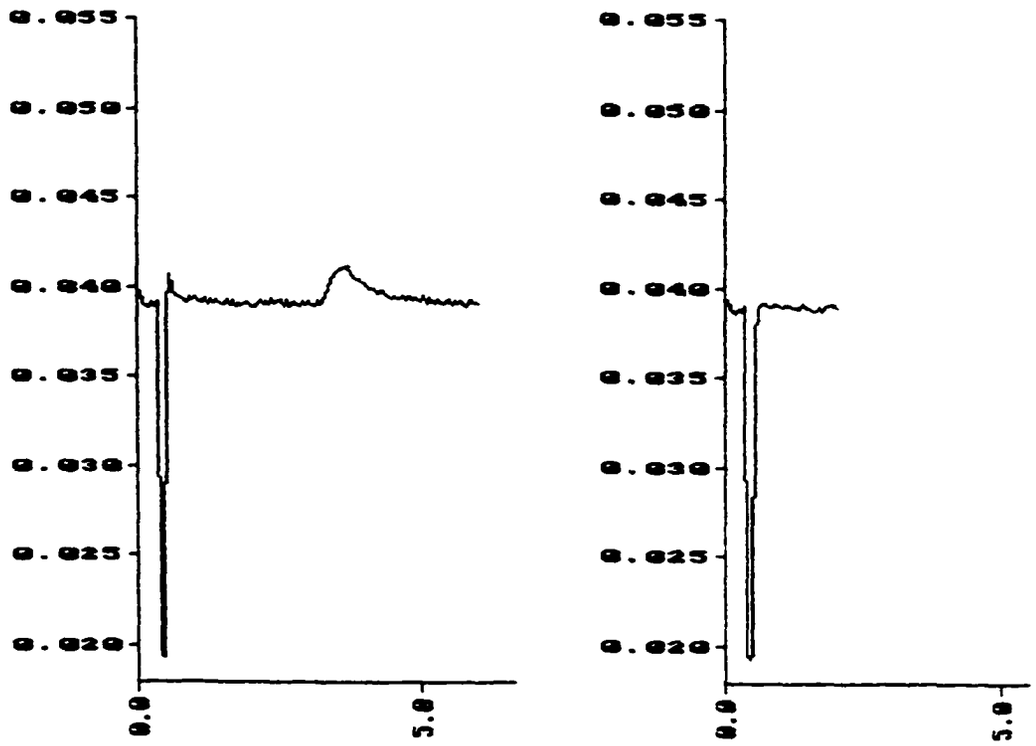

C_{16} 76:19:5 $CH_3OH:CH_3CN:H_2O$

Figure 7-6 (Continued)

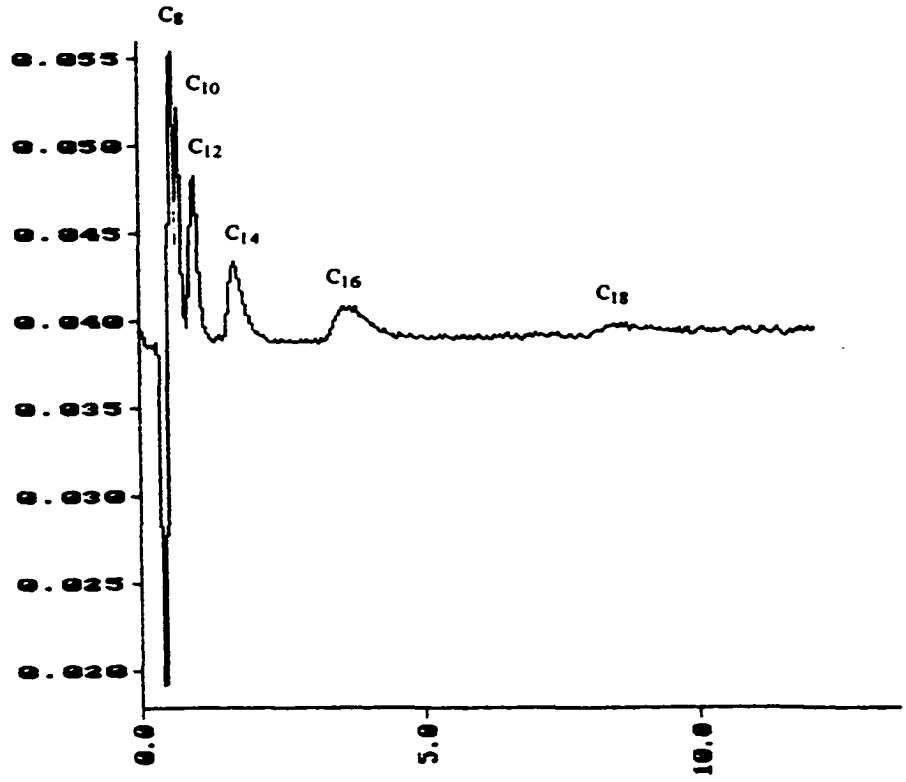

C_8, C_{10}, C_{12}, C_{14}, C_{16} and C_{18} mixture

Figure 7-6 (Continued)

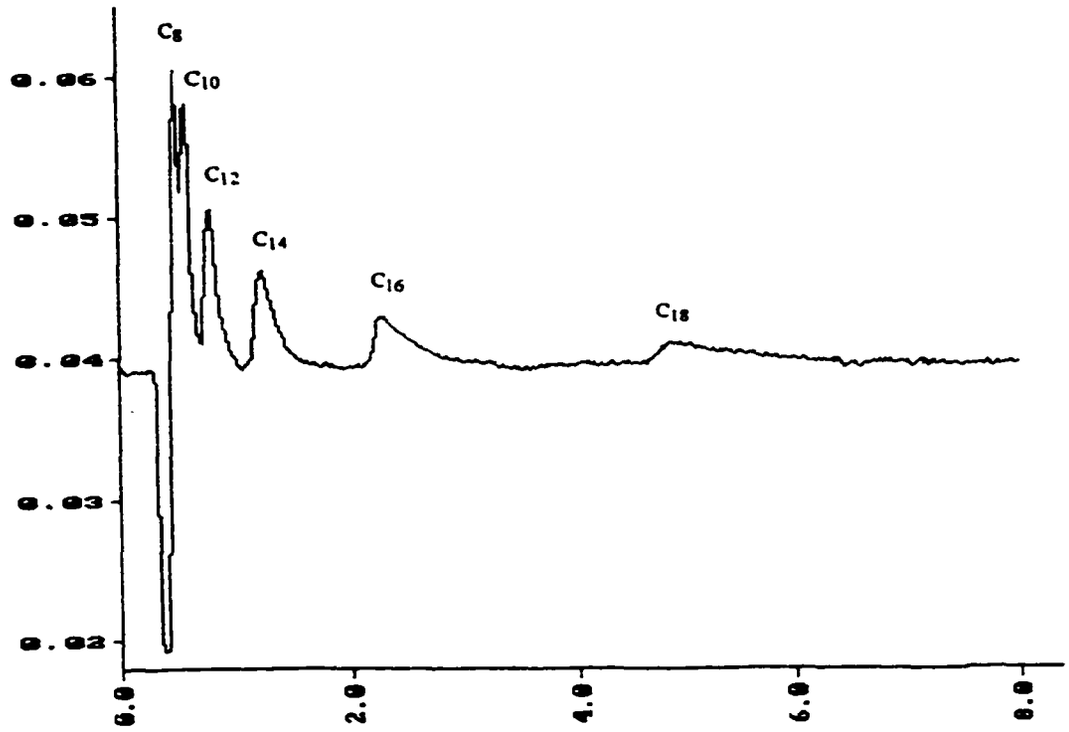

C_8, C_{10}, C_{12}, C_{14}, C_{16} and C_{18} mixture

Figure 7-7 Chromatogram of $(C_nN)_2(OH)_2$ surfactants (1 m*M* each) with 2.5% H_2O in mobile phase

Mobile phase:	78:19.5:2.5 CH_3OH:CH_3CN:H_2O, 5 m*M* *p*-TSA and 5 m*M* *p*-TSNa
UV detection:	255 nm
Flow rate:	1.0 mL/min
Column:	3x3 C18 (33 x 4.6 mm)
Injection volume:	10 μl
Temperature:	25 °C

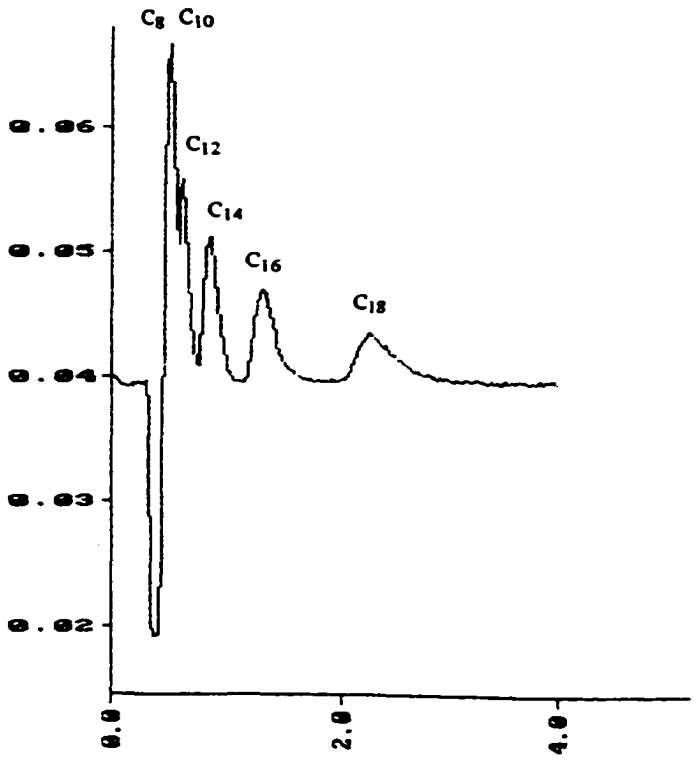

C_8, C_{10}, C_{12}, C_{14}, C_{16} and C_{18} mixture

Figure 7-8 Chromatogram of $(C_nN)_2(OH)_2$ surfactants (1 m*M* each) with 0% H_2O

Mobile phase:	80:20:0 CH_3OH:CH_3CN:H_2O, 5 m*M* *p*-TSA and 5 m*M* *p*-TSNa
UV detection:	255 nm
Flow rate:	1.0 mL/min
Column:	3x3 C18 (33 x 4.6 mm)
Injection volume:	10 μl
Temperature:	26 °C

7.3.3 Sodium *p*-toluenesulfonate and *p*-toluenesulfonic acid as ion-interaction reagents

As mentioned in Section 5.3.3, tailing problems are common for ammonium compounds in RP-HPLC, because of their affinity for residual silanol groups on the packing material. The chromatographic peaks of $(C_nN)_2OH$ and $(C_nN)_2(OH)_2$ surfactants are slightly tailed. A reason might be that the residual silanol groups on the stationary phase and ammonium groups on the analyte cannot be effectively covered by *p*-toluenesulfonate ions. Since one of the requirements for ion-interaction reagents here is UV absorption, sodium *p*-toluenesulfonate and *p*-toluenesulfonic acid were chosen, even though the tailing cannot be overcome completely.

7.4 Separation Mechanism

7.4.1 Ion-interaction mechanism

The ion-interaction mechanism for $(C_nN)_2OH$ and $(C_nN)_2(OH)_2$ gemini surfactants is illustrated in Figure 7-9, which is similar to the mechanism of alkanesulfonates (Section 3-4).

(a) As discussed in Section 3.4.1, before injection of the sample, the surface of the stationary phase is at equilibrium with the mobile phase. The distribution equilibrium of ion-interaction reagents, sodium *p*-toluenesulfonate and *p*-toluenesulfonic acid, is dynamic.

(b) After injection of the sample, the previous equilibrium is disturbed. The analyte ions can adsorb onto the stationary phase in two ways as shown in Figure 7-9, process A and process B.

Process A occurs if the coverage of the stationary phase surface is high. Cationic gemini surfactants are retained by the stationary phase mainly through electrostatic interaction between the ionic groups of surfactants and ion-interaction reagents adsorbed on the stationary phase. The alkyl chains point towards the mobile phase.

Process B occurs if the coverage of the stationary phase surface is low. The retention is caused by the London dispersion force between surfactants and the C18 stationary phase and by the electrostatic interaction between the ionic

groups of surfactants and ion-interaction reagents. Addition of the positively charged species to the negatively charged primary adsorption layer has the net effect of neutralizing the negative change in this layer. More negatively charged ion-interaction reagent ions can adsorb onto the stationary phase if there is enough surface left.

Theoretical calculations and the surface coverage calculation shown in the next two sections suggest that process B is predominant.

In process B, adsorption of more ion-interaction ions decreases its concentration in the eluent, and results in a negative peak in the early part of chromatograms which is observed in Figure 7-3 to 7-8.

(c) When an analyte ion leaves the surface, an excess negative charge is left behind. The partition equilibrium is disturbed again. An ion-interaction reagent ion can leave the surface to reestablish the equilibrium. Thus, apparently the pair of ions travels through the column and reaches the detector producing the UV absorption signal.

Detector response calculations (Section 7.4.4) suggest a 1:1 ratio of the oppositely charged surfactant and *p*-toluenesulfonate ions in the eluent instead of 1:2 ratio based on the charges of ions.

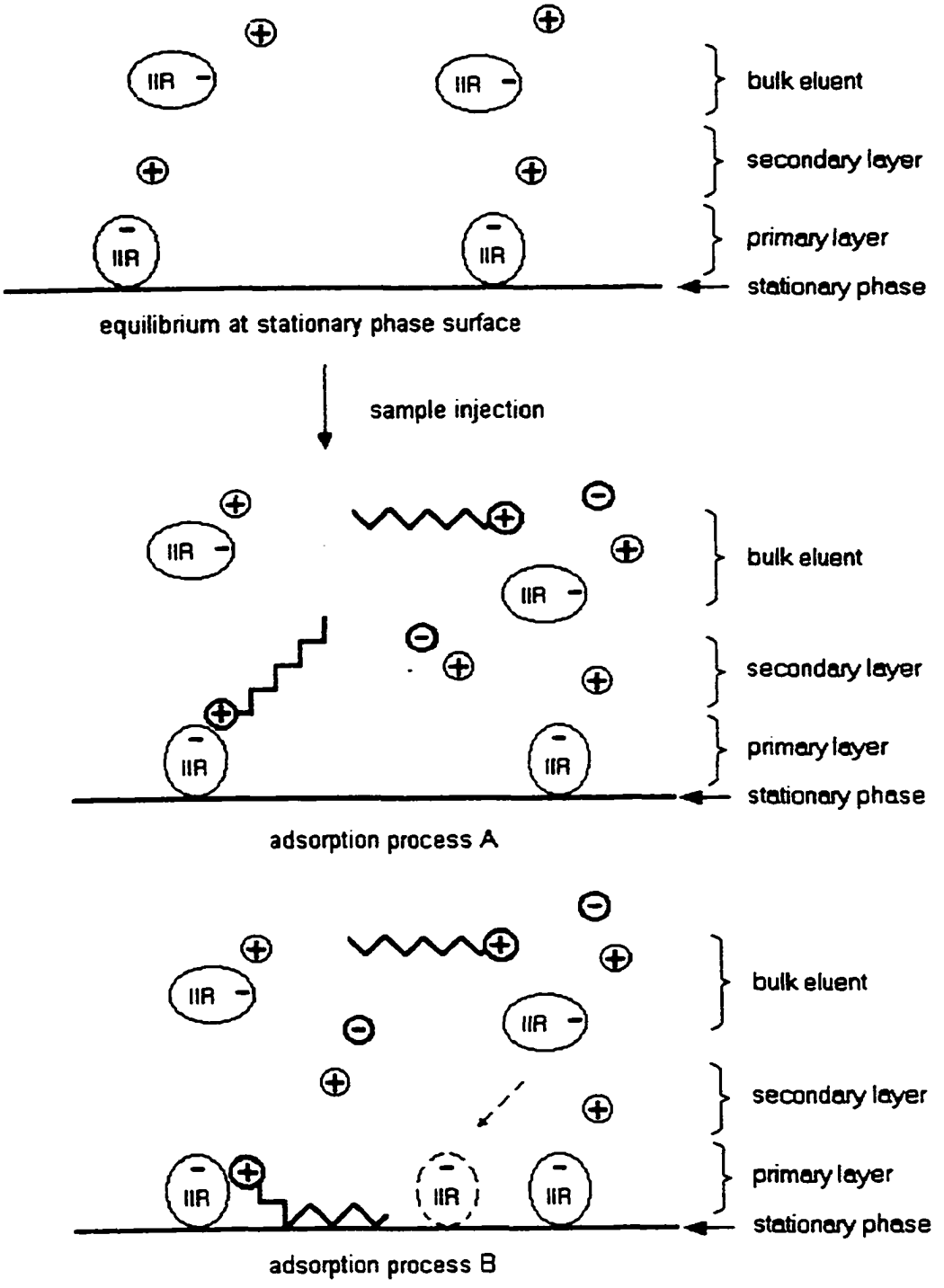

Figure 7-9 Schematic diagram of $(C_nN)_2OH$ and $(C_nN)_2(OH)_2$ retention mechanism

7.4.2 Thermodynamic considerations

In Chapter 5, using equations (1-5), (1-15) and (5-1), equation (5-3) was obtained.

$$\ln k' = - \frac{\Delta H^\circ}{RT} + \frac{\Delta S^\circ}{R} - \ln \frac{V_m}{V_s} \qquad (5\text{-}3)$$

For two compounds (B>A) in a homologous series chromatographed under the same condition, the following relationship holds:

$$\ln k'_B - \ln k'_A = - \frac{\Delta H^\circ_B - \Delta H^\circ_A}{RT} + \frac{\Delta S^\circ_B - \Delta S^\circ_A}{R} \qquad (7\text{-}1)$$

$$\ln \frac{k'_B}{k'_A} = \ln \alpha = - \frac{\Delta (\Delta H^\circ)_{B\text{-}A}}{RT} + \frac{\Delta (\Delta S^\circ)_{B\text{-}A}}{R} \qquad (7\text{-}2)$$

The α is the selectivity factor of a column[72].

$$\alpha = \frac{k'_B}{k'_A} \qquad (7\text{-}3)$$

where k'_B is the capacity factor for the more strongly retained species B and k'_A is the capacity factor for the more rapidly eluted species A.

Plotting ln α vs. $1/T$ should give a straight line (Figures 7-10 and 7-11), if ΔH° and ΔS° are approximately constant in the temperature range. The slope and the intercept are

$$\text{slope} = - \frac{\Delta (\Delta H^\circ)_{B\text{-}A}}{R} \qquad (7\text{-}4)$$

$$\text{intercept} = \frac{\Delta(\Delta S^{\circ})_{B-A}}{R} \qquad (7\text{-}5)$$

Where R = 8.314 J/K·mol.

One can use the plot of ln α vs. $1/T$ to calculate $\Delta(\Delta H^{\circ})_{B-A}$ and $\Delta(\Delta S^{\circ})_{B-A}$ of two analytes transferring from the mobile phase to the stationary phase in chromatography. Table 7-3 shows calculated $\Delta(\Delta H^{\circ})_{B-A}$ and $\Delta(\Delta S^{\circ})_{B-A}$ values for $(C_nN)_2OH$ and $(C_nN)_2(OH)_2$ surfactants, where all $\Delta(\Delta H^{\circ})_{B-A}$ and $\Delta(\Delta S^{\circ})_{B-A}$ values are negative. The following discussion shows the process B in the retention mechanism is a more likely one. These considerations are similar as used for the aromatic gemini surfactants (Section 5.4.3).

(a) $\Delta(\Delta H^{\circ})_{B-A}$

In process A (Figure 7-9), the longer chain surfactant is not energetically favored over the shorter chain surfactant. Here the electrostatic interactions are similar for two homologs, but the alkyl chains exposed to a hydrophilic environment (secondary counterion layer) can cause a difference. The enthalpy of the system with a longer surfactant in the counterion layer could be higher, and ΔH°_B of the longer surfactant will be less negative than ΔH°_A of the shorter one, or approximately equal to ΔH°_A if this difference is similar in the mobile phase. Therefore $\Delta(\Delta H^{\circ})_{B-A}$ should be positive or close to zero, and the slope of ln α vs. $1/T$ should be negative or close to zero.

In process B, the longer alkyl chain has a larger

dispersion interaction with the C18 stationary phase. $\Delta H°_B$ will be more negative than $\Delta H°_A$. $\Delta(\Delta H°)_{B-A}$ should be negative and the slope of ln α vs. $1/T$ should be positive.

Figures 7-10 and 7-11 show positive slopes, and Table 7-3 shows negative $\Delta(\Delta H°)_{B-A}$ values. Considering $\Delta(\Delta H°)_{B-A}$ of transferring two homologs from the mobile phase to the stationary phase, B is the predominant mechanism.

(b) $\Delta(\Delta S°)_{B-A}$

In the process A, the hydrophobic chain stays in the similar environments, $\Delta S°_B$ and $\Delta S°_A$ will approximately equal to each other. Therefore $\Delta(\Delta S°)_{B-A}$ should be close to zero, and the intercept should be about zero.

In process B, the longer chain system will be more ordered than the shorter chain system after the hydrophobic chain transfers from the bulk polar eluent to the C18 phase. Thus, $\Delta S°_B$ will be more negative or less positive than $\Delta S°_A$. The values of $\Delta(\Delta S°)_{B-A}$ will be negative, and the intercept of ln α vs. $1/T$ should be negative.

Table 7-3 shows that $\Delta(\Delta S°)_{B-A}$ values are all negative. Therefore, a more likely mechanism is B.

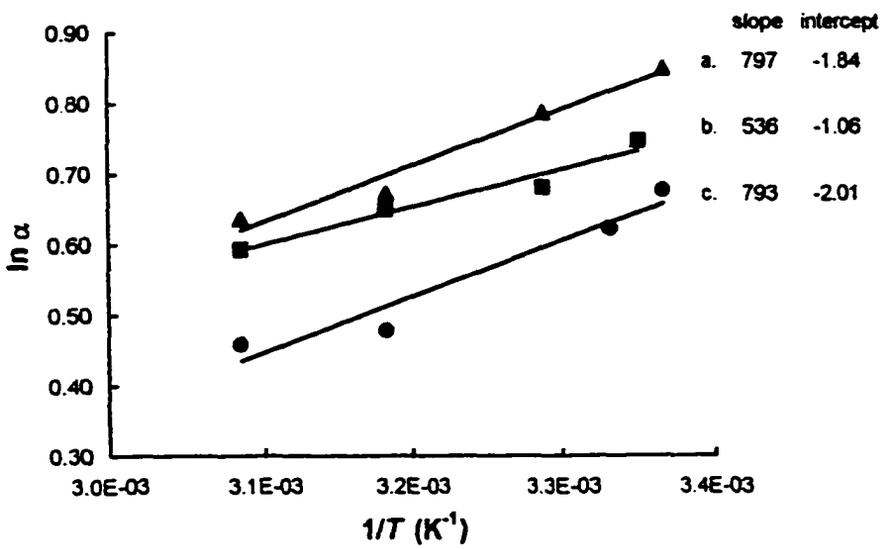

Figure 7-10 ln α vs. 1/*T* for $(C_{12}N)_2OH$ and $(C_{14}N)_2OH$
a. 76:19:5 $CH_3OH:CH_3CN:H_2O$, 5 m*M* *p*-TSA, 5m*M* *p*-TSNa
b. 78:19.5:2.5 $CH_3OH:CH_3CN:H_2O$, 5 m*M* *p*-TSA, 5m*M* *p*-TSNa
c. 80:20:0 $CH_3OH:CH_3CN:H_2O$, 5 m*M* *p*-TSA, 5m*M* *p*-TSNa

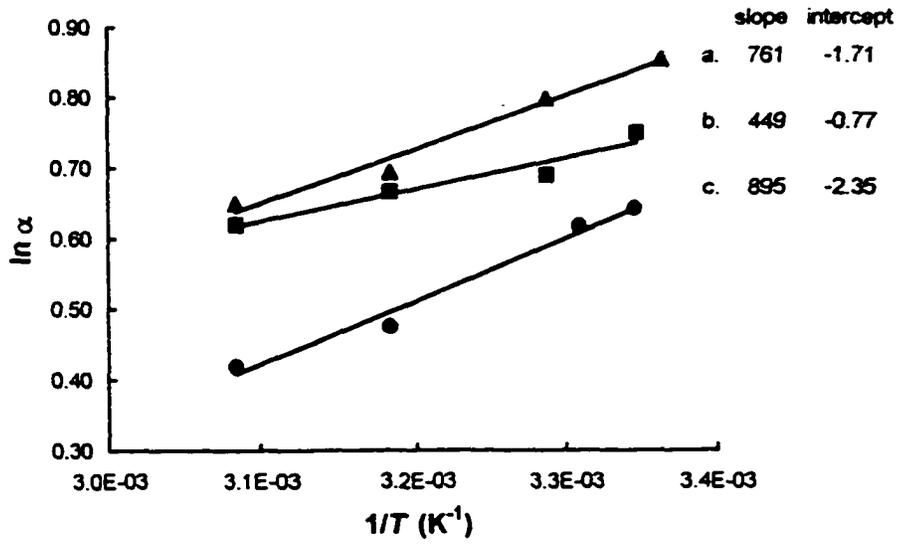

Figure 7-11 ln α vs. $1/T$ for $(C_{12}N)_2(OH)_2$ and $(C_{14}N)_2(OH)_2$
a. 76:19:5 $CH_3OH:CH_3CN:H_2O$, 5 mM *p*-TSA, 5mM *p*-TSNa
b. 78:19.5:2.5 $CH_3OH:CH_3CN:H_2O$, 5 mM *p*-TSA, 5mM *p*-TSNa
c. 80:20:0 $CH_3OH:CH_3CN:H_2O$, 5 mM *p*-TSA, 5mM *p*-TSNa

Table 7-3 $\Delta(\Delta H°)_{B-A}$ and $\Delta(\Delta S°)_{B-A}$ of $(C_nN)_2OH$ and $(C_nN)_2(OH)_2$

		$(C_nN)_2OH$		$(C_nN)_2(OH)_2$	
Mobile phase	B-A	$\Delta(\Delta H°)_{B-A}$ kJ/mol	$\Delta(\Delta S°)_{B-A}$ J/mol	$\Delta(\Delta H°)_{B-A}$ kJ/mol	$\Delta(\Delta S°)_{B-A}$ J/mol
80:20:0	C_{10}-C_8	-2.24	-0.3	-1.51	-0.8
CH_3OH:CH_3CN:H_2O	C_{12}-C_{10}	-7.23	-19.6	-6.32	-16.3
5 m*M* *p*-TSA & *p*-TSNa	C_{14}-C_{12}	-6.59	-16.7	-7.44	-19.6
	C_{16}-C_{14}	-6.78	-16.8	-6.00	-14.3
	C_{18}-C_{16}	-7.61	-19.3	-7.67	-19.6
78:19.5:2.5	C_{10}-C_8	-3.64	-6.0	-4.27	-9.5
CH_3OH:CH_3CN:H_2O	C_{12}-C_{10}	-4.04	-8.1	-4.86	-11.0
5 m*M* *p*-TSA & *p*-TSNa	C_{14}-C_{12}	-4.45	-8.8	-3.73	-6.4
	C_{16}-C_{14}	-5.02	-10.2	-5.27	-11.1
	C_{18}-C_{16}	-5.48	-11.3	-5.47	-11.4
76:19:5	C_{10}-C_8	-5.01	-11.6	-6.25	-15.7
CH_3OH:CH_3CN:H_2O	C_{12}-C_{10}	-5.91	-13.3	-6.08	-13.9
5 m*M* *p*-TSA & *p*-TSNa	C_{14}-C_{12}	-6.63	-15.3	-6.33	-14.2
	C_{16}-C_{14}	-7.79	-18.5	-7.86	-18.7
	C_{18}-C_{16}	-7.75	-17.8	-6.93	-15.3

7.4.3 Surface coverage

Following the discussion in Section 3.4.5, an estimated amount of toluenesulfonate ions adsorbed is given by

1×10^{-3} *M* x 1 x 10^{-3} L/min x 10 min x (1.00 -0.90)/2

$= 5 \times 10^{-7}$ mol

Where 1×10^{-3} *M* is the molarity of sodium *p*-toluenesulfonate plus *p*-toluenesulfonic acid in the mobile phase; other values are the same as listed and explained in Section 3.4.5.

Using the same assumption made previously for the surface area of the column packing material, an estimated surface coverage of the toluenesulfonate ion is approximately 1.5×10^{-2} molecules/nm^2 or 60 nm^2/molecule. Since the surface area of one *p*-toluenesulfonate ion is about 0.2 nm^2, most of the C18 stationary surface is not covered and is accessible to the analyte. This calculation provides additional support for process B.

7.4.4 Detector response

The peaks in Figure 7-3 to 7-8 are produced by the co-elution of the UV absorbing *p*-toluenesulfonate ion and the non-UV absorbing surfactant ion. The calculated detector response is given in Table 7-4, which is the peak area per mole of the analyte. The relative detector response in Table 7-4 is the ratio of the detector response from the co-elution of surfactants and ion-interaction reagents to the detector response of ion-interaction reagents. If there were strongly bonded ion-pairs, the relative detector response would have been 2 approximately since a gemini surfactant carries two ionic groups with a 2+ total charge and could combine with two *p*-toluenesulfonate ions. However, the calculated relative detector response is close to 1. The data suggest an approximately 1:1 ratio of the $(C_nN)_2OH$ or $(C_nN)_2(OH)_2$ ion and the *p*-toluenesulfonate ion co-eluted. These ions do not seem to be strongly bonded.

Table 7-4 Detector response of *p*-toluenesulfonate and $(C_nN)_2OH$ or $(C_nN)_2(OH)_2$ co-elution

	$(C_nN)_2OH^*$		$(C_nN)_2(OH)_2^{**}$	
	Detector response (area/mol)x10^{-12}	Relative detector response***	Detector response (area/mol)x10^{-12}	Relative detector response
C_8	4.95	1.13	4.29	0.98
C_{10}	4.96	1.13	4.33	0.99
C_{12}	4.94	1.13	4.85	1.11
C_{14}	4.97	1.13	4.28	0.98
C_{16}	5.07	1.16	4.07	0.93
p-TSA+*p*-TSNa	4.38	1	4.38	1

* Data based on Figure 7-3.
** Data based on Figure 7-6.
*** Detector response ratio of C_n to *p*-TSA + *p*-TSNa.

Chapter 8

log CMC, pC_{20} and log k' of Nonaromatic Quaternary Ammonium Geminis

8.1 Correlation between log CMC, pC_{20} and log k'

Two series of nonaromatic quaternary ammonium gemini surfactants, $(C_nN)_2OH$ and $(C_nN)_2(OH)_2$, have the same unusual surface and micellar properties as the aromatic quaternary ammonium gemini surfactant discussed in Section 6-1. The surface tension measurement results[70,73] show that log CMC and pC_{20} values of the larger homologs deviate from regularity. The $(C_nN)_2OH$ and $(C_nN)_2(OH)_2$ surfactants with an n value 14 or greater have higher CMC values and lower pC_{20} values than the expected. This unusual property causes the deviation in the log CMC and log k', pC_{20} and log k' correlations. Because there is no micelle formation in the chromatographic mobile phases used in our work, plots of log k' vs. the carbon number are almost linear. The following equations apply to the C_8, C_{10} and C_{12} surfactants in the series.

$$\log CMC = - m\log k' + c \qquad (1\text{-}25)$$

$$pC_{20} = m' \log k' + c' \qquad (1\text{-}27)$$

Plotting the literature log CMC and pC_{20} values[70,73] vs. our experimental log k' gives the straight line for the C_8, C_{10} and C_{12} as showed in Figures 8-1, 8-2, 8-3, and 8-4. The deviations of the larger members from this linear trend are discussed in the next section.

Tables 8-1 and 8-2 list the literature[70][73] and calculated log CMC and pC_{20} values, where the summary is the average over all calculated values. Because of the low solubility of $(C_{18}N)_2OH$, $(C_{16}N)_2(OH)_2$, and $(C_{18}N)_2(OH)_2$ under the CMC and pC_{20} measurement conditions, there are no log CMC and pC_{20} values for these surfactants. The calculated values in the tables were obtained using our log k' values and equations (1-25) and (1-27). The parameters in the equations were defined with the C_8 and C_{12} data.

The results show good agreement between experimental and calculated values for $(C_{10}N)_2OH$ and $(C_{10}N)_2(OH)_2$ surfactants. The standard deviation over all calculated values is small. But the calculated log CMC values of $(C_nN)_2OH$ and $(C_nN)_2(OH)_2$ with $n \geq 14$ are smaller than the experimental data, and the pC_{20} values are larger. These deviations are similar to the surface tension measurement results (see Section 8-2). The results suggest that the prediction of log CMC and pC_{20} using log k' is only applicable for surfactants showing normal behavior.

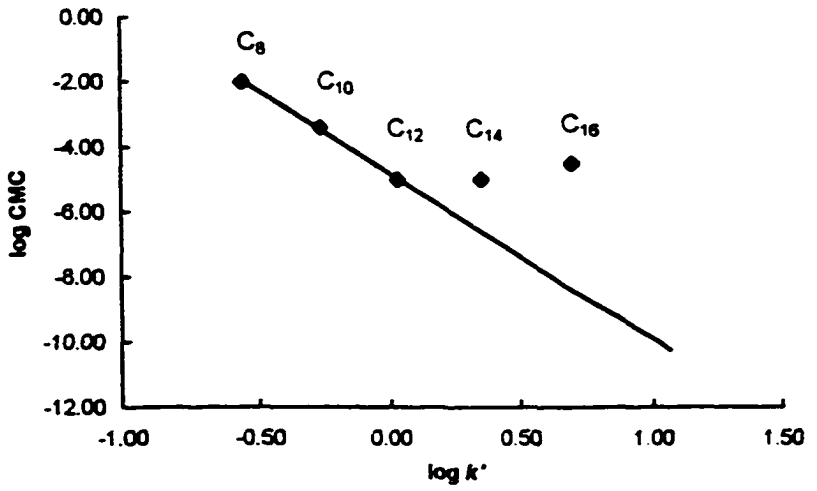

(a)

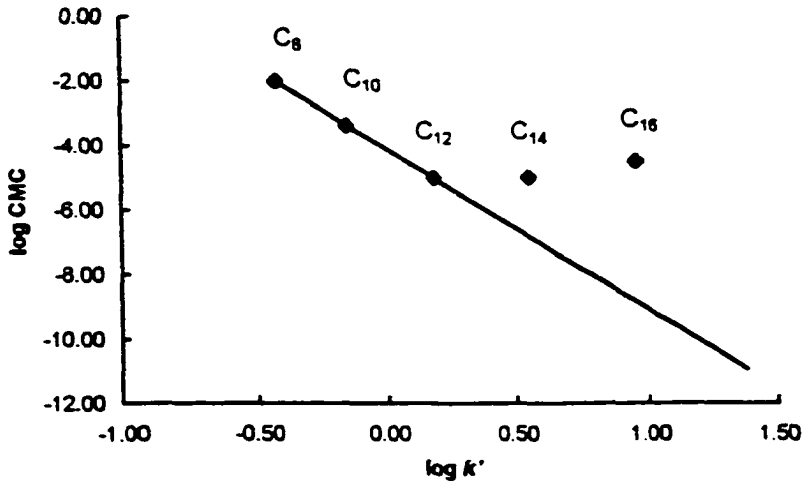

(b)

Figure 8-1 Correlation between log CMC and log k' for $(C_nN)_2OH$
(a) log k': 78:19.5:2.5 CH_3OH:CH_3CN:H_2O, 5 m*M* *p*-TSA & *p*-TSNa, 25 °C
(b) log k': 76:19:5 CH_3OH:CH_3CN:H_2O, 5 m*M* *p*-TSA & *p*-TSNa, 25 °C

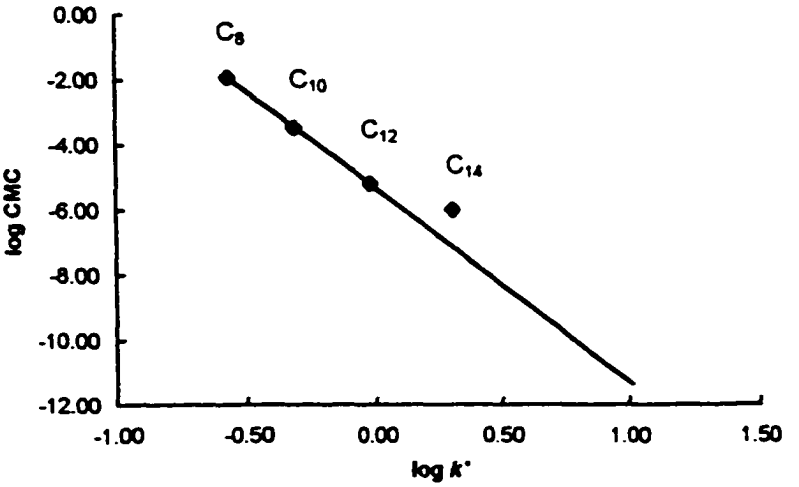

(a)

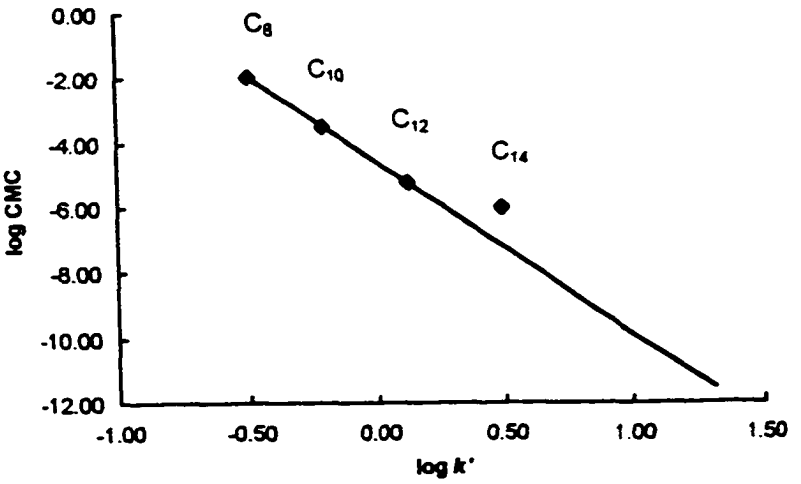

(b)

Figure 8-2 Correlation between log CMC and log k' for $(C_nN)_2(OH)_2$
(a) log k': 78:19.5:2.5 CH_3OH:CH_3CN:H_2O, 5 mM *p*-TSA & *p*-TSNa, 25 °C
(b) log k': 76:19:5 CH_3OH:CH_3CN:H_2O, 5 mM *p*-TSA & *p*-TSNa, 25 °C

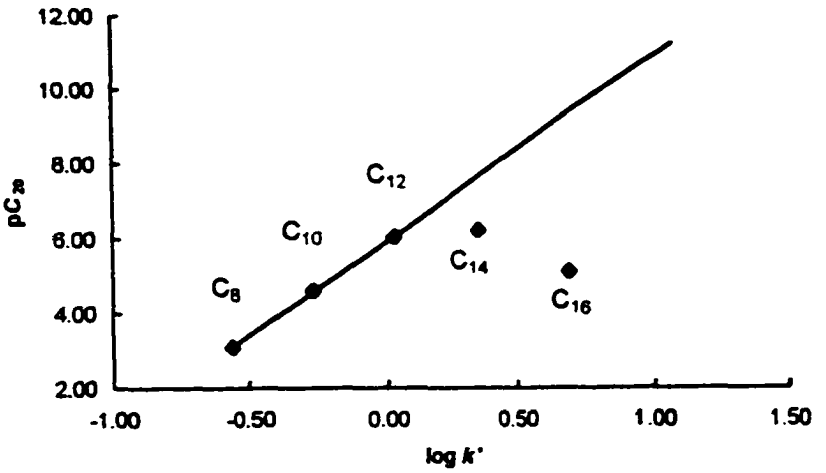

(a)

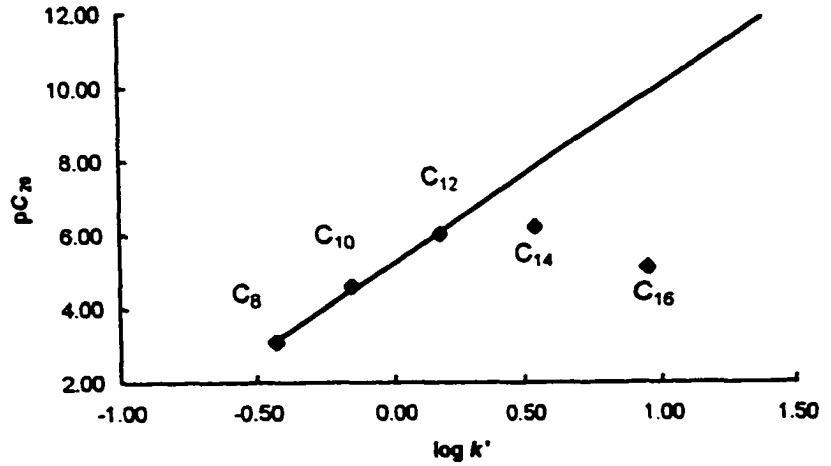

(b)

Figure 8-3 Correlation between pC_{20} and log k' for $(C_nN)_2OH$
(a) log k': 78:19.5:2.5 CH_3OH:CH_3CN:H_2O, 5 mM *p*-TSA & *p*-TSNa, 25 °C
(b) log k': 76:19:5 CH_3OH:CH_3CN:H_2O, 5 mM *p*-TSA & *p*-TSNa, 25 °C

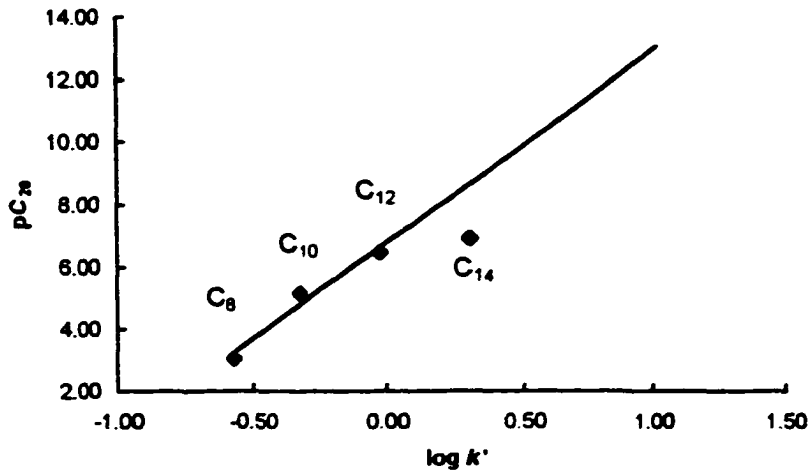

(a)

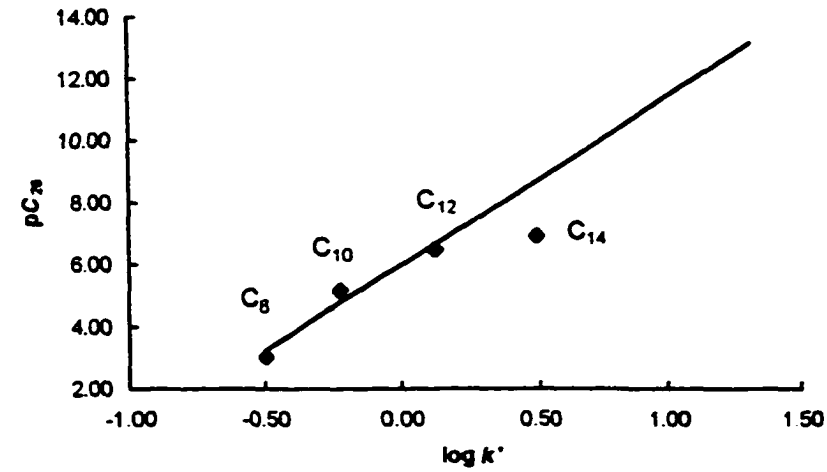

(b)

Figure 8-4 Correlation between pC_{20} and log k' for $(C_nN)_2(OH)_2$
(a) log k': 78:19.5:2.5 CH_3OH:CH_3CN:H_2O, 5 m*M* *p*-TSA & *p*-TSNa, 25 °C
(b) log k': 76:19:5 CH_3OH:CH_3CN:H_2O, 5 m*M* *p*-TSA & *p*-TSNa, 25 °C

Table 8-1 log CMC and pC_{20} of nonaromatic quaternary ammonium geminis $(C_nN)_2OH$

			Exp*	C_8**	C_{10}	C_{12}**	C_{14}	C_{16}	C_{18}
			log CMC	-2.02	-3.40	-5.02	-5.00	-4.50	-
			pC_{20}	3.10	4.60	6.04	6.22	5.10	-
HPLC Condition	T (°C)	Cal.							
80:20:0 $CH_3OH:CH_3CN:H_2O$	24	log CMC	-	-3.38	-	-6.66	-8.44	-10.30
5 mM *p*-TSA, 5 mM *p*-TSNa		pC_{20}	-	4.44	-	7.65	9.39	11.22
	27	log CMC	-	-3.45	-	-6.75	-8.70	-10.75
		pC_{20}	-	4.50	-	7.74	9.65	11.66
	41	log CMC	-	-4.17	-	-6.25	-7.65	-9.08
		pC_{20}	-	5.20	-	7.24	8.61	10.02
	51	log CMC	-	-4.06	-	-6.21	-7.55	-8.92
		pC_{20}	-	5.10	-	7.21	8.52	9.86
78:19.5:2.5 $CH_3OH:CH_3CN:H_2O$	25	log CMC	-	-3.51	-	-6.66	-8.43	-10.31
5 mM *p*-TSA, 5 mM *p*-TSNa		pC_{20}	-	4.56	-	7.65	9.38	11.22
	31	log CMC	-	-3.58	-	-6.67	-8.45	-10.38
		pC_{20}	-	4.63	-	7.65	9.40	11.29
	41	log CMC	-	-3.54	-	-6.66	-8.37	-10.22
		pC_{20}	-	4.59	-	7.64	9.32	11.14
	51	log CMC	-	-3.57	-	-6.64	-8.37	-10.21
		pC_{20}	-	4.61	-	7.62	9.32	11.13
76:19:5 $CH_3OH:CH_3CN:H_2O$	24	log CMC	-	-3.38	-	-6.84	-8.83	-10.94
5 mM *p*-TSA, 5 mM *p*-TSNa		pC_{20}	-	4.44	-	7.82	9.77	11.84
	31	log CMC	-	-3.36	-	-6.79	-8.72	-10.80
		pC_{20}	-	4.42	-	7.77	9.67	11.71
	41	log CMC	-	-3.16	-	-6.77	-8.73	-10.87
		pC_{20}	-	4.22	-	7.76	9.68	11.78
	51	log CMC	-	-3.45	-	-6.83	-8.75	-10.83
		pC_{20}	-	4.50	-	7.82	9.70	11.73
Summary		log CMC	-	-3.55	-	-6.64	-8.42	-10.30
		stdev	-	0.29	-	0.21	0.42	0.67
		pC_{20}	-	4.60	-	7.63	9.37	11.22
		stdev	-	0.28	-	0.20	0.41	0.65

* CMC and pC_{20} were measured in 0.1 *M* NaCl, at 25 °C (ref.[70]).

** Used to determine parameters in equations (1-25) and (1-27).

Table 8-2 log CMC and pC_{20} of nonaromatic quaternary ammonium geminis $(C_nN)_2(OH)_2$

		Exp*	C_8**	C_{10}	C_{12}**	C_{14}	C_{16}	C_{18}
		log CMC	-1.96	-3.48	-5.22	-6.00	-	-
		pC_{20}	3.05	5.17	6.47	6.90	-	-
HPLC Condition	T (°C)	Cal.						
80:20:0 $CH_3OH:CH_3CN:H_2O$	25	log CMC	-	-3.45	-	-7.07	-9.08	-10.86
5 mM *p*-TSA, 5 mM *p*-TSNa		pC_{20}	-	4.61	-	8.41	10.52	12.38
	29	log CMC	-	-3.63	-	-7.06	-9.07	-11.20
		pC_{20}	-	4.80	-	8.40	10.50	12.73
	41	log CMC	-	-3.71	-	-7.02	-9.10	-11.07
		pC_{20}	-	4.88	-	8.35	10.53	12.60
	51	log CMC	-	-3.69	-	-6.76	-8.66	-10.54
		pC_{20}	-	4.87	-	8.08	10.08	12.05
78:19.5:2.5 $CH_3OH:CH_3CN:H_2O$	25	log CMC	-	-3.46	-	-7.15	-9.21	-11.36
5 mM *p*-TSA, 5 mM *p*-TSNa		pC_{20}	-	4.63	-	8.49	10.65	12.90
	31	log CMC	-	-3.68	-	-7.23	-9.43	-11.33
		pC_{20}	-	4.85	-	8.58	10.88	12.87
	41	log CMC	-	-3.55	-	-7.28	-9.38	-11.24
		pC_{20}	-	4.72	-	8.63	10.82	12.78
	51	log CMC	-	-3.66	-	-7.19	-9.20	-10.97
		pC_{20}	-	4.84	-	8.53	10.64	12.50
76:19:5 $CH_3OH:CH_3CN:H_2O$	24	log CMC	-	-3.44	-	-7.18	-9.32	-11.51
5 mM *p*-TSA, 5 mM *p*-TSNa		pC_{20}	-	4.60	-	8.52	10.76	13.06
	31	log CMC	-	-3.42	-	-7.15	-9.25	-11.45
		pC_{20}	-	4.58	-	8.50	10.69	13.00
	41	log CMC	-	-3.46	-	-7.06	-9.04	-10.90
		pC_{20}	-	4.62	-	8.40	10.47	12.42
	51	log CMC	-	-3.55	-	-7.11	-9.08	-10.88
		pC_{20}	-	4.72	-	8.45	10.51	12.40
Summary		log CMC	-	-3.56	-	-7.11	-9.15	-11.11
		stdev	-	0.11	-	0.13	0.20	0.29
		pC_{20}	-	4.73	-	8.45	10.59	12.64
		stdev	-	0.12	-	0.14	0.21	0.30

* CMC and pC_{20} were measured in 0.1 *M* NaBr, at 25 °C (ref.[73]).

** Used to determine parameters in equations (1-25) and (1-27).

8.2 Discussion

8.2.1 Irregularity of $(C_{14}N)_2OH$, $(C_{16}N)_2OH$, and $(C_{14}N)_2(OH)_2$

The irregularity in the surface tension and micellar properties of the $(C_nN)_2OH$ and $(C_nN)_2(OH)_2$ series of surfactants in water are shown in Figures 8-5[70] and 8-6[73]. As mentioned in Section 6.2.1, the proposed reason is the formation of premicellar aggregates with little or no surface activity before the micelle formation.

Because of the formation of premicellar aggregates instead of micelles, the CMC and pC_{20} values of these longer chain surfactants obtained using the surface tension measurement cannot be used to calculate the slopes and intercepts in the equations (1-25) and (1-27). However, equations (1-25) and (1-27) can be used to estimate what the CMC and pC_{20} would be if there were no premicellar aggregates. The calculated log CMC and pC_{20} values of $(C_{14}N)_2OH$, $(C_{16}N)_2OH$ and $(C_{14}N)_2(OH)_2$ using log k' data correspond well with the expected values extrapolated from the linear relationships between the log CMC, pC_{20} and the alkyl chain length (Tables 8-3 and 8-4).

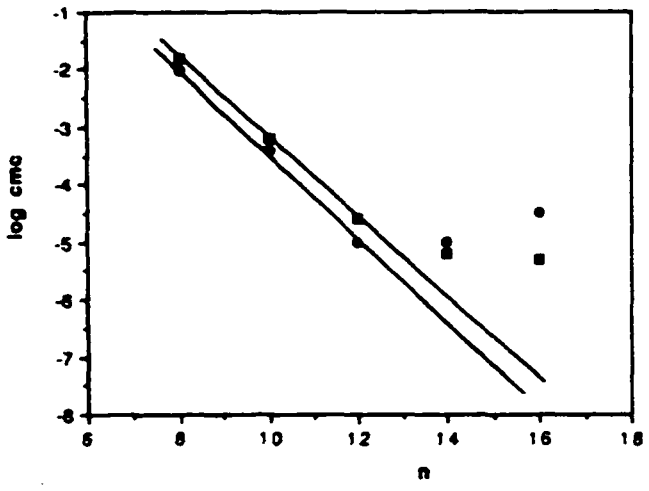

log CMC vs. carbon number

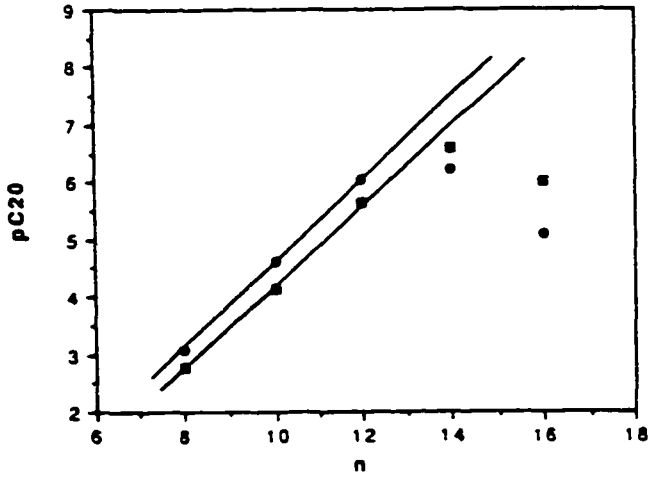

pC_{20} vs. carbon number

Figure 8-5 Unexpected surface properties of nonaromatic quaternary ammonium gemini surfactants $(C_nN)_2OH$[70] In 0.1 *M* NaCl: ● at 25 °C; ■ at 50 °C.

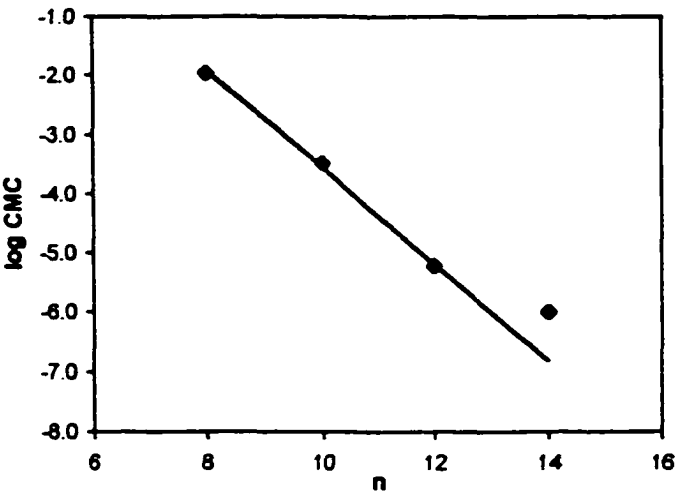

log CMC vs. carbon number

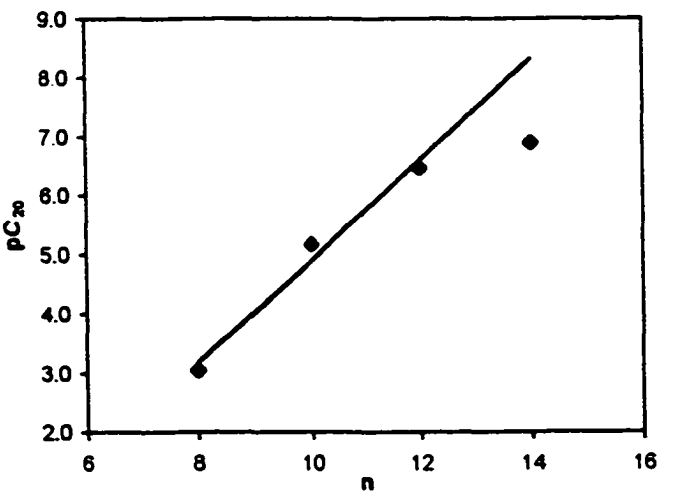

pC_{20} vs. carbon number

Figure 8-6 Unexpected surface properties of nonaromatic quaternary ammonium gemini surfactants $(C_nN)_2(OH)_2$[73] In 0.1 *M* NaBr, at 25 °C.

Table 8-3 Expected log CMC and pC_{20} of $(C_{14}N)_2OH$, $(C_{16}N)_2OH$ and $(C_{18}N)_2OH$

Method	C_{14}	C_{16}	C_{18}
log CMC			
log CMC vs. carbon atom number*	-6.52	-8.02	-9.52
log CMC vs. log k'**	-6.64	-8.42	-10.30
pC_{20}			
pC_{20} vs. carbon atom number*	7.51	8.98	10.45
pC_{20} vs. log k'**	7.63	9.37	11.22

* CMC and pC_{20} in 0.1 *M* NaCl, at 25 °C[70].
** The summary values in Table 8-1.

Table 8-4 Expected log CMC and pC_{20} of $(C_{14}N)_2(OH)_2$, $(C_{16}N)_2(OH)_2$ and $(C_{18}N)_2(OH)_2$

Method	C_{14}	C_{16}	C_{18}
log CMC			
log CMC vs. carbon atom number*	-6.85	-8.49	-10.12
log CMC vs. log k'**	-7.11	-9.15	-11.11
pC_{20}			
pC_{20} vs. carbon atom number*	8.18	9.89	11.60
pC_{20} vs. log k'**	8.45	10.59	12.64

* CMC and pC_{20} in 0.1 *M* NaBr, at 25 °C[73].
** The summary values in Table 8-2.

8.2.2 log CMC and log k'

The values of the slope and intercept for the equation (1-25) are listed in Table 8-5 (for the $(C_nN)_2OH$ series) and Table 8-6 (for the $(C_nN)_2(OH)_2$ series).

$$\log CMC = - m\log k' + c \qquad (1\text{-}25)$$

They are calculated using C_8 and C_{12} data. The log k' values are the averages over various sets of chromatographic experiments.

As mentioned in Section 4.2.1, the slope is a measure of different tendencies for a homologous series of surfactants to partition onto the HPLC stationary phase (the monomer adsorbing onto the interface) and to self-associate (micellization) in aqueous solution. The change in the log k' under various HPLC conditions will change the intercept. For these two series of surfactants, the chromatographic mobilities vary slightly. Therefore these parameters do not change substantially.

(a) $(C_nN)_2OH$

The slopes are in the range of -4.9 to -6.6, but there is no obvious trend. The intercept is between -4.2 to -7.4. It becomes more negative with decreasing water percentage in the mobile phase and increasing HPLC temperature.

(b) $(C_nN)_2(OH)_2$

The slope is in the range of -5.3 to -8.7. The intercept is between -4.6 to -8.6. These parameters become more

negative with decreasing water percentage and increasing temperature.

Table 8-5 Parameters in the log CMC* and log k' correlation equation for $(C_nN)_2OH$ surfactants

HPLC condition	T (°C)	Slope	Intercept
80:20:0 $CH_3OH:CH_3CN:H_2O$	24	-5.59	-5.71
5 m*M* *p*-TSA, 5 m*M* *p*-TSNa	27	-6.42	-5.90
	41	-5.91	-6.77
	51	-6.00	-7.35
78:19.5:2.5 $CH_3OH:CH_3CN:H_2O$	25	-5.08	-4.88
5 m*M* *p*-TSA, 5 m*M* *p*-TSNa	31	-5.57	-5.36
	41	-5.80	-5.85
	51	-6.28	-6.11
76:19:5 $CH_3OH:CH_3CN:H_2O$	24	-4.93	-4.15
5 m*M* *p*-TSA, 5 m*M* *p*-TSNa	31	-5.17	-4.53
	41	-6.00	-4.85
	51	-6.57	-5.68

* In 0.1 *M* NaCl, at 25 °C[70].

Table 8-6 Parameters in the log CMC* and log *k'* correlation equation for $(C_nN)_2(OH)_2$ surfactants

HPLC condition	T (°C)	Slope	Intercept
80:20:0 $CH_3OH:CH_3CN:H_2O$	25	-6.64	-6.54
5 m*M* *p*-TSA, 5 m*M* *p*-TSNa	29	-6.86	-6.76
	41	-8.72	-8.15
	51	-8.43	-8.65
78:19.5:2.5 $CH_3OH:CH_3CN:H_2O$	25	-5.94	-5.36
5 m*M* *p*-TSA, 5 m*M* *p*-TSNa	31	-6.74	-6.00
	41	-7.14	-6.67
	51	-7.33	-6.87
76:19:5 $CH_3OH:CH_3CN:H_2O$	24	-5.28	-4.59
5 m*M* *p*-TSA, 5 m*M* *p*-TSNa	31	-5.58	-5.00
	41	-6.12	-5.33
	51	-6.71	-6.18

* In 0.1 *M* NaBr, at 25 °C[73].

8.2.3 pC_{20} and log k'

The values of the slope and intercept from equation (1-27) are listed in Table 8-7 (the $(C_nN)_2OH$ series) and Table 8-8 (the $(C_nN)_2(OH)_2$ series).

$$pC_{20} = m' \log k' + c' \qquad (1\text{-}27)$$

They are obtained using C_8 and C_{12} data. The log k' values are averages over various sets of chromatographic experiments.

This slope is a measure of the different tendency to partition between the mobile-stationary interface and the water-air interface, for a homologous series of surfactants. The change in the log k' under various HPLC conditions changes the intercept. As mentioned previous, for these two series of surfactants these parameters do not change substantially.

(a) $(C_nN)_2OH$

The slope is in the range of 4.8 to 6.4, but there is no obvious trend. The intercept becomes more positive as the water percentage is decreased and temperature increased because of the decrease in log k'. Its value is between 5.2 to 8.3.

(b) $(C_nN)_2(OH)_2$

The slope is in the range of 5.5 to 9.1. The intercept varies from 5.8 to 10.1. These parameters increase with decreasing water percentage in the mobile phase and increasing temperature.

The slopes and intercepts in equations (1-25) and (1-27)

vary with the chromatographic conditions and the various homologous series. Since two series of surfactants are chromatographed under the same conditions, the differences in these parameters are produced by surfactants themselves. The comparison can be made for the two series of nonaromatic quaternary ammonium gemini surfactants, $(C_nN)_2OH$ and $(C_nN)_2(OH)_2$. Tables 8-5 to 8-8 show that the values of parameters are different for these two homologous series. All absolute values are larger with the $(C_nN)_2(OH)_2$ series.

Table 8-7 Parameters in the pC_{20}^{*} and log k' correlation equation for $(C_nN)_2OH$ surfactants

HPLC condition	T (°C)	Slope	Intercept
80:20:0 CH_3OH:CH_3CN:H_2O	24	5.48	6.71
5 m*M* *p*-TSA, 5 m*M* *p*-TSNa	27	6.29	6.90
	41	5.79	7.76
	51	5.88	8.32
78:19.5:2.5 CH_3OH:CH_3CN:H_2O	25	4.98	5.91
5 m*M* *p*-TSA, 5 m*M* *p*-TSNa	31	5.46	6.37
	41	5.69	6.85
	51	6.15	7.10
76:19:5 CH_3OH:CH_3CN:H_2O	24	4.83	5.19
5 m*M* *p*-TSA, 5 m*M* *p*-TSNa	31	5.07	5.56
	41	5.88	5.87
	51	6.44	6.68

* In 0.1 *M* NaCl, at 25 °C[79].

Table 8-8 Parameters in the pC_{20}^{*} and log k' correlation equation for $(C_nN)_2(OH)_2$ surfactants

HPLC condition	T (°C)	Slope	Intercept
80:20:0 $CH_3OH:CH_3CN:H_2O$	25	6.96	7.85
5 mM *p*-TSA, 5 mM *p*-TSNa	29	7.19	8.08
	41	9.14	9.54
	51	8.84	10.06
78:19.5:2.5 $CH_3OH:CH_3CN:H_2O$	25	6.23	6.61
5 mM *p*-TSA, 5 mM *p*-TSNa	31	7.06	7.29
	41	7.48	7.99
	51	7.68	8.20
76:19:5 $CH_3OH:CH_3CN:H_2O$	24	5.54	5.81
5 mM *p*-TSA, 5 mM *p*-TSNa	31	5.85	6.24
	41	6.42	6.58
	51	7.03	7.48

* In 0.1 *M* NaBr, at 25 °C[73].

8.3 m/m', CMC/C_{20} and $\Delta G^{\circ}_{mic}/\Delta G^{\circ}_{ad}$

The CMC/C_{20} ratio is an important parameter which serves as a measure of surfactant effectiveness[15,74]. A larger value of the CMC/C_{20} indicates a greater tendency of the surfactant to adsorb at the surface relative to the tendency to form micelles. Relating the ratio of the slopes, m and m', in equations (1-25) and (1-27) to the CMC/C_{20} and to the ratio of ΔG°_{mic} and ΔG°_{ad} has been investigated.

By rearranging equations (1-25) and (1-27), we obtain

$$m = - \frac{\log CMC - c}{\log k'} \qquad (4\text{-}1)$$

$$m' = \frac{pC_{20} - c'}{\log k'} \qquad (4\text{-}2)$$

The ΔG°_{mic}[75] and ΔG°_{ad}[76] are

$$\Delta G^{\circ}_{mic} = 2.3RT\log CMC + K \qquad (4\text{-}3)$$

$$\Delta G^{\circ}_{ad} = - 2.3RTpC_{20} + K' \qquad (4\text{-}4)$$

The K and K' values involve the molar concentration of water and contributions from counterions of the surfactant. The K' is also related to the surface area per adsorbed molecule for monolayer adsorption. In most situations the value of the area/molecule at the interface for a homologous series of surfactants does not change much with increase in the chain length of the hydrophobic group. The K and K' can be

considered as constants.

Because the constants in each equation are not the same, no direct relationship can be written between m/m' and CMC/C_{20}, or m/m' and $\Delta G°_{mic}/\Delta G°_{ad}$. One could relate these parameters if the constants were known, but it might be a circular calculation, and is not significant or convenient.

Table 8-9 lists the CMC/C_{20} ratio and the log CMC/pC_{20} ratio of $(C_nN)_2OH$[70] and $(C_nN)_2(OH)_2$[73] surfactants. The comparison of the slopes in equations (1-25) and (1-27) is shown in Tables 8-10 and 8-11, where different sets of literature CMC and pC_{20} values are used. The $(C_nN)_2(OH)_2$ series has larger CMC/C_{20} ratios (see Table 8-9). But in Table 8-10 the absolute values of the m/m' are smaller with the $(C_nN)_2(OH)_2$ series. Here, the ratios of the log CMC/pC_{20} and the m/m' have the same trend of slightly less negative for the $(C_nN)_2(OH)_2$ series. However, in Table 8-11 the absolute values of the m/m' are larger with the $(C_nN)_2(OH)_2$ series. Therefore due to the constant terms in each equation one can not simply relate these parameters.

Table 8-9 CMC/C_{20} ratio of $(C_nN)_2OH$ and $(C_nN)_2(OH)_2$

Surfactant	CMC (M)	C_{20} (M)	CMC/C_{20}	log CMC/pC_{20}
$(C_nN)_2OH^*$				
C_8	9.55×10^{-3}	7.94×10^{-4}	12.0	-0.65
C_{10}	3.98×10^{-4}	2.51×10^{-5}	15.8	-0.74
C_{12}	9.55×10^{-6}	9.12×10^{-7}	10.5	-0.83
$(C_nN)_2(OH)_2^{**}$				
C_8	1.10×10^{-2}	8.91×10^{-4}	12.3	-0.64
C_{10}	3.30×10^{-4}	6.76×10^{-6}	48.8	-0.67
C_{12}	6.00×10^{-6}	3.39×10^{-7}	17.7	-0.81
$(C_nN)_2(OH)_2^{***}$				
C_{10}	1.00×10^{-3}	3.98×10^{-5}	25.1	-0.68
C_{12}	2.10×10^{-5}	9.33×10^{-7}	22.5	-0.78

* In 0.1 M NaCl, 25 °C[70].
** In 0.1 M NaBr, 25 °C[73].
*** In 0.1 M NaCl, 25 °C[73].

Table 8-10 Comparison of the slopes in log CMC, pC_{20} and log k' correlations (I)

		$(C_nN)_2OH^+$			$(C_nN)_2(OH)_2^{++}$		
HPLC condition	T(°C)	m	m'	m/m'	m	m'	m/m'
80:20:0	25	-5.59	5.48	-1.02	-6.64	6.96	-0.95
$CH_3OH:CH_3CN:H_2O$	28	-6.42	6.29	-1.02	-6.86	7.19	-0.95
	41	-5.91	5.79	-1.02	-8.72	9.14	-0.95
	51	-6.00	5.88	-1.02	-8.43	8.84	-0.95
78:19.5:2.5	25	-5.08	4.98	-1.02	-5.94	6.23	-0.95
$CH_3OH:CH_3CN:H_2O$	31	-5.57	5.46	-1.02	-6.74	7.06	-0.95
	41	-5.80	5.69	-1.02	-7.14	7.48	-0.95
	51	-6.28	6.15	-1.02	-7.33	7.68	-0.95
76:19:5	24	-4.93	4.83	-1.02	-5.28	5.54	-0.95
$CH_3OH:CH_3CN:H_2O$	31	-5.17	5.07	-1.02	-5.58	5.85	-0.95
	41	-6.00	5.88	-1.02	-6.12	6.42	-0.95
	51	-6.57	6.44	-1.02	-6.71	7.03	-0.95

* CMC and C_{20} in 0.1 *M* NaCl, 25 °C[70].
** CMC and C_{20} in 0.1 *M* NaBr, 25 °C[73].

Table 8-11 Comparison of the slopes in log CMC, pC_{20} and log k' correlations (II)

		$(C_nN)_2OH^+$			$(C_nN)_2(OH)_2^{++}$		
HPLC condition	T(°C)	m	m'	m/m'	m	m'	m/m'
80:20:0	25	-5.59	5.48	-1.02	-6.27	6.09	-1.03
$CH_3OH:CH_3CN:H_2O$	28	-6.42	6.29	-1.02	-7.24	7.04	-1.03
	41	-5.91	5.79	-1.02	-9.66	9.38	-1.03
	51	-6.00	5.88	-1.02	-9.25	8.99	-1.03
78:19.5:2.5	25	-5.08	4.98	-1.02	-5.67	5.51	-1.03
$CH_3OH:CH_3CN:H_2O$	31	-5.57	5.46	-1.02	-7.34	7.13	-1.03
	41	-5.80	5.69	-1.02	-7.18	6.98	-1.03
	51	-6.28	6.15	-1.02	-7.89	7.67	-1.03
76:19:5	24	-4.93	4.83	-1.02	-4.98	4.84	-1.03
$CH_3OH:CH_3CN:H_2O$	31	-5.17	5.07	-1.02	-5.19	5.04	-1.03
	41	-6.00	5.88	-1.02	-5.81	5.65	-1.03
	51	-6.57	6.44	-1.02	-6.73	6.54	-1.03

* CMC and C_{20} in 0.1 *M* NaCl, 25 °C[70].
** CMC and C_{20} in 0.1 *M* NaCl, 25 °C[73].

Chapter 9

Conclusions and Further Study

9.1 Conclusions

Throughout this thesis, the application of ion-interaction reversed-phase chromatography to ionic surfactants, including three series of the new gemini type of surfactants and alkanesulfonates, has been demonstrated. We also have presented a discussion of the retention mechanism for each series of surfactants under the chromatographic conditions. The correlations between log CMC and log k', pC_{20} and log k' have been explored as well.

9.1.1 RP-HPLC of ionic surfactants

For RP-HPLC separation of ionic surfactants, the ion-interaction technique is needed. The ion-interaction reagents can be chosen from organic or inorganic salts based on the analytes and separation conditions. In this work dodecylpyridinium bromide is used for alkanesulfonates; sodium perchlorate is the ion-interaction reagent for the aromatic quaternary ammonium gemini surfactants $(C_nN)_2Ar$; for the nonaromatic quaternary ammonium gemini surfactants $(C_nN)_2OH$ and

$(C_nN)_2(OH)_2$, the ion-interaction reagent is sodium *p*-toluenesulfonate and *p*-toluenesulfonic acid.

If a UV detector is used, indirect UV detection can provide a detection method for the non UV absorbing analytes. This technique is used in the analysis of alkanesulfonates and nonaromatic quaternary ammonium gemini surfactants $(C_nN)_2OH$ and $(C_nN)_2(OH)_2$.

The 33 x 4.6 mm short C18 column was shown to give satisfactory RP-HPLC separation for the surfactants studied in our work. This column provides the advantages of a short separation time, less solvent consumption and lower price compared with a 15 cm column.

The separation methods developed in our work provide a fast and economic RP-HPLC analysis for the three series of gemini surfactants ($(C_nN)_2Ar$, $(C_nN)_2OH$, $(C_nN)_2(OH)_2$) and the series of alkanesulfonates.

9.1.2 The retention mechanism

The study of the retention mechanism indicates that no matter what kind of the ion-interaction reagent is used there are no tightly bonded ion pairs formed, even though the analyte and the ion-interaction reagent co-elute. The oppositely charged ions are separated by the polar solvent molecules. The separation is improved because of the electrostatic interaction and/or dispersion force between the ion-interaction reagent and the analyte. Since the oppositely

charged ions are not tightly bonded, excess ion-interaction reagents are always needed in the mobile phase to enhance the interaction.

9.1.3 The correlations between log CMC and log k', pC_{20} and log k'

The results demonstrate that when the surface and micellar properties of a series of surfactants are normal, there will be linear relationships between log CMC and log k', or pC_{20} and log k'.

$$\log CMC = - m\log k' + c \qquad (1\text{-}25)$$

$$pC_{20} = m'\log k' + c' \qquad (1\text{-}27)$$

The slopes and intercepts in equations (1-25) and (1-27) vary with the surfactants and the experimental conditions. In this work the slopes and intercepts are experimentally evaluated. Therefore, the log CMC and pC_{20} can be calculated using above equations and the log k', if two values of log CMC and pC_{20} in a homologous series are available for the computation of the parameters in the correlation equations.

9.2 Further Study

(a) The gemini surfactants $(C_nN)_2Ar$, $(C_nN)_2OH$, and $(C_nN)_2(OH)_2$ and alkanesulfonates can be quantitatively analyzed using the methods described in this thesis. The detection limit and the linear concentration range could be further studied.

(b) Since only the UV detector and the C18 column were used in this work, other types of detectors and columns could be tried.

(c) The ion-interaction reagents for the analysis of $(C_nN)_2OH$ and $(C_nN)_2(OH)_2$ geminis in our work were limited to ones with UV chromophores. Using the ion-interaction reagents sodium *p*-toluenesulfonate and *p*-toluenesulfonic acid, chromatographic peaks of these surfactants are slightly tailed. Therefore, finding a better ion-interaction reagent, such as benzenesulfonate or xylenesulfonate, could be the next step of the study.

(d) The values of the parameters in the log CMC, pC_{20} and log k' correlation equations (1-25) and (1-27) lie within a certain range for a series of surfactants and change with certain trend with the change of variables. If a large number of series of surfactants could be tested in a systematic way, the range and the trend could be investigated.

References

[1] M.J.Rosen. *Surfactants and Interfacial Phenomena*, 2nd ed.; John Wiley & Sons Inc.: New York, **1989**, 84-85.

[2] M.J.Rosen. *Surfactants and Interfacial Phenomena*, 2nd ed.; John Wiley & Sons Inc.: New York, **1989**, 86-87.

[3] W.C.Preston. *J. Phys. Colloid Chem.* **1948**, *52*, 85.

[4] M.J.Rosen. *Surfactants and Interfacial Phenomena*, 2nd ed.; John Wiley & Sons Inc.: New York, **1989**, 110-111.

[5] J.C.Jacquier and P.L.Desbène. *J. Chromatogr A.* **1995**, *718*, 167-75.

[6] H.B.Klevens. *J. Am. Oil Chem. Soc.* **1953**, *30*, 74-80.

[7] M.J.Rosen. *Surfactants and Interfacial Phenomena*, 2nd ed.; John Wiley & Sons Inc.: New York, **1989**, 135-136.

[8] IUPAC Analytical Chemistry Division, Commission on Analytical Nomenclature (1974). *Pure Appl. Chem.* *37*, 447.

[9] K.Robards, P.R.Haddad, and P.E.Jackson. *Principles and Practice of Modern Chromatographic Methods*; Academic Press: San Diego, **1994**, 38-39.

[10] V.Castro and J.-P.Canselier. *J. Chromatogr.* **1986**, *363*, 139-146.

[11] A.J.P.Martin. *Biochem. Soc. Symp.* **1949**, *3*, 4-20.

[12] G.Shaw, W.H.Elliott, and B.G.Barisas. *Mikrochim. Acta* **1991**, *III*, 137-145.

[13] M.J.Rosen. *Surfactants and Interfacial Phenomena*, 2nd ed.; John Wiley & Sons Inc.: New York, **1989**, 150-154.

[14] M.J.Rosen. *Surfactants and Interfacial Phenomena*, 2nd ed.; John Wiley & Sons Inc.: New York, **1989**, 86.

[15] M.J.Rosen. *CHEMTECH* **1993**, *March*, 30-33.

[16] K.Robards, P.R.Haddad, and P.E.Jackson. *Principles and Practice of Modern Chromatographic Methods*; Academic Press: San Diego, **1994**, 344-345.

[17] S.Eksborg and G.Schill. *Anal. Chem.* **1973**, *45*, 2092-2100.

[18] C.F.Poole and S.K.Poole. *Chromatography Today*; Elsevier: Amsterdam, **1991**, 412.

[19] B.-A.Persson and B.L.Karger. *J. Chromatogr.Sci.* **1974**, *12*, 521-528.

[20] J.C.Kraak and J.F.K.Huber. *J. Chromatogr.* **1974**, *102*, 333-351.

[21] J.H.Knox and G.R.Laird. *J. Chromatogr.* **1976**, *122*, 17-34.

[22] D.P.Wittmer, N.O.Nuessle, and W.G.Haney,Jr.. *Anal. Chem.* **1975**, *47*, 1422-1423.

[23] E.Fitzgerald. *Anal. Chem.* **1976**, *48*, 1734-1735.

[24] C.F.Poole and S.K.Poole. *Chromatography Today*; Elsevier: Amsterdam, **1991**, 417-418.

[25] B.A.Bidlingmeyer, S.N.Deming, W.P.Price,Jr., B.Sackok, and M.Petrusek. *J. Chromatogr.* **1979**, *186*, 419-34.

[26] B.A.Bidlingmeyer. *J. Chromatogr. Sci.* **1980**, *18*, 525-39.

[27] G.Schill and E.Arvidsson. *J. Chromatogr.* **1989**, *492*, 299.

[28] T.M.Schmitt. *Analysis of Surfactants, Surfactant Science Series, Volume 40;* Marcel Dekker, Inc.: New York, **1992**, 167-180.

[29] H.Ullner, I.Koenig, C.Sander, and U.Schwenk. *Tenside* **1980**, *17*, 167-170 (German).

[30] B.A.Bidlingmeyer and F.V.Warren,Jr.. *Anal. Chem.* **1982**, *54*, 2351-2356.

[31] F.Smedes, J.C.Kraak, C.F.Werkhoven-Goewie, U.A.Th. Brinkman, and R.W.Frei. *J. Chromatogr.* **1982**, *247*, 123-132.

[32] V.Castro and J.-P.Canselier. *J. Chromatogr.* **1985**, *325*, 43-51.

[33] G.Eppert and G.Liebscher. *J. Chromatogr.* **1986**, *356*, 372-378 (German).

[34] G.Liebscher, G.Eppert, H.Oberender, H.Berthold, and H.G.Hauthal. *Tenside* **1989**, *26*, 195-197 (German).

[35] K.J.Irgolic and J.E.Hobill. *Spectrochim. Acta, Part B* **1987**, *42B*, 269-273.

[36] G.R.Bear. *J. Chromatogr.* **1988**, *459*, 91-107.

[37] H.König and W.Strobel. *Fresenius'Z. Anal. Chem.* **1988**, *331*, 435-438.

[38] D.J.Pietrzyk, P.G.Rigas, and D.Yuan. *J. Chromatogr. Sci.* **1989**, *27*, 485-90.

[39] L.Chen, X.Liu, and Q.Wang. *Fenxi Ceshi Tongbao* **1991**, *10*, 11-15 (Chinese).

[40] T.M.Schmitt. *Analysis of Surfactants, Surfactant Science Series, Volume 40;* Marcel Dekker, Inc.: New York, **1992**, 203-208.

[41] A.Nakae, K.Kunihiro, and G.Muto. *J. Chromatogr.* **1977**, *134*, 459-466.

[42] R.C.Meyer. *J. Pharm. Sci.* **1980**, *69*, 1148-1150.

[43] K.Nakamura, Y.Morikawa, and I. Matsumoto. *J. Am. Oil Chem. Soc.* **1981**, *58*, 72-77.

[44] K.Nakamura and Y.Morikawa. *J. Am. Oil Chem. Soc.* **1982**, *59*, 64-68.

[45] S.L.Abidi. *J. Chromatogr.* **1985**, *324*, 209-230.

[46] S.L.Abidi. *J. Chromatogr.* **1986**, *362*, 33-46.

[47] G.Ambrus, L.T.Takahashi, and P.A.Marty. *J. Pharm. Sci.* **1987**, *76*, 174-176.

[48] M.Denkert, L.Hackzell, G.Schill, and E.Sjögren. *J. Chromatogr.* **1981**, *218*, 31-43.

[49] P.Helboe. *J. Chromatogr.* **1983**, *261*, 117-122.

[50] J.Kawase, Y.Takao, and K.Tsuji. *J. Chromatogr.* **1983**, *262*, 293-298.

[51] C.B.Huang. *J. Liq. Chromatogr.* **1987**, *10(6)*, 1103-1125.

[52] C.J.Dowle, W.C.Campbell, and B.G.Cooksey. *Analyst* **1989**, *114*, 883-885.

[53] T.Suortti and H.Sirvio. *J. Chromatogr.* **1990**, *507*, 421-425.

[54] The Perkin-Elmer Corp. *The Liquid Chromatography Supplies Catalog* **1991**.

[55] Alltech Associates, Inc. *Chromatography Catalog 350* **1994**.

[56] D.A.Skoog and J.J.Leary. *Principles of Instrumental Analysis*, 4th ed.; Saunders College Publishing: **1992**, 586-587.

[57] K.Robards, P.R.Haddad, and P.E.Jackson. *Principles and Practice of Modern Chromatographic Methods*; Academic Press: San Diego, **1994**, 49-53.

[58] W.J.Moore. *Physical Chemistry*, 4th ed.; Prentice-Hall, Inc.: New Jersey, **1972**, 425-35.

[59] D.A.Skoog and J.J.Leary. *Principles of Instrumental Analysis*, 4th ed.; Saunders College Publishing: **1992**, 150-154.

[60] H.B.Klevens. *J. Phys. Colloid Chem.* **1948**, *52*, 130-148.

[61] P.Mukerjee and K.J.Mysels. *Critical Micelle Concentrations of Aqueous Surfactant Systems*. NSRDS-NBS 36: **1971**, 121-53.

[62] M.J.Rosen. *Surfactants and Interfacial Phenomena*, 2nd ed.; John Wiley & Sons Inc.: New York, **1989**, 72-73.

[63] M.Dahanayake, A.W.Cohen, and M.J.Rosen. *J. Phys. Chem.* **1986**, *90*, 2413-2418.

[64] A.L.M.Lelong, H.V.Tartar, E.C.Lingafelter, J.K.O'Loane, and R.D.Cadle. *J. Am. Chem. Soc.* **1951**, *73*, 5411-5414.

[65] J.K.Weil, F.D.Smith, A,J.Stirton, and R.G.Bistline. *J. Am. Oil Chem. Soc.* **1963**, *40*, 538.

[66] H.V.Tartar and K.A.Wright. *J. Am. Chem. Soc.* **1939**, *61*, 539-544.

[67] M.J.Rosen and L.D.Song. *J. Colloid Interface Sci.* **1996**, *179*, 261-268.

[68] Albemarle ADMA Compound Description, **1994**.

[69] C.F.Poole and S.K.Poole. *Chromatography Today*; Elsevier: Amsterdam, 1991, 459.

[70] L.D.Song and M.J.Rosen. *Langmuir* **1996**, *12*, 1149-1153.

[71] L.T.Liu and M.J.Rosen. *J. Colloid Interface Sci.* **1996**, *179*, 454-459.

[72] D.A.Skoog and J.J.Leary. *Principles of Instrumental Analysis*, 4th ed.; Saunders College Publishing: **1992**, 584-585.

[73] M.J.Rosen and L.T.Liu. *J. Am. Oil Chem. Soc.* **1996**, *73*, 885-890.

[74] D.Myers. *Surfaces, Interfaces, and Colloids, Principles and Applications*; VCH Publishers, Inc.: New York, **1991**, 153-157.

[75] M.J.Rosen. *Surfactants and Interfacial Phenomena*, 2nd ed.; John Wiley & Sons Inc.: New York, **1989**, 154-155.

[76] M.J.Rosen. *Surfactants and Interfacial Phenomena*, 2nd ed.; John Wiley & Sons Inc.: New York, **1989**, 92-93.

IMAGE EVALUATION TEST TARGET (QA-3)

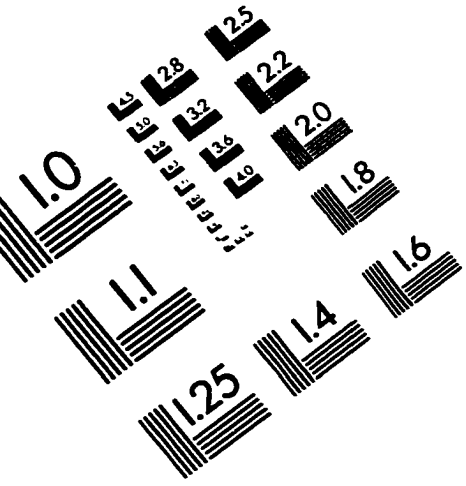

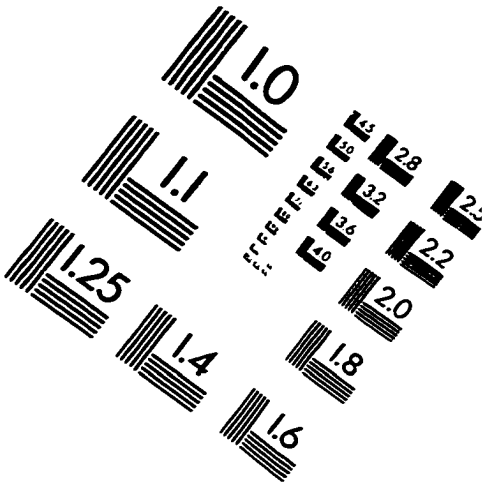

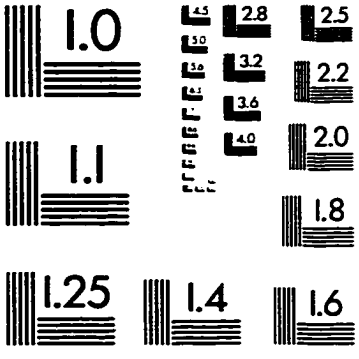

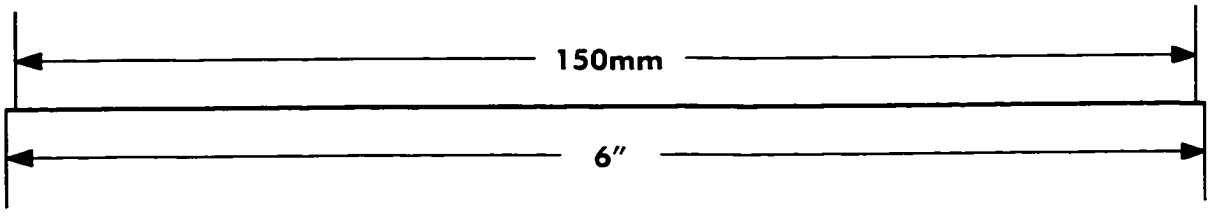

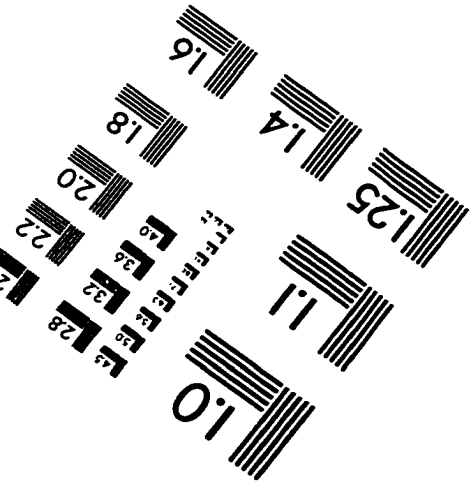

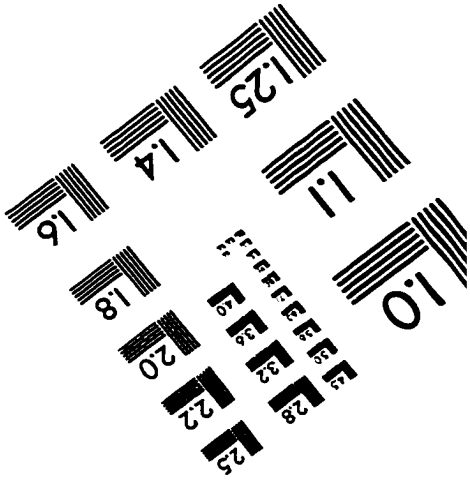

APPLIED IMAGE, Inc
1653 East Main Street
Rochester, NY 14609 USA
Phone: 716/482-0300
Fax: 716/288-5989